Destabilisation and inactivation of foam and foam-forming microorganisms in poultry slaughterhouse wastewater

By

Cynthia Dlangamandla
Student number: 209134402

Thesis submitted in fulfilment of the requirements for the degree
Doctor of Engineering in Chemical Engineering

Faculty of Engineering and Built Environment
Cape Peninsula University of Technology

Supervisor: Dr. M. Basitere
External supervisor: Prof. S.K.O. Ntwampe
Co-Supervisor: Dr. B.S. Chidi
Co-Supervisor: Dr. B.I. Okeleye

Cape Town

August 2022

DECLARATION

I, **Cynthia Dlangamandla**, declare that the contents of this thesis represent my unaided work and that the thesis has not previously been submitted for academic examination towards any qualification. Furthermore, it represents my own opinions and not necessarily those of the Cape Peninsula University of Technology and the National Research Foundation of South Africa.

All intellectual concepts, theories, methodologies, material derivations, and model developments used in this thesis and published in various scientific journals (except those that the candidate is not the first author in) were derived solely by the candidate and/or first author of the published manuscripts. Where appropriate, the intellectual property of others was acknowledged by using appropriate references. The contribution of co-authors for the conference and the published manuscript was in a training capacity, research assistance, and supervisory capacity.

Signed:  **Date:** 15 February 2023

ABSTRACT

Poultry slaughterhouse wastewater (PSW) contains a high concentration of nutrients such as ammonium nitrogen (NH_4^+-N), phosphorous, particulate matter, proteins, detergents as well as fats, oil, and grease (FOG), and includes a high biochemical oxygen demand (BOD) and chemical oxygen demand (COD). This makes PSW toxic if it is discharged into the environment. FOG leads to the fouling of diffusers and membranes in wastewater treatment plants (WWTPs); moreover, it enhances the proliferation of actinomycetes that contain hydrophobic cell walls and produces biosurfactants that result in excessive biofoam formation. For wastewater treatment, conventional activated sludge (AS) systems are used. However, the major drawback of AS systems is the accumulation of biofoam that is associated with the presence of FOG and proteins. To reduce biofoam, the AS systems are periodically dosed with synthetic defoamers; however, these compounds are toxic to the environment, and they are a short-term solution because they only deal with the symptoms and not the cause of biofoaming. As a consequence, this study focused on the production of biodefoamers that destabilizes and inactivate foam-forming microorganisms in PSW treatment systems.

Biodefoamer-producing microorganisms were isolated from PSW, and were assessed for their foam reduction efficiency as a foam collapse rate, under various response surface methodology (RSM) conditions, i.e. (pH 7-10) and biodefoamer concentration (1-4 % v defoamer/ v MLSS and PSW mixture). The isolates that achieved high foam reduction efficiency at a high foam collapse rate were identified and characterised. These isolates were found to be *Bacillus subtilis*, *Aeromonas veronii*, *Klebsiella grimontii,* and *Comamonas testosteroni testosteroni*, which were then mixed as a consortium and further tested for their foam reduction efficiency and foam collapse rate. At 4% (v defoamer/v MLSS and PSW), the crude biodefoamer had 96% foam reduction efficiency at a 1.7 mm/s foam collapse rate, whereas at 4% (v [active silicone polymer antifoam A by Sigma-Aldrich synthetic antifoam] / PSW), a synthetic defoamer obtained 96% foam reduction efficiency at 2.5 mm/s foam collapse rate achieved in less than 50s. The use of a biodefoamer resulted in compacted flocs whereas the use of synthetic defoamers resulted in flocs with protruding filaments. Fourier transform infrared spectroscopy (FTIR) showed that the biodefoamer had alkanes, amines, carboxyl, and hydroxyl groups which indicated that the defoamer was a polysaccharide. ^{1}H nuclear magnetic resonance spectroscopy confirmed that the biodefoamer was a carbohydrate polymer.

The mixed liquor of suspended solids (MLSS) that was used to assess biodefoamer efficiency was assessed using metagenomics, and the dominant microorganisms were identified as *Nostocoida limicola*, *Gordonia kroppenstedtii*, *Candidatus Microthrix parvicella*, *Nocardioides insulae* and *Bacteroides nordii,* which are biofoamers. Foaming reactors were also designed to assess the effect of reactor design on foamability and foam stability using the mixed liquor of biofoamers. The highest foam stability of 5.1 cm was achieved using a 150 mL sample in a 250 mL foaming rector at 3080 mg/L

MLSS concentration, culminating in a foaming potential of 51.3 mL/L. Whereas the lowest foam stability of 0.94 cm was achieved using a 250 mL sample with 4090 mg/L MLSS concentration in a 500 mL foaming reactor, which was the highest concentration of MLSS used in this study. For this setup, a foaming potential of 83.5 mL/L was observed. It was evident that reactor configuration was influential in foamability and foam stability. Furthermore, there was a high concentration of FOG and NH_4^+-N in PSW, hence it was crucial to assess the effect of these contaminants on the biodefoamer consortium growth as well as the ability of the consortium to biodegrade these contaminants to avoid biofoaming. The highest biodefoamer reduction of NH_4^+-N from 49 mg/L to 15.8 mg/L was observed at 216 h with FOG decreasing from a concentration of 170 mg/L to 6 mg/L. This indicated that the consortium also produced lipases. To elucidate foam destabilisation in terms of foam drainage and foam collapse rates, biodefoamer kinetics were developed using 3 models, namely the rate law, Monod's model, and exponential decay formula. The rate law model could predict both foam drainage and collapse, with R^2 of 1 and adjacent R^2 values of 0.98 respectively. Further, it had low variance of 6.99E-19 and 0.0148 and standard deviation was 2.2 E-10 as well as 0.001. These statistical aspects are a requirement for a good predictive model. Therefore, the rate law was significant in the prediction of the kinetic constants.

The biodefoamer consortium was cultured in PSW and MLSS nutrients to further assess its growth rate in the presence of high FOG and protein concentration as well as foam reduction efficiency. The highest growth rate was observed on day 3, whereby an exponential reduction of FOG from 672 mg/L to 400 mg/L was observed; moreover, proteins were also reduced from 130.8 - 96 mg/L. The foam reduction efficiency of 1.33 mm/s was obtained on day 5, which indicates that the biodefoamers are not only produced during the exponential growth phase but are also produced during cell lysis. The biodefoamer consortium was assessed for its antimicrobial activity by quantifying volumetric zones of inhibition (VZI) on the MLSS and PSW microbial community. The highest growth inhibition was 1.39 L/mL which was observed in the presence of the biodefoamer consortium. The other highest antimicrobial activity of 1.32 L/mL was observed when a biodefoamer produced by *Aeromonas veronii* and *Klebsiella grimontii* was used. This revealed that these microorganisms work better when they are in a consortium culture than as monocultures. The consortium was deemed competent for biodefoamer-supported AS systems, but this assertion needed to be evaluated.

Therefore, a miniaturised AS wastewater treatment system which consisted of a primary sedimentation tank, aeration tank, and a secondary clarifier was subsequently designed. The air flow rate in the aeration tank was 7L/min, and a 26-day-old sludge was collected from a local municipal WWTP near Cape Town, South Africa (SA). Subsequently, 1L of the MLSS was added into the aeration thank and PSW was pumped into the reactor using a Gilson® Minipuls Evolution peristaltic pump at a flow rate of 3.4 mL/ min at a hydraulic retention time (HRT) of 24 h. The sludge was recycled from the MLSS recycle steam back into the AS tank using a Gilson® Minipuls Evolution peristaltic pump at a flow rate of 3.2

mL/ min at a sludge retention time (SRT) of 10 days. The biodefoamer consortium was supplemented at 4% (v/v) (biodefoamer: PSW) for the removal of FOG, soluble proteins, total suspended solids (TSS), and COD in the PSW. The results indicated that the biodefoamer-AS aerobic tank can remove up to 94% FOG, 99% soluble proteins, 93.3% TSS, and 85.4% COD; whereas the synthetic defoamer supported AS (Syn-AS) system removed 74% FOG, 79% soluble proteins, 83.2% TSS as well as 61% COD. Furthermore, the conventional activated sludge (CAS) achieved removal of up to 72.3% FOG, 68% soluble proteins, 87% TSS and 50.5% COD. Meanwhile, in the secondary clarifier, the Biodefoamer-AS system removed a further 85% FOG, 99% soluble proteins, 86% TSS, and 67% COD, when compared with Syn-AS which removed FOG, soluble proteins, TSS, and COD by 67%, 92.2%, 86%, and 44.1% respectively. It was therefore concluded that the Biodefoamer-AS system was more efficient in the removal of the contaminants as compared to the Syn-AS and CAS systems. Overall, this study is the first to report on the efficacy of biodefoamer consortium for application in AS systems; however, further development regarding this approach is needed.

Keywords: Activated sludge; biodefoamers; biofoam; biodegradation; biodelipidation; filamentous bacteria; foamability; foam formation, foam collapse; foam drainage; foam reduction efficiency, foam stability; poultry slaughterhouse wastewater; synthetic defoamers, volumetric zone of inhibition, wastewater treatment plants.

DEDICATION

I dedicate this thesis to everyone who supported me throughout this journey, especially my late mother (Sylvia Nomaledi Dlangamandla), my late father (Nceba Webster Londa), and my daughter Luhluthando Dlangamandla who gave me motivation when I thought it was impossible to finish my studies.

I dedicate this thesis to every woman out there who is willing to live up to the challenge and pursue her dreams and embrace every single opportunity she receives.

To those who taught me and instilled the importance of research which is the ability to acquire new knowledge.

To those who had faith in me and my abilities and those who inspire me to do more.

ACKNOWLEDGEMENTS

I would like to thank:

- God for the courage and strength
- Dlangamandla and Londa families for their support throughout this journey
- Lillian Nombulelo Thomas, Ntombekhaya Eunice Dlangamandla, Yanga Dlangamandla, Nakhane Dlangamandla, and Miranda Msiwa for supporting me and taking care of my baby through the duration of my studies
- My supervisors Prof. SKO Ntwampe, Dr. M. Basitere, Dr. B.S. Chidi, and Dr. B.I. Okeleye for their assistance, guidance, and technical advice throughout my studies
- Dr. Ncumisa Mpongwana, Yolanda Phelisa Mpentshu, Melody Ruvimbo Mukandi, Zandile Estella Jingxi, and Dr. Nkosikho Dlangamandla for technical support and advice
- My Friends Nangamso Cawe, Mathabo Ludaka, Zandile Mdingi, Andiswa Same, Nomzamo Gecelo, Vuyiswa Biyo, Busisiwe Prudence Keva, Bukelwa Qwashu, Wongeka Mdlokova, Vuyiswa Njokweni, Ntombethemba Nkohla, Siyasanga Mbulawa, Nomaphelo Dameni, Sizeka Dyantyi and Thuletu Mbita for being there for me throughout my hardships
- The University Research Fund (RK16) and the National Research Foundation Thuthuka funding for financially supporting this research, the Cape Peninsula University of Technology postgraduate fund, and
- All the postgraduate students in the Bioresource Engineering Research Group (BioERG), Faculty of Applied Sciences and Faculty of Engineering & the Built Environment, CPUT.

RESEARCH OUTPUTS

The following research outputs represent the contributions of the candidate to scientific knowledge and development during the doctoral candidacy (2017-2022):

DHET-accredited manuscripts published/accepted for publication form part of this thesis

Dlangamandla, C., Mukandi M.R., Basitere, M., Okeleye, B.I., Chidi, B.S. & Ntwampe, S.K.O. 2023. Production, Application, and Efficacy of Biodefoamers from Bacillus, Aeromonas, Klebsiella, Comamonas spp. Consortium for the Defoamation of Poultry Slaughterhouse Wastewater. *MDPI Water*, 15(4): 655. https://doi.org/10.3390/w15040655.

Dlangamandla, C., Basitere, M., Okeleye, B.I., Chidi, B.S. & Ntwampe, S.K.O. 2020. Biofoam formation and defoamation in global wastewater treatment systems. *Water Practice & Technology*, 16(1): 1-18. https://doi.org/10.2166/wpt.2020.113.

Additional DHET-accredited manuscripts published/accepted for publication that does not form part of this thesis

Dlangamandla, C., Ntwampe, S.K.O. & Basitere, M. 2018. A bioflocculant-supported dissolved air flotation system for the removal of suspended solids, lipids, and protein matter from poultry slaughterhouse wastewater. *Water Science and Technology*, 78(2): 452-45. https://doi.org/10.2166/wst.2018.324.

Mpongwana, N., Ntwampe, S.K.O., Omodanisi, E.I., Chidi, B.S., Razanamahandry, L.C., **Dlangamandndla, C**. & Mukandi, M.R. 2020. Bio-Kinetics of Simultaneous Nitrification and Aerobic Denitrification (SNaD) by a Cyanide-Degrading Bacterium Under Cyanide-Laden Conditions. *MDPI Applied sciences*, 10(14): 4823. https://doi.org/10.3390/app10144823.

Submitted manuscripts

Cynthia Dlangamandla, Seteno K.O. Ntwampe, Moses Basitere, Boredi S. Chidi, Benjamin I. Okeleye, Ncumisa Mpongwana. Biokinetic modelling of biofoam destabilisation by biodefoamers in poultry slaughterhouse wastewater treatment. Submitted to *Bioengineering* (under review).

Cynthia Dlangamandla, Seteno K.O. Ntwampe, Moses Basitere, Boredi S. Chidi, Benjamin I. Okeleye. Antagonistic characteristics of biodefoamers against biofoam formers in poultry slaughterhouse wastewater. Submitted to *Bioengineering* (under review).

Cynthia Dlangamandla, Moses Basitere, Seteno K.O. Ntwampe, Boredi S. Chidi, and Benjamin I. Okeleye. Biodefoamer supported activated sludge for the treatment of poultry slaughterhouse wastewater. Submitted to *Bioengineering* (under review).

LAYOUT OF THESIS

The general aim of this study was to design a bench-scale activated sludge system and supplement it with biodefoamer-producing microorganisms for 1) biofoam defoamation, 2) the inactivation of biofoamers, and 3) the reduction of biofoam from poultry slaughterhouse wastewater. The experimental work of this study was conducted at the Cape Peninsula University of Technology, Bioresource Engineering Research Group (BioERG) laboratory, South Africa. The references are listed as per the CPUT Harvard method of referencing. The thesis was compiled as a thesis by publication.

- **Chapter 1**: Introduction: this chapter provides the background information about poultry slaughterhouse wastewater treatment and the challenges that affect the aerobic treatment of this wastewater, especially its constituents such as FOG, proteins, and NH_4^+-N, i.e., contaminants that enhance the proliferation of biofoamers. Furthermore, it includes a research problem statement, hypothesis, aims, objectives, significance, and delineation of the study.

- **Chapter 2**: This chapter focuses on the literature consulted to provide a detailed background of biofoam formation and defoamation in global wastewater treatment systems. Moreover, environmentally benign, economical, and sustainable methods that can be used to overcome biofoam challenges were also reviewed.

- **Chapter 3**: This chapter focuses on the listing of methods and materials that were utilised to achieve the aims of the study.

- **Chapter 4**: This chapter focuses on the production, application, and efficacy of biodefoamers for defoamation of poultry slaughter wastewater.

- **Chapter 5**: This chapter discusses biokinetic modelling of biofoam destabilisation by biodefoamers in poultry slaughter wastewater treatment systems.

- **Chapter 6**: This chapter focuses on the antimicrobial activity of biodefoamers against poultry slaughterhouse wastewater and municipal wastewater mixed liquor suspended solids microbial communities.

- **Chapter 7**: This chapter presents the design and efficacy of biodefoamer-supported activated sludge for the treatment of poultry slaughterhouse wastewater.

- **Chapter 8:** This chapter provides the overall study summary and conclusions, and it also answers all the research questions and provides recommendations for future studies.

TABLE OF CONTENTS

LIST OF FIGURES

LIST OF TABLES

GLOSSARY

Abbreviations	Meaning
AS	Activated sludge
NH_4-N	Ammonium nitrogen
ANOVA	Analysis of variance
BOD_5	Five-day biochemical oxygen demand
Bio-AS	Biodefoamer supported activated sludge
tCOD	Total chemical oxygen demand
CFU	Colony-forming unit
CAS	Conventional activated sludge
CMC	Critical micelle concentration
DO	Dissolved oxygen
EPS	Extracellular polymeric substances
FOG	Fats, oils and grease
FCR	Foam collapse rate
FRE	Foam reduction efficiency
LCFAs	Long chain fatty acids
MLSS	Mixed liquor suspended solids
NO_3-N	Nitrate nitrogen
NO_2-N	Nitrite nitrogen
NMR	Nuclear magnetic resonance
PCR	Polymerase chain reaction

PSW	Poultry slaughterhouse wastewater
RSM	Response surface methodology
Syn-AS	Synthetic defoamer supported activated sludge
TSS	Total suspended solids
VZI	Volumetric zones of inhibition
WWTP	Wastewater treatment plant

Symbols	**Definition (units)**
$°C$	Degree celsius
h	Liquid or foam height
Δh^F	Level changes in foam height
Δh^S	Level changes of the solution
H_0	Initial liquid height before aeration (cm)
H_t	Foam-liquid interface post aeration (cm)
ki	Kinetic defoamation constant
μ	Specific growth rate (h^{-1})
Q	Air flow rate L_{air}/min
R^2	Correlation coefficient
r_a	Rate of foam destabilisation
S	Area of the cylinder (cm^2)
t	Time (h/day)
ΔT	Change in aeration time (min)

CHAPTER 1

GENERAL INTRODUCTION

CHAPTER 1

GENERAL INTRODUCTION

1.1 Introduction

The South African poultry industry includes 470 slaughterhouses that produce 65.5% of animal protein that is consumed locally (Basitere et al., 2016). Poultry slaughterhouses utilise a high quantity of clean water during animal slaughtering for the cleaning of utensils as well as sanitising of the facilities (Basitere et al., 2017). Up to 24% of the wastewater in the food processing industry is generated from the meat processing industry (Bustillo et al., 2016). Poultry slaughterhouse wastewater (PSW) contains fats, grease and lipids (FOG), which contribute to an increase in insoluble COD, high concentration of suspended solids which decreases the efficiency of an- and aerobic treatment systems due to deterioration of biomass within such systems (Del Nery et al., 2007). This wastewater also contains detergents that are used for cleaning the plant as well as the utensils (Coskun et al., 2015). The detergents in the wastewater are biodegradable but their degradation process is very slow; hence, they become problematic in wastewater treatment plants (WWTPs) since they cause foam in the aerobic treatment processes as well as the secondary clarifiers (Jenkins et al., 2004). The foaming is stabilised by the presence of surfactants that make up the detergents as well as the presence of filamentous bacteria with hydrophobic membranes. The filamentous bacteria are generated by high dissolved oxygen (DO) in the treated wastewater due to aeration. These constituents can be removed by the activated sludge treatment system before their introduction into the secondary clarifier.

Activated sludge (AS) is a biologically engineered system that uses suspended biomass to remove contaminants. It consists of a metagenomic complex microbial community that is introduced into the system as an influent (Liu et al., 2019). The main focus of this system is to make the chemo-heterotrophic microorganisms take up the dissolved organic matter such as nitrogen (N), phosphorous (P) as well a carbon (C) and convert it to biomass (sludge) and carbon dioxide (CO_2). The biomass aggregates the solids such that compact biomass is formed, so that when they enter the secondary clarification tank, the sludge and clear water can be physically separated by gravity. If the sludge disintegrates and deflocculation occurs, this reduces the system efficacy and results in a loss in biomass, excess sludge wastage and discharge into the environment, as well as sludge flotation in the secondary clarifier and biofoam formation due to overgrowth of actinomycetes (Li et al., 2016; Zhang et al., 2021). To overcome deflocculation, synthetic flocculants are added into the system; hence, flocculants are used to efficiently separate hydrophobic material from the wastewater by modifying particle (lipids and suspended solids) charges to enhance the flocculation (Li et al., 2014). When the

particulate material is flocculated, macro flocs are formed which in turn result in the clarification of the wastewater in the secondary clarifier. Chemical flocculants are used often in the treatment of industrial wastewater because they are efficient and economical; however, they are toxic to humans and the environment (Dlangamandla et al., 2017). To tame biofoam, synthetic defoamers are used; however, they are a temporary solution that treats the symptom (foam) not the cause (deflocculation) (Dlangamandla et al., 2020).

Therefore, there is a need to produce as well as screen non-toxic and biodegradable biodefoamers that are highly efficient. These biodefoamers must have bioflocculation activity which in turn minimises biofoaming. Biodefoamers are intracellular and extracellular polymeric structures that include proteins, polysaccharides and amino acids that are produced by microorganisms during their growth and death phase (Liu et al., 2015; Dlangamandla et al., 2020). These biodefoamers can also be incorporated within the AS system for the removal of suspended solids as well as lipids and hydrophobic filamentous bacteria. Biodefoamers are produced by different isolates that are found in many habitats. This study focused on the production of biodefoamers by microorganisms from PSW for use in AS for PSW treatment. The destabilisation of foam by biodefoamers, kinetics as well as the inactivation of biofoam-forming bacteria, was studied to understand the different dynamics involved in biofoam destabilisation or reduction of foam formation in AS. The biodefoamer-supported activated sludge (Bio-AS) wastewater treatment system must therefore work better to remove FOG, TSS, proteins and COD, while deactivating biofoam-forming microorganisms for it to be developed into a system that can be adopted on a large scale.

1.2 Statement of the research problem

Macromolecules such as FOG and proteins from food processing industries and households are a major problem for WWTPs as it is difficult to treat them using conventional biological treatment methods. In most instances, they result in treatment system fouling. Fats solidify at low temperatures, resulting in clogging of pipes and reduced system efficiency, and causing irreparable damage to equipment. This may result in increased operational costs, especially in aerobic treatment systems whereby FOG decreases the rate at which dissolved oxygen is transferred; meanwhile, in anaerobic treatment system, FOG elevates the number of actinomycetes such as *Nocardia amarae*, causing scum formation and foaming, which leads to poor sludge activity, and therefore decreasing treatment efficiency of the WWTPs (Jeganathal et al., 2006). The current source of these pollutants to be studied is poultry slaughterhouses producing wastewater containing FOG, proteins, phosphorous, nitrogen, blood, and other organic matter (Escamilla-Silva et al., 2005). Most industries that produce waste materials from a biological origin are often more amenable to the application of bio-based processes for their wastewater remediation. However, it is difficult to treat this kind of wastewater in bioreactors since it contains a high quantity of suspended solids, as well as FOG (Del Nery et al., 2007). Therefore, there

is a need to design an AS system in which biodefoamers are used for the flocculation of sludge and biodefoamation of the treated wastewater. Additionally, there is a need to focus on the destabilisation and inactivation of foam including foam-forming microorganisms in PSW to minimise foam formation. An added benefit will be if such biodefoamers can also solubilise FOG.

1.3 Hypothesis

Using an AS supported with biodefoamers can efficiently inactivate foam-forming microorganisms and destabilise foam in a PSW treatment system.

1.4 Research questions

- Can the single isolates and consortium microorganisms produce sufficient biodefoamers suited for AS systems`?
- Will the biodefoamer activity (foam reduction efficiency and foam collapse) be suitable for AS-PSW treatment system?
- Which of the commonly used mathematical models can be used to predict biodefoamation?
- Will the biodefoamers be active in the presence of both PSW and total suspended solids (TSS), i.e., mixed liquor suspended solids (MLSS)?
- Will the biodefoamers be able to biodefoam and inactivate biofoamers in the AS-PSW treatment process?

1.5 Aim and objectives of the study

This study aimed to design a bench-scale AS system supplemented with biodefoamers for the inactivation of foam-forming microorganisms and reduction of biofoam for PSW treatment. This aim was reached by achieving the following objectives:

- To isolate and asses the microorganisms in PSW for their ability to produce biodefoamers with high foam reduction efficiency and foam collapse rate.
- To characterise the biodefoamers' functional groups using FTIR and ^{1}H Nuclear magnetic resonance (NMR).
- To evaluate the bio-kinetics and defoaming activity of the biodefoamers against foam-forming microorganisms.
- To assess the antimicrobial activity of the crude biodefoamer against biofoam generation microorganisms in the presence of suspended solids,
- To design and operate a bench-scale Bio-AS to reduce biofoaming and increase inactivated foam-forming microorganisms and compare such a PSW treatment system to: 1) that which uses synthetic defoamers and 2) the conventional AS system.

1.6 Delineation of study

This study did not research on the modelling of the AS microbial processes and the impact of spargers on the biodefoamers.

1.7 Significance of research

Physical, chemical, and biological treatments have been applied to PSW for the removal of pollutants. Although these treatments have been in use, suspended solids and FOG including other contaminants remain a huge problem in treatment systems where AS is used. FOG solids build up and clog piping systems, resulting in system failure. Cleaning clogged piping systems is costly. This necessitates the implementation of a Bio-AS with a high efficacy in the removal of solids, FOG and proteins among others, with the ultimate aim of reducing biofoam and the proliferation of biofoam-producing organisms. The presence of actinomycetes in AS results in sludge deflocculation and biofoaming and these results in the system inefficiency, which will increase operational cost. Although synthetic flocculants and defoamers have been used in AS processes for generations, their use is harmful to the environment. This study focussed on the use of a Bio-AS system not only to reduce pollutants that are used by biofoam-forming microorganisms in PSW, but to ensure that the effluent from a treatment system enters the secondary clarifier with minimal nutrient content that does not favour the growth of actinomycetes. This is the first study to assess an AS system by using this approach.

CHAPTER 2

LITERATURE REVIEW

***Published as*: Dlangamandla, C**., Basitere, M., Okeleye, B.I., Chidi, B.S. & Ntwampe, S.K.O. 2020. Biofoam formation and defoamation in global wastewater treatment systems. *Water Practice & Technology*, 16(1): 1-18. https://doi.org/10.2166/wpt.2020.113

CHAPTER 2

LITERATURE REVIEW

2.1 Introduction

Activated sludge (AS) systems are commonly used in wastewater treatment systems. They are efficient in removing organic matter in the form of dissolved solids, nutrients, and dissolved biodegradable carbon (Pal et al., 2014). Wastewater treatment plants (WWTPs) are common worldwide. A conventional municipal WWTP has a primary clarifier, aeration tank/basin and secondary tank/clarifier including a recycle stream that recycles sludge from the secondary clarifier to the aeration basin (Tchobanoglus et al., 2003). Mixed liquor suspended solids (MLSS) in the aeration basin contain suspended microbial growth responsible for aerobic nitrification and subsequent anoxic denitrification as well as phosphorus removal (Saunders et al., 2015). The microorganisms in the AS aeration basin feed continuously on the nutrients in the influent.

The primary purpose of AS is to degrade organic matter and pollutants in the wastewater so that the treated wastewater meets the discharge standards (Islam et al., 2013). Liquid-solid separation occurs in the clarifiers. In the secondary clarifier, after the primary AS system, the solids (sludge) are returned to the aeration basin, while the clarified liquid goes to tertiary treatment systems. AS systems can be classified as primary bioengineered systems designed to mimic natural processes; however, wastewater treatment is done rapidly such that the wastewater throughput is sustained for high volume treatment plant efficiency.

A major challenge in AS systems is sludge bulking and foaming (Xia et al., 2018). Sludge bulking is considered a challenge due to its ability to render WWTPs inoperable, unlike foam formation. Foaming is generally neither studied nor monitored sufficiently, and usually arises from the presence of surfactants, proteins, fats, oil, and grease (FOG), as well as the presence of filamentous bacteria such as *Gordonia amarae* (*G. amarae*) (previously known as *Nocardia amarae* (*N. amarae*)), *Microthrix parvicella* (*M. parvicella*), Eikelboom types 021N, 1701, 1863, 0041/0675, 0092, 0803, 0914, 1851 and other actinomycetes with cell wall containing filaments (Wanner et al., 1998). These microorganisms are highly hydrophobic and thus readily accumulate in organic matter-polluted wastewater, particularly in the aeration basin where they are buoyant because they easily attach to air bubbles and float to the wastewater surface, proliferating rapidly due to nutrient availability. Subsequently, they release extracellular polymeric substances (EPSs), some of which are biosurfactants, to facilitate the hydrolyzation of organic pollutants including FOG into long-chain fatty acids (LCFAs), which then form their primary nutrient and carbon

source (Xia et al., 2018; Lemmer et al., 2000). When the concentration of FOG is high, foam formation due to actinomycetes proliferation is inevitable and biofoam defoamation becomes crucial.

Various studies have been done outlining aspects of chemical, physical, and biological biofoam control (Pitt & Jenkins, 1990; Mamais et al., 2011; Shao & Kao, 2014; Khairnar et al., 2014). The current review provides an insight into different approaches, including an eco-friendly and environmentally benign approach. The objective of the review was to highlight biofoamation as a major hindrance for AS systems and consolidate information on the causes of foaming in WWTPs including defoaming methods and strategies, and highlight the efficacy of biodefoamers.

2.2 What causes foam in WWTPS?

Foaming arise from the overgrowth of filamentous bacteria that falls under the mycolata taxon in AS systems. (Wanner, 1994). Madoni et al (2000) carried out a survey of biological foaming agents in 167 Italian WWTPs. They found abundant *M. parvicella* in foaming, whereas *Nocardiaform actinomycetes*, Eikelboom types 0041, 0092, 021N, 0675, and *Thiothrix,* were only detected in very low concentrations. Guo & Zhang (2012) also used throughput-sequencing to profile dominant microorganisms associated with biofoaming in 14 WWTPs worldwide. In their study, *M. parvicella*, *Nostocoida limicola I* and *II*, *Mycobacterium fortuitum,* and Eikelboom type 1863 were identified as dominant biofoamers. Overall, foaming occurs in AS systems largely because of aeration in the presence of synthetic and biosurfactants from filamentous bacteria (Nielsen et al., 2009; Osama, 2014; Mulligan, 2005). It is also associated with the presence of proteins and FOG, including foam-facilitating operating conditions at WWTPs (Rossetti et al., 2005). Generally, the presence of biosurfactants in combination with proteins produces a stable foam, with the proteins, composed of nitrogen, carbon, hydrogen, and oxygen, being used as carbon and nitrogen sources by the foam-forming filamentous bacteria (Wiley et al., 2008). These foam-forming bacteria can also use soluble hexadecane and acetate as readily available carbon sources during their growth. Under such conditions, the organisms will excrete biosurfactants. Microorganisms such as *M. parvicella* and *N. amarae* proliferate in FOG-containing wastewater, as they degrade the lipids and solubilize them by producing biosurfactants (Pal et al., 2014; Dunkel et al., 2018).

N. amarae is a gram-positive non-motile organism that depends on the wastewater characteristics and sparging, to enhance their buoyancy to the wastewater surface. It has relatively low food requirements and depends on the effluent for a continuous supply of biodegradable FOG for growth (Tandoi et al., 2017). *M. parvicella* however, is gram-positive and slow-growing and has unbranched filamentous strands that appear between flocs, disrupting floc formation. Like *N. amarae*, *M. parvicella* has a low food to microorganism

ratio (f/m). It is also microaerophilic and can grow in any AS zone, particularly dead zones. The optimum pH range for *M. parvicella* is 6.7-8 and the microorganism is likely to be limited by high dissolved oxygen (DO) concentration (Rossetti et al., 2005). It also has a hydrophobic cell surface containing filamentous strands that attach to foam layers. The filamentous network ensures entrapment in bubbles, resulting in a buoyant movement to the wastewater surface. *M. parvicella* cannot use acetyl coenzyme A to generate LCFAs for growth but depends on the FOG in the influent or sludge (Tandoi et al., 2017). Table 2.1 outlines the different environmental conditions that promote the growth of various filamentous microorganisms associated with biofoam development.

Table 2.1: Environmental conditions promoting different types of filamentous organisms associated with biofoaming (The Water Network, 2019; Liu et al., 2019; Nielsen et al., 2009

Environmental condition	**Organism(s)**
High DO concentration	*Sphaerotilus natans*, Eikelboom type 021N
Low f/m ratio	Eikelboom types: 0041, 0675, 1851
Grease and oil availability	*Nocardia* sp., *Microthrix parvicella*, Eikelboom type 1863
Low pH	Fungi
Protein availability	Chloroflexi, Eikelboom types 0092 and 0041

2.3 Modern molecular methods for identification of biofoam producers

Conventionally, filamentous bacteria were characterized based on their morphology using staining and light microscopic techniques (Eikelboom, 1975). However, it was shown that filament characterization and identification using microscopic techniques were inaccurate for the identification of filamentous bacteria. Therefore, new methods like fluorescence *in situ* hybridization (FISH) were developed in order to identify biofoamers (Nielsen et al., 2009). Polymerase chain reaction (PCR) is another molecular method that is used to amplify specific DNA sequences for microorganism identification. Generally, real-time quantitative PCR (qPCR) detects a targeted DNA sequence for a certain specie during PCR (Nittami et al., 2017). Other newly available techniques include 16S rRNA sequencing on the Illumina platform, which uses a reversible dye terminator method (Dunkel et al., 2018). Metagenomics of *in-situ* mixed cultures and the MiDAS 2.1 database were also designed to profile AS bacteria (Speirset et al., 2015).

2.4 Control methods for excessive foam in WWTPs

Various methods have been used to control excessive foaming in AS systems, but it persists. Some foam control methods were successful in laboratory studies, but when scaled-up they were costly, and after a time they reduced AS efficiency (Mamais et al., 2011). Foam reduction or complete removal is complex, and a sustainable solution requires more in-depth research. Methods reported in previous studies included the adjustment of AS operating conditions, water spraying, steaming, use of "feast-fast" reactors in series, and the use of chemical defoamers which require to be added to the wastewater more often and this results in increased running costs (Shao & Kao, 2014; Hoyle et al., 2006; Tsang et al., 2008).

2.5 Non-specific foam control strategies

2.5.1 Adjustment of AS system operating conditions

The operating conditions used to control foam formation include the mean biomass (cell) residence time (MCRT) within the AS system, i.e., the average residence time (days) of the microorganisms within the AS system. Pitt & Jenkins (1990) reported that lowering the MCRT reduced *N. amarae* growth in 6 days. On this basis, reducing MCRT to less than 8 days was deemed an appropriate strategy for managing *M. parvicella* proliferation (Pal et al., 2014). However, it was inefficient for removing excessive foam in industrial-scale operations, whereby nitrification is also required. Generally, many other foam producers are present in excess in AS systems and can survive MCRT reduction. Richard et al. (1989) reduced air in the aeration basin so that the bubbles in it were significantly minimised, thus reducing excessive foaming. This led to incomplete nitrification as well as an excess of suspended solids in the secondary clarifier.

2.5.2 Application of water sprays to control excessive foam

Water spraying has also been used to control excessive foaming in AS systems. Water is sprayed onto the foam surface so that the bubbles collapse rapidly. The sprays can be suspended in the AS system. Using sprays does not minimise the foam former proliferation but the filamentous bacteria are returned to the AS system and integrated into the MLSS. This method tends to assist in the reintegration of filamentous organisms, some of which will be embedded in the AS solids and recycled back via the secondary clarifier, promoting bulking or the generation of more foam, which will require more spraying, subsequently increasing the plant's operating costs (Saby et al., 2002).

2.5.3 Application of steam to reduce filamentous bacteria

Hoyle et al. (2006) conducted a study whereby steam was applied to reduce foam-causing filamentous bacteria. The steam was delivered to a reactor containing a 0.5 L foam sample. Various pressure and time combinations were tested from 207 to 483 kPa and 10 to 60 minutes respectively. *Nocardia* sp. filament growth decreased gradually at 483 kPa after 60 minutes' exposure, but this did not affect *M. parvicella* growth. As a result, foam-forming potential was unaffected although foam stability was reduced. Although the study demonstrated a reduction of *Nocardia* sp. filaments, the system is energy-intensive and other microbial structures might evolve to perform differently, with temperature-sensitive microorganism cells lysing.

2.5.4 "Feast-fast" operation

Tsang et al. (2008) and Chua et al. (2000) used a "feast-fast" process, whereby floc formers were separated from foam formers by harnessing their growth conditions in separate reactors prior to the passing of wastewater containing LCFAs and FOG. The two reactors operated in series were named feast (reactor 1) and fast (reactor 2). The feast reactor influent favoured floc former growth because it contained a high f/m ratio of 0.75 BOD/gMLSS/d, while the fast flask contained a low f/m ratio that favoured the growth of filamentous foam formers (Tsang et al., 2008). Since floc and foam formers were harnessed in different growth reactors, there was minimal competition for the nutrients. This technique reduced the sludge volume index from 300 to 80 mL/g, as well as foam stability in the system. Some 95% of BOD was removed and *N. amarae* growth decreased, while the system stability improved. Although the results were good at laboratory scale, operation at full-scale operation is impractical.

2.5.5 Chemical dosing to reduce excessive foaming in WWTPs

Chemicals – e.g., chlorine and chemical polymers or coagulants – have also been used to reduce excessive foaming. They are a short-term solution because consistent dosing is required for foam reduction. Dosing chlorine into the aeration tank can also be inefficient as it causes floc disintegration and can lead to sludge bulking, which renders the AS system inefficient (Eckenfelder & Garu, 1998). Chlorine also breaks microorganism cell walls and affects their metabolism. Other than that, when chlorine is added to organic matter, it may form chlorinated oxidation by-products like trihalomethanes (Pasinetti et al., 2005) that might cause further damage to the microbial population in AS systems (Dai et al., 2013; Liu, 2003) while raising the soluble COD concentration in the treated wastewater (Cotruvo & Amato, 2019).

Mamais et al. (2011) investigated the addition of coagulants such as ferric chloride, ferrous chloride, polyaluminium chloride, hydrated aluminium sulphate, and cationic polymers. In the study, polyaluminium chloride with a cationic polymer was determined as the most effective foam reduction combination. Adding polyaluminium chloride at 31.5 mg/L improved sludge settleability while good foam reduction was achieved with 0.6 mg/L of the cationic polymer. Microscopic analyses showed that polyaluminium chloride improves floc density and enhances floc formation. The study also showed *M. parvicella* and *N. amarae* filaments embedded within the flocs, and thus deprived of a nutrient-rich environment (Nielsen et al., 2005). At this polyaluminium chloride dose, biofoam reduction was between 75 and 100% (Pal et al., 2014).

Although these coagulants achieved significant results, they may not be suitable for use in full-scale WWTPs. Most wastewater discharge regulations and/or standard guidelines specify that the treated water discharged must contain 0.25 mg/L or less total chloride, so using chemicals with a significant chloride content – e.g., chloride-based coagulants – will not be ideal.

2.5.6 Inhibition of filamentous bacterial growth by deselection mechanism

Biofoam formation and sludge bulking can be inhibited by a deselection mechanism whereby conditions are made unfavourable for filamentous growth but favour floc formers. Several filamentous foam forming bacteria occur in AS, including alphaproteobacteria, bacterioidetes, etc., (Nielsen et al., 2009) with alphaproteobacteria taking up most of the nutrients and subsequently storing polyhydroxyalkanoate which facilitates sludge bulking. These types of organisms can be deselected by adding a dehydrogenation treatment stage or creating a selective reactor configuration for their removal (Kragelund et al., 2005). Apart from *M. parvicella*, bacterioidetes such as *Curvibacter* and TM7 cause neither bulking nor foaming (Kreguland et al., 2008). Additionally, *M. parvicella* can be controlled by removing FOG to degrade surface active lipases. All these filamentous, foam-forming bacteria can be controlled selectively using a deselection mechanism whereby anoxic and anaerobic selectors can control their growth, assisted by chemical dosing. Table 2.2 lists biofoamers and general AS biofoam control strategies in various countries.

Table 2.2: Biofoamers and general AS control strategies in various countries (by country)

Country	Biofoamers	Control strategies	References
Argentina	*S. natans*, *M. parvicella*, *Nocardia* sp. *Thiothrix* I, Eikelboom Types: 021N, 1701, 1863, 0041, 0092	Chlorination, oxidant, or coagulant addition	Di Marzio (2002)
Australia	*M. parvicella*, Eikelboom Types: 0041/0675, 0092 and *H. hydrossis*	Chlorination, aeration, and f/m ratio 0.4 manipulation and reducing sludge age	Seviour et al. (1989), Seviour et al. (1994), Seviour et al. (1997)
Czech Republic	*M. parvicella*, Eikelboom Type 0092	FEX-120 supplementation, reducing sludge, water sprays, mechanical skimming, use of contact zone selectors, chlorination	Krhutkova et al. (2002), Kragelund et al. (2010)
Denmark	*M. parvicella*, Eikelboom Types: 0041/0675, 021N, 0092, 0803, 0914, 1851 and *N. limicola*	FEX-120, chlorination, addition of PAX-14, use of selectors	Kristensen et al. (1994), Kragelund et al. (2010)
France	*M. parvicella*, Nocardioform Eikelboom Types: 0041/0675, 021N, Type 0092 and *M. limicola*	Chlorination, contact zone loading rate manipulation	Pujol (1994)
Germany	*M. parvicella*, Eikelboom Types: 0041/0675, 021N, 0092 and 1701	Coagulants ($FeCl_3$, $Ca(OH)_2$), oxidants (H_2O_2, Cl_2), antifoam and coagulant use, contact zone use, reduction of sludge age, DO reduction and mechanical skimming	Kunst & Reins (1994)
Italy	*M. parvicella*, NALO, Eikelboom Types: 0041/0675 and 0092	SRT reduction, maintaining DO at >2 mg/L. Influent delipidation, chlorine and PAX-14 usage.	Rossetti et al. (1994), Madoni et al. (2003), Rossetti et al. (2005)
Japan	Eikelboom Types: 021N, 1701, 0041/0675 *S. natans* and *Thiothrix* sp.	DO reduction, use of coagulants and feast-fast technique	Mino (1995), Chua et al. (2000)

Netherlands	*M. parvicella*, *H. hydrossis*, Eikelboom Types: 021N, 0041/0675, 0092 and 701	Decreasing f/m ratio and SRT. Delipidation and polymers addition with DO at >2 mg/L	Eikelboom (1977), Eikelboom (1994), Kruit et al. (2002), Mino (1995)

Cont. Table 2.2

South Africa	*M. parvicella*, Eikelboom Types: 1851, 0041/0675 and 0914	Chlorine, O_3, H_2O_2 and polymer addition. Use of a defoamer, DO adjustment, sludge age reduction, physical skimming	Blackbeard et al. (1986), Blackbeard (1988), Mangundu (2017), Pitman (1996)
United Kingdom	*M. parvicella*, Eikelboom Type 021N, *N. limicola*, and NALO	Manipulation of DO and f/m, and reduced MLSS at 2.5 g/L	Foot (1992), Foot & Robinson (2003)
Unites States of America	*M. parvicella*, NALO, Eikelboom Types: 1701, 021N, 0092,0041/0675 and NALO	Addition of coagulant	Strom & Jenkins (1984), Switzenbaum et al. (1992), Jenkins et al. (1993)

2.6 Specific foam control methods: future perspectives

2.6.1 Application of microbial cells as defoamers

Chemical and physical methods are short-term solutions to excessive foaming in AS systems, and novel approaches are required to overcome their limitations (de los Reyes, 2010). The novel biological approaches studied include the use of bacteriophages to reduce foam formers. Bacteriophages are specific to individual microorganism types/species. Withey et al. (2005) showed that bacteriophages could reduce mycolata cell numbers sufficiently for foam formation to be reduced significantly. Petrovski et al. (2011a) used multi-spectrum DNA phages, i.e., GTE2 and GTE7, isolated from an AS system. They were screened for their ability to lyse 65 different mycolata species. In their study, GTE7 lysed all the 65 mycolata species while GTE2 was lytic against only five (Petrovski et al., 2011a; Petrovski et al., 2011b).

Khairnar et al. (2014) isolated and characterised three bacteriophages, NOC1, NOC2 and NOC3, to lyse *Nocardia* sp., which they did efficiently under laboratory conditions (at 30 °C for 2 days). Pajdak-Stós et al. (2017) conducted further, full-scale studies for reducing foam-forming microorganism using rotifers, which ingest and minimise filaments in sludge, thus reducing excessive foam. Three rotifers – isolates *Lecane tenuiseta*, *Lecane inermis*, and *Lecane pyriformis* – were used successfully against *M. parvicella* and Eikelboom type 0092 filaments, with significant reduction of these organisms within two weeks. In general, the rotifers can reduce some actinomycetes populations significantly. *Lecane inermis* was then introduced into a full-scale WWTP, which was monitored for a year. It was further discovered that the introduction of rotifers reduced *M. parvicella* and other actinomycetes on a large scale.

2.6.2 Antimicrobial characteristics of biodefoamers (microbial defoamers)

Antimicrobial defoamers can either lyse or inhibit the growth of the filamentous bacteria present in AS systems. If they can lyse bacterial cell walls, they are called bactericidal, but if they inhibit foam formers' growth, they are bacteriostatic. Khairnar et al. (2014) used bactericidal phages to eliminate the growth of filamentous bacteria. Microbial cells can also be used as antibacterial agents to lyse other cells or to inhibit the growth of other microorganisms. The extra- and intra-cellular structures of compatible microorganisms can be used as defoamers to inhibit or lyse filamentous bacteria known for foam formation. These isolates can be taken from the AS and cultured further using a microbial culture/inoculum development programme, for subsequent reintroduction into the wastewater to be treated. This is the strategy adopted for the Bio-AS treating PSW in this study.

2.7 Characterisation of foam stability and destabilisation

2.7.1 Parameters associated with foam stability and instability

Foam stability and instability science is complex. Foam can be characterised by various parameters – e.g., the dynamic foam test, where foam height is tested against time, surface rheology, surface tension, conductivity, bulk viscosity, and/or foam drainage, which can be measured by foam dispersion imaging procedures (Sakker et al., 1997). The parameters used vary with the distribution of gas molecules in the liquid. In the foam decay test, foam is produced mechanically by air sparging, agitation, and pouring (Iglesias et al., 1995). The Ross-Miles simple method is conducted by pouring a foaming solution at a definite height through a minute aperture of known diameter while measuring the foam's height over time. The amount of gas introduced into the solution, i.e., the gas dispersion rate, cannot be controlled (Ross & Miles, 1941). Pneumatic methods that measure the amount of gas distributed through the solution also exist but are time-consuming and unusable as standard procedures (Pinazo et al., 2001). Lunkenheimer et al. (2010) measured foam's rheological characteristics under defined gas dispersion and applied deviation and transition time simultaneously by measuring the changes in foam volume and foam drainage. Deviation and transition time characterise different stages of foam decay, of which there are three: the initial stage when the lamellae are still unruptured, described by Equation 2.1:

$$\frac{\Delta h^F}{\Delta h^S} = 1 \text{ and/or } \Delta h^F - \Delta h^S = 0 \qquad (2.1)$$

Whereby any level changes of the foam/air (Δh^F) or the solution/foam (Δh^S) boundaries can be quantified simultaneously as a function of time. When the foam drainage and lamellae rupture, the transition stage occurs concurrently – Equation 2.2 – and the ratio between the changes in foam/or air and solution/ foam must exceed unity.

$$\frac{\Delta h^F}{\Delta h^S} > 1 \text{ and/or } \Delta h^F - \Delta h^S > 0 \qquad (2.2)$$

If in the final stage, lamellae rupture is dominant and negligible, the liquid is drained from the foam, and Equation 2.3 applies.

$$\frac{\Delta h^F}{\Delta h^S} \geq 1 \text{ and/or } \Delta h^F - \Delta h^S \geq 0 \qquad (2.3)$$

The initial deviation time (t_{dev}) occurs towards the end of the initial stage whereas the time transition (t_{tr}) occurs during the transition and final stages. For unstable foams t_{tr} is < 10s, for stable foams it exceeds 10s, or 100s for very stable foams (Lunkeinheimer et al., 2010). Stable foam crust can also occur in the presence of biofoamers -e.g., *M. parvicella* and *N. amarae* where t_{tr} >100s. The Ross-Miles foam height test can be applied with minor modifications and is still used as a standard operating procedure despite its drawbacks.

2.7.2 Factors affecting foam stability and destabilisation

Foam stabilisation and destabilisation can be controlled by many factors including liquid surface tension, surface viscosity, lamellae rupture, surface elasticity, disjoining pressure, critical micelle concentration and foam drainage. Increases in viscous film thickness, surface viscosity, and/or critical micelle concentration, like decreases in intact lamellae or disjoining pressure, lead to bubble deflocculation, and minute thin liquid film drainage, and stabilise the foam. Table 2.3 lists the major factors that affects foam stability and destabilisation.

Table 2.3: Factors affecting foam stability and destabilisation

Factors	Foam stability	Foam destabilisation	References
Surface tension	Decreases due to hydrogen bond disruption resulting in increased interfacial area and energy	Increases due to the undisrupted hydrogen bonds, resulting in decreased interfacial area and energy	Pradhan & Bhattacharyya (2017)
Surface viscosity	As viscous modulus increases, the surface viscosity also increases	Viscous modulus and surface viscosity decreases	Wang et al. (2019)
Lamellae film	Electrical double layer is formed, repulsive forces are produced to stabilise the lamellae	Lamellae rupture and results in bubble drainage	Keal et al. (2016)
Surface elasticity	Increase in elasticity elongates foam life	Decreased elasticity reduces foam life	Wang et al. (2016)

Cont: Table 2.3

Disjoining pressure	Strong attractive interactions between the liquid and gas phases strengthen the interfacial film so that it remains intact	Weak repulsive disjoining pressure causes rupture of the gas-liquid film.	Schramm (1994)
Critical micelle concentration (CMC)	Increased beyond CMC	Falls below CMC	Malysa et al. (2008)
Foam drainage	Bubble deflocculation leads to decreased rate of bubble collision. This lowers the pressure exerted on the thin liquid film and minute liquid drainage.	Bubble flocculation causes the thin liquid film to break. The pressure in the lamellae is lower than that inside the bubble, causing the film to rupture, which increases liquid drainage	Narsimhan & Xiang (2018)

2.7.3 Factors enhancing foam stability in wastewater

2.7.3.1 Influences of wastewater characteristics on foam formation and stability

Foam is formed by gas dispersion and aqueous surfactants (Osei-Bonsu et al., 2015) and/or biosurfactants (Santos et al., 2016). The surfactants prevent bubble coalescing and reduce the wastewater's surface tension (Malysa et al., 2008). Foam stability is determined by assessing foam height or volume with generation time (Osama, 2014). Foam stability and foamability are co-related because a stable foam means that the solution has high foamability. Surfactant concentration up to the critical micelle concentration (CMC) triggers foam formation under reduced surface tension conditions (Malysa et al., 2008). Foam stability also depends on the foam film's electric double layer, bubble drainage by gravity, surface elasticity, and bulk viscosity (Osama, 2014).

The disjoining pressure difference is the total pressure variation between the gaseous and aqueous phase within a film and is highly dependent on film thickness, which, in turn, is influenced by the surface tension (Schramm, 1994). The difference arises from repulsive electrostatic and attractive van der Waals forces (Derjaguin & Landau, 1993). The van der Waals forces arise from the induction of dipole-

dipole interactions that dominate in the absence of surfactants, with the disjoining pressure within the film being reduced (Derjaguin & Landau, 1993). Any surfactants present penetrate the gas-liquid film and create an electrical double layer. Subsequently, repulsive forces are generated and stabilize the lamellae, which means that the wastewater's ionic strength is crucial for foam stability (Almajid & Kovscek, 2016).

The presence of proteins contributes to the uniform distribution of bubbles, and they stabilize foam at low concentration, i.e., 0.1% (Halling, 1981). Soluble proteins diffuse to the air-water interface and reduce surface tension (Narsimhan & Xiang, 2018). Their polar groups attach to the aqueous phase while their hydrophobic groups attach to the non-aqueous phase (Fameau & Salonen, 2014). They are adsorbed at the lamellae and stabilize foam formation by reducing interfacial tension, increasing the liquid phase's viscosity and elasticity, and strengthening the film; however, this depends on the temperature, pH, and protein concentration (Zayaz, 1997). Proteins are surface-active, yielding wet foam and reducing foam drainage in the presence of other surface-active agents. The quaternary structure of the proteins present can lead to foam formation in reactors, so it is important that its constituents are known. The quaternary structure of proteins contains more than one polypeptide chain based on their amino acid sequence. A protein structure is stabilized by hydrogen, ionic, and disulfide bonds (Willey et al., 2008), with the disulfide bonds stabilizing the foam at the interface if not disrupted (Zayaz, 1997).

The effects of oil on foam stability are also complex and influenced by many factors such as the lightness or thickness of the FOG. Tang et al. (2018) state that light oil in wastewater disrupts foam whereas thick FOG stabilises foam in the presence of surfactants. Some studies showed that emulsified FOG lengthens foam life and that a pseudo-emulsion film (the film between air and oil droplets) can be used to determine the foam stability thermodynamics (Tang et al., 2018). The length of the FOG-hydrocarbon chains in the wastewater also affects foam stability. Shorter chain hydrocarbons adsorb into the foam's liquid-gas interface disrupting the film, which, in turn, disrupts the lamellae leading to foam coalescence (Jones et al., 2016). However, long-chain hydrocarbons stabilise the foam. At high surfactant concentrations, long half-life foam films are stable because the disjoining pressure decreases, leading to slower gas-liquid film disruption.

2.7.3.2 Surfactants' influence on foam stability

Surfactants, which can be ionic, cationic, and non-ionic, have been applied widely, e.g., in the pharmaceutical, food, and petroleum industries (Osei-Bonsu et al., 2017). They have been used for flocculation, foaming, and de-emulsification (Mulligan, 2005), and can increase detergent power, wetting ability, and foaming strength (Mulligan & Gibbs, 1993), as well as to solubilise FOG, enhance the solubility of polar substances, reduce surface tension, lower the CMC, and reduce interfacial tension

(De Almeida et al., 2018). The critical CMC is influenced by the surfactant's strength (hydrophile-lipophile balance (HLB) number), pH, temperature, and ionic strength (Rosen & Kunjappu, 2013). Surfactants may generate unstable foam in the presence of FOG, but it has been shown that stable foam can be generated in such circumstances when a surfactant with long hydrocarbon chains is used (Yekeen et al., 2016). The liquid-film thinning is caused by FOG influences spreading on the gas-liquid interface (Derjaguin & Landau, 1993), thus affecting foam stability mechanisms. Foam stability is affected by FOG because it enters and spreads across the gas-liquid interface and an unstable bridge can be formed that could cause lamellar rupture. FOG spreading across the foam film can also result in pseudo film instability. Foam stability in the presence of FOG can be described by Equations 2.4, 2.5 and 2.6:

$$\mathrm{E} = \sigma_{\mathrm{gw}} + \sigma_{\mathrm{ow}} - \sigma_{og} \tag{2.4}$$

$$\mathrm{S} = \sigma_{\mathrm{gw}} - \sigma_{\mathrm{ow}} - \sigma_{og} \tag{2.5}$$

$$B = \sigma_{\mathrm{gw}}^2 + \sigma_{\mathrm{ow}}^2 - \sigma_{og}^2 \tag{2.6}$$

Where σ_{gw} is the surface tension between the gas and liquid film, σ_{ow} is the surface tension between the FOG and liquid, while σ_{og} is the interfacial tension between the FOG and gas phase (Simjoo et al., 2013).

If *E* is positive, the FOG can enter the liquid-gas interface. If *S* is positive, the FOG droplet stretches and spreads in the liquid gas layer and cause the thinning and rupture of the foam film. If *S* is negative, the FOG will form a lens and the liquid gas interface will not rupture; however, an unstable bridge (*B*) that can destabilize foam in some circumstances can be created.

2.7.3.3 Impact of biofoamers in stabilising excessive biofoam

Biofoamers affect AS systems globally and many attempts have been made to determine the predominant biofoamers so that control strategies can be developed. FOG is the major contributor to biofoam stability because it can be biodegraded and assimilated by the biofoamers (Cisterna-Osorio & Arancibia-Avila, 2019; Almajid & Kovscek, 2016; Osei-bonsu et al., 2017). Foam stability depends not only on the hydrophobicity of the cells of biofoam-producing organisms, but also on the presence of solids, the filaments attach to suspended solids and float on the wastewater surface (Fryer et al., 2011). In gram-negative organisms, cell lipopolysaccharides and phospholipids are the main contributors to cell hydrophobicity, whereas, in gram-positive organisms, polypeptides enhance hydrophobicity, which influences filament formation and nutrient uptake. The nutrients present in the wastewater are also major contributors to foam formation. During starvation, the polysaccharide slime capsules of the filaments are lost due to carbon source limitations. Hence, in the presence of poor hydrophobic cells

and low uronic acid concentrations, the foam surface can become unstable. The presence of uronic acid is an indicator of phosphorus deficiency in gram-positive microorganisms and a substitute for polyol phosphate chains of the teichoic acids, required for filament formation (Miłobędzka et al., 2016).

2.7.3.4 Effect of biosurfactants in excessive biofoam stability

Biosurfactants are surface-active biomolecules that are produced by microorganisms during their growth from various nutrient sources, e.g., sugars, oils, alkanes, etc. (Lin, 1996). Biosurfactant CMC varies from 1 to 200 mg/L, and it is relatively better than that of synthetic surfactants because biosurfactants are biodegradable (Osei-Bonsu et al., 2017). Microorganisms excrete biosurfactants during nutrient reduction in wastewater, e.g., during the reduction of nitrogen availability, with an example being *Pseudomonas aeruginosa* which produces rhamnolipids under nutrient limited conditions. Other microorganisms produce biosurfactants to emulsify and take up the lipids and fatty acids in FOG that are readily available in the wastewater. Actinomycetes have been found to produce surface-active lipid molecules in AS that lower surface tension (Zhang et al., 2018). They also produce EPS or by-products such as biosurfactants that enable them to solubilise, biodegrade, and emulsify the hydrophobic material as their carbon and nitrogen source. Actinomycetes such as *N. amarae* in conventional AS produce sufficient biosurfactants to form foam. The *N. amarae* cells and biosurfactants contribute to foam stabilisation in AS systems (Pagilla et al., 2002).

2.8 Factors that influence foam destabilisation in wastewater

2.8.1 Conditions associated with foam destabilisation

Foams are thermodynamically unstable and rupture easily if bubbles coalesce (Pajdak-Stós et al., 2017), with rupturing occurring as the gas-liquid film thins. Many techniques have been employed to stabilize foam, but they are not suitable for AS systems in which foam is an unwanted nuisance (Fryer et al., 2011). The presence of dissolved solids in the wastewater may stabilize or destabilize foam. Soluble solids in the micelle may make foam stable because of their agglomeration in the gas-liquid interphase, leading to a need for the presence of hydrophilic substances to destabilize the foam (Garett, 2014; Miller, 2008). The lamellae in the foam can also rupture due to bridging (Rafati et al., 2016).

Foam decay behaviour, gravity drainage, bubble coalescence, and the lamellae number, should all be considered for foam destabilisation (Pajdak-Stós et al., 2017). Foam can be destabilized by silicone and oils that contain short alkane chains which solubilize in the micelle, further reducing micelle volume and the repulsive forces between the micelle, diminishing stratification in the foam film, and leading to faster foam destabilisation (Hill & Eastoe, 2017). Spreading of the oil in the gas-liquid plateau (lamellae connection points) increases lamellae thinning and leads to foam destabilisation and bubble film

deformation, which ultimately lead to foam instability and disjoining pressure differentiation. The pressure differentiation increases foam decay as the lamellae thins. Svarz (1990) invented a good antifoam/defoamer consisting of a polyether surfactant and polyhydric alcohol fatty acid ester. However, its constituents, which are toxic to microorganisms, could damage the environment and reduce sludge efficacy (Conley & Kabara, 1973).

2.8.2 Defoamer impact on foam destabilisation

Antifoamers are used to prevent foam generation, whereas defoamers reduce foam that already exists. These terms are sometimes used interchangeably. For example, Denkov et al. (2014) describe defoamers as chemicals used to collapse foam that incorporate various short-chain alkane oils and hydrophobic molecules, while antifoamers prevent unwanted foam from forming (Gastrock & Heid, 1938). Prevention of foam dates back to the 1930s when mechanical devices, e.g., skimmers, etc., that consume a large amount of energy were used. In the late 1940s, chemical methods were introduced, including the use of essential oils, kerosene, and alcohol. For this reason, post 1970, oils and hydrophobic particles have been used as defoamers (Gunderson & Denman, 1948; Jacoby & Bischmann, 1948; Ross & McBain, 1944).

Although a wide variety of biodefoamers have been commercialised, they are not suitable for all systems and their composition is not always clearly outlined, which makes it difficult to determine a suitable defoamer for any particular system. Even when this has been done, the defoamer might deteriorate in the system, especially when environmental conditions vary; a trait of open-air biological processes, e.g., AS, systems (Mangundu, 2017). Therefore, a defoamer's mechanism must be determined, i.e., whether it imparts defoamation through bridging and/or stretching. Under normal circumstances, a defoamer enters the FOG-water and gas-liquid interface, and the FOG droplet is spread across the interface, forming a bridge that stretches in all directions and causing a rupture at its centre (Figure 2.1). Since the FOG droplet is hydrophobic when it enters the foam interface, the interface dehydrates. A higher defoamer concentration is then required for it to be efficient. Defoamers can also reduce AS efficiency, reducing the ability of microorganisms to degrade foam and use it as a carbon source. Few microorganisms can degrade FOG constituents in sludge containing LCFAs (Kougias et al., 2015).

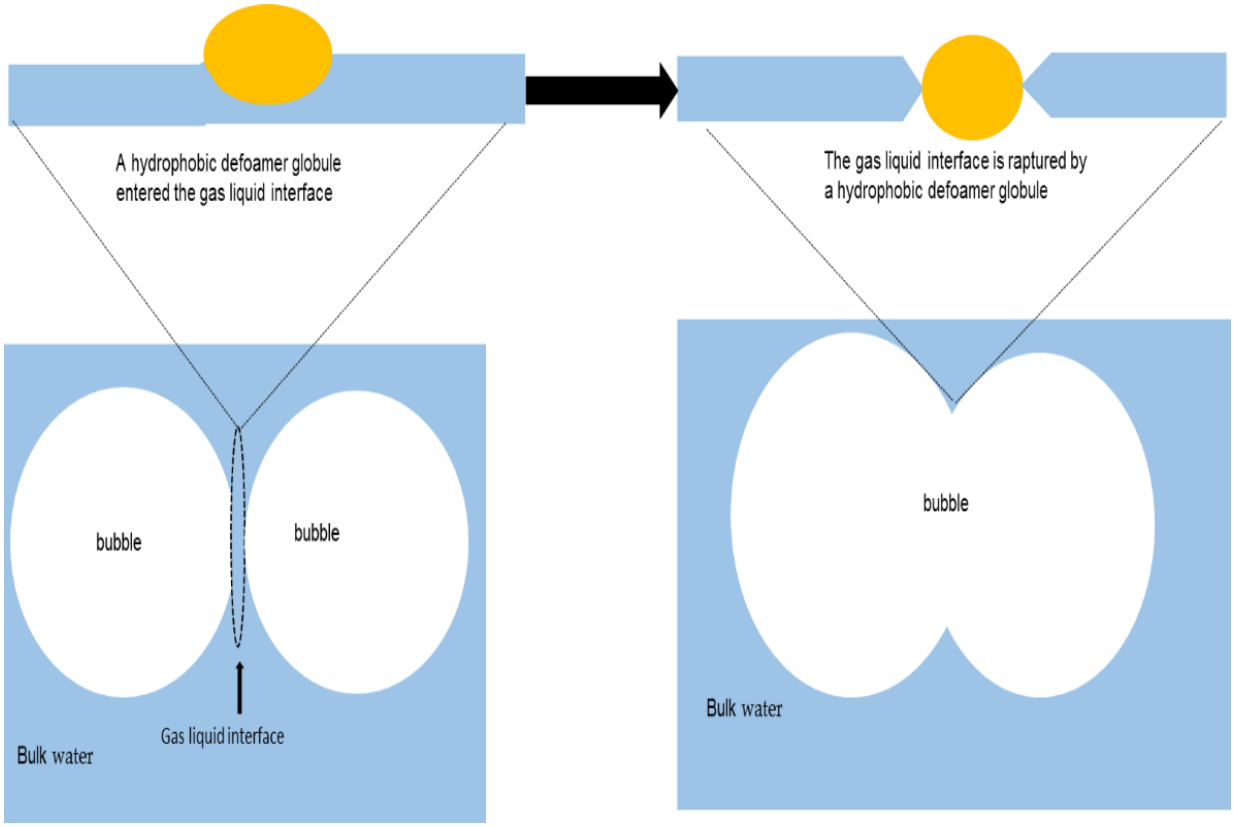

Figure 2.1: Rupture of a gas-liquid interface by a hydrophobic defoamer

Chemical-based defoamers are added to surfactants to reduce detergency, i.e., foam formation, but yield by-products that cannot be biodegraded and are toxic (Cook et al., 1997; Brown et al., 2005). Brown et al. (2005) invented an efficient defoamer containing halogens, epoxy oxygen and an alkyne group. However, halogens are highly reactive, corrosive, and toxic to aquatic life (Pourmoghaddas & Stevens, 1995). Surfactants containing a non-silicone type anti-foaming agent such as polyether might also be unsuitable for large-scale use due to their toxicity and/or relatively low levels of solubility at low temperatures (Jin et al., 1997). The use of synthetic defoamers such as polyhydric alcohol fatty acid esters destabilise AS systems (Denkov et al., 2014). Many defoamers/antifoamers may be efficient but Pitt & Tenkins (1990) confirmed that microorganism-produced foams are resistant to chemical antifoamers, thus biodefoamers may be required.

2.8.3 Foam destabilisation by biodefoamer application

Biodefoamers are environmentally benign and biodegradable when compared to silicone- or oil-based defoamers. They are based on agricultural oils or EPS (microbial polymers secreted by the cell) constituents of microbial origin which contain no fats. They are dioxin precursor compliant and non-toxic (Bajpai, 2017). Their major advantages include improved bubble drainage and reductions in chemical and energy use, and they can be added directly to the AS aeration basin.

Microorganisms can also produce polymers intra- and/or extra-cellularly that can play a definite role in biodefoamer production. In oily wastewaters, such microorganisms can be isolated to produce EPS independent of the AS system, with their bioproducts being concentrated for use as defoaming agents. If a microorganism from oily wastewater is used to treat the same wastewater, that ecosystem will usually be harnessed and become undisturbed within that treatment system.

2.8.4 Quantifying biofoam destabilisation kinetics

Mathematical models of foam destabilisation are required, because foaming mechanisms are complex, and such models will provide a better understanding and optimisation of the foam destabilisation process and the opportunity to determine foam destabilisation efficiency. Studies of foam destabilisation kinetics will improve understanding of the processes causing foam decay, liquid drainage disproportionation, and foam collapse when a biodefoamer is used. Liquid foam destabilisation occurs when the lamellae become thin, thus causing the bubbles to disintegrate, leading to liquid drainage. Gas entrapment in a bubble can also be disproportionately higher than atmospheric pressure, potentially causing bubble bursts. Sceni & Wagner (2007) noted that some mechanisms, which can be described using defoamation kinetic models, occur concurrently because of the breakage of the interfacial film, which results in the foam collapsing. They studied the destabilisation kinetics of sodium caseinate dispersion in foam using multiple-scattering, quick-scan, optical microscopy, and traditional volumetric analysis. A kinetic model for estimating liquid drainage and foam collapse was then formulated (Equation 2.7):

$$\alpha_{(t)} = \alpha_{max} \frac{t^n}{t^n + t_{1/2}^n} \qquad (2.7)$$

Where: $\alpha(t)$ is the volume of liquid drainage as a function of time, α_{max} is the maximum volume of drained liquid, n is the sigmoidal character of the curve, and $t_{1/2}$ is the half-life of drainage or collapse (the time needed to drain half of the maximum volume) (Sceni & Wagner, 2007; Delgado-Sánchez et al., 2017).

This method can be used for foam collapse kinetics with the area $\alpha(t)$ of collapse as the function of time and α_{max} as the maximum area of the collapse both of which can be estimated. Equation 2.8 can also be fitted to kinetic profiles generated using a multiple-scattering quick-scan and data obtained using optical microscopy under different defoamer concentrations (Jin et al., 1997).

$$BS_{(t)} = \mathrm{a} + \mathfrak{b}(-t \,/\, k) \tag{2.8}$$

Where: $BS_{(t)}$ is backscattering as a function of time *t*. $a + b$ is the proximity of $BS_{(max)}$, and *k* is inversely proportional to the $BS_{(t)}$ fall rate.

Only chemical- and FOG-based defoamer destabilisation kinetics have been studied to date, with no biodefoamer studies reported. To elucidate defoamer globule influences on foam destabilisation kinetics, a pneumatic defoamer movement must also be understood as bubbles under turbulence float defoamer globules pneumatically. Foam bubbles aggregate in the presence of defoamer globules, which is what determines bubble longevity. Defoamer efficiency can thus be estimated by quantifying the ratio (*F*) of the foam volume (V_1/V_2) generated in the presence of the defoamer (V_2) in comparison with foam volume (V_1) generated in the absence of a defoamer (Equation 2.9). The parameters required for Equation 2.9 are: bubble size distribution [*P(rb)*] and the probability of bubble persistence (*qiCiY(rb)Zi*) for a bubble with the radius r_b that is bound to antifoam droplets (*CiY(rb)Zi*). Similarly, the concentration of the defoamer droplets (*Ci*) of specie *i*, and the function of bubble size dissemination, *Y(rb)*, including the average length of the mono bubble (*L*) during mixing (*Z*), are all required. Defoamer globule dispersion during mixing is quantified according to size which can also be estimated as $\left({}^{4}/_{3}\right)\pi\rho \int_0^\infty \mathcal{X} r_i^3 \, dr_i$, where *r* is the size of a defoamer aggregate of specie *i*, and *P* the defoamer's average density.

$$F = \frac{V_2}{V_1} = \frac{\int_0^\infty P(r_b) r^3 {}_{bq_i} CiY(r_b) Z \, dr_b}{\int_0^\infty P(r_b) r_b^3 \, dr_b} \tag{2.9}$$

Usually, some of this model's functions are unknown, e.g., *Zi*, *qi*, *P(rb)*, *Y(rb)* but they can be used to understand the experimental data (Karakashev & Grozdanova, 2012).

2.9 Conclusion

Foam can be removed or reduced in various ways, i.e., using physical, chemical, and/or biological methods in AS systems. All these methods, however, have limitations. Physical methods often require additional and costly WWTP equipment, while chemical dosing can reduce microbial (AS) system efficiency over time. Therefore, biocontrol methods for foam formation might be appropriate as they are generally environmentally benign and can be applied in full-scale WWTPs. Bacterial cells and their intra- and extra-cellular polymeric bioproducts can be used as bio-controllers to reduce foam generation.

Such microorganisms can be isolated from the wastewater to be treated so that, once harnessed to produce defoamers, there are no negative effects on the wastewater treatment system. This in turn will improve WWTP operability while reducing the abundance of the microbial filaments that provide the buoyancy of the foam-producing microbial populations in WWTPs. Future biodefoamer application in different wastewater treatment apparatuses could lead to advances in WWTP designs. The current study proposes the use of biodefoamers instead of chemical defoamers in activated sludge treatment systems.

CHAPTER 3

METHODS AND MATERIALS

CHAPTER 3

METHODS AND MATERIALS

3.1 General introduction

The experiments were divided into 4 phases such that the aim and objectives in Chapter 1 were achieved and the research questions were properly answered.

3.2 Phase 1: Isolation, optimisation, consortium development, and biodefoamer production

The aim of this phase was to isolate and assess the foam reduction efficiency and foam collapse rate of the biodefoamer, i.e., as produced by a consortium of isolates identified to produce biodefoamers in the presence of MLSS and a PSW microbial community.

3.2.1 Isolation and identification

The isolates were collected using sterile swabs from a PSW discharge spout of a commercial poultry producer (Cape Town, South Africa). Serial dilutions were performed and the nutrient agar plates were inoculated using the swabs by a spread plating technique subsequent to incubation at 37˚C overnight. Thereafter, they were cultivated into fresh nutrient agar plates, and the agar plates with pure colonies were stored at 4˚C and recultured daily for further experiments, and the pure cultures (n = 9) were subjected to mixed liquor suspended solids (MLSS) prior to biofoam generation to determine their efficiency with regard to foam reduction efficiency and foam collapse. Of the identified isolates, some (n = 4) were highly efficient; they were gram stained and viewed under a microscope to determine their gram reaction. The pure culture plates were sent to Inqaba Biotechnical Industries (Pty) Ltd (Muckleneuk, Pretoria, South Africa) for DNA analysis and identification. The DNA of the pure isolates was extracted using the Quick-DNA Fungal/Bacterial Miniprep Kit (Zymo Research, Irvine, California, USA, Catalogue No. D6005). The 16S rRNA target region was amplified using OneTaq® Quick-Load® 2X Master-Mix (New England Biolabs, Ipswich, Massachusetts, USA, NEB Catalogue No. M0486) with primers 16S-27F and 16S-1492R with the sequence (5'-3') AGAGTTTGATCMTGGCTCAT and CGGTTACCTTGTTACGACTT, respectively.

The extracted fragments were sequenced in both the forward and reverse directions using NimaGen BrilliantDye™ Terminator Cycle Sequencing kit v3.1, (NimaGen B.V., CG Nijmegen, Netherlands, BRD3- 100/1000), and were purified by Zymo Research ZR-96 DNA Sequencing Clean-up Kit™

(Zymo Research, Irvine, California, USA, Catalogue No. D4050). The purified DNA fragments were analysed on the Applied Biosystems™ 3500xL Genetic Analyzer (Applied Biosystems, Waltham, Massachusetts, USA) for each sample. A Qiagen CLC Main Workbench (Hilden, Germany, v7.6) was used to analyse the ab1 files generated by the ABI 3500xL genetic analyser and the results were obtained by a Basic Local Alignment Search Tool (BLAST) search provided by the National Centre for Biotechnology Information (NCBI, http://www.ncbi.nlm.nih.gov).

3.2.2 Metagenomics analysis of the MLSS microbial community

From the MLSS samples collected using 4 L polypropylene bottles (n = 9) from an aeration tank of a WWTP near Cape Town, South Africa, 100 mL of the MLSS samples was filtered through a 0.22 µm millipore membrane filter (Merck Millipore, Burlington, Massachusetts, USA) and the cells were re-suspended in 5 mL sterile millipore water for DNA extraction. DNA was extracted from the suspension solution using commercially available DNA extraction kits (Promega, Madison, Wisconsin, USA), using the manufacturer's instructions. The 16S rRNA target regions were sequenced and amplified using a OneTaq® Quick-Load® 2X Master-Mix (New England Biolabs, Ipswich, Massachusetts, USA, Catalogue No. M0486) with the primers 16S-27 F and 16S-518 R with the sequence (5-3) AGAGTTTGATCMTGGCTCAG and ATTACCGCGGCTGCTGG respectively. Moreover, the V1 and V3 targeted sequences were used for PCR amplification of the purified DNA sequence. The PCR amplicons were sent for sequencing at Inqaba Biotechnical Industries (Pty) Ltd (Muckleneuk, Pretoria, South Africa.

The purified PCR amplicons were gel purified and repaired and the amplicons were sequenced on the PacBio Sequel II system (Pacific Biosciences Inc, California, USA). Raw subreads were processed through the SMRT(R) Link (v9.0) Circular Consensus Sequences (CCS) algorithm which estimates/computes consensus sequences to produce highly accurate reads (>QV40). These reads were then processed through Vsearch (https://github.com/torognes/vsearch) and taxonomic information was determined based on the QIIME 2™. The results were acquired through basic local alignment search tool (BLAST) provided by the National Centre for Biotechnology Information (NCBI, http://www.ncbi.nlm.nih.gov). The sequences were further deposited into the national NCBI and the sequence read archive (SRA) databases before acquiring the accession numbers of single species.

3.2.3 Biodefoamer production and extraction

The pure culture isolates (n = 4) growing on nutrient agar plates were all inoculated as a consortium in nutrient broth (50mL) where conical flasks (250 mL) were used and subsequently incubated at 37°C for 24 h at 120 rpm (Labwit ZWYR-240 shaking incubator, Labwit Scientific, Burwood East, Vic.,

Australia) to produce a seed culture. A volume (1mL) of the 24 h old seed culture in the form of a consortium was inoculated into 99 mL of nutrient broth to a final volume of 100 mL in 250 mL conical flasks and further incubated at a temperature of 37°C at 120 rpm for 24 h. Thereafter, 15 mL of each sample was centrifuged (Hermle-Z233M-2 centrifuge, Labortechnik GmbH, Wasserburg, Germany) at 15 000 rpm for 30 min to sediment the cells and the supernatant was extracted and used as a crude biodefoamer. All experiments were done in triplicate.

3.2.4 Response surface methodology

Response surface methodology (RSM) was used to determine optimum pH and concentration for the biodefoamer production, i.e., foam reduction efficiency and foam decay rate, for either the bio- or synthetic defoamers. Foam reduction efficiency and foam decay rate were the output variables. The design of experiments in RSM was used to generate various experimental conditions (pH 7-10) and concentration (1-4 % v defoamer/ v MLSS and PSW mixture) (Deval et al., 2017; Bukhari et al., 2020). A two-factor, 5-level central composite design with 13 experimental runs was carried out. A t-test was conducted to evaluate the statistical importance of the regression coefficient to be utilised to estimate biodefoamer production and a Fisher (F) test was employed to ensure the precision of the model obtained, i.e., to describe optimal conditions for biodefoamer production. The determination coefficient (R^2) was determined to assess the appropriateness of the model which described optimal biodefoamer production. See Table 3.1 for coded levels and description.

Table 3.1: Media constituents included in central composite design (CCD) experiments and their corresponding high, medium and low pH and concentration

Variables	Code	Units	High level (+)	Medium (0)	Low levels (-)
pH	A	-	10.60	8.50	6.30
Concentration	B	% (v/v)	4.60	2.50	1.00

3.2.5 Foaming behaviour tests

3.2.5.1 Foam reduction efficiency

The PSW used in this study was collected from a slaughterhouse near Cape Town, South Africa, using 25 L polypropylene bottles, transported to the laboratory at 4°C and used when received. A volume (100 mL) of PSW and mixed liquor suspended solids (MLSS) at a ratio of 1:2 was added to 250 mL graduated cylinders (foaming reactor see Figure 3.1 and the specification of this reactor are tabulated on Table 3.1) subsequent to pneumatic mixing through air sparging using Mott element 6500 diffusers (Mott element 6500, Mott Corporation, New York, United States of America) at 40 mL/min. Thereafter, foam was generated by sparging air using a Resun air pump (Resun Ac 9906, Shenzhen

Xing Risheng Industrial Co. Ltd., Baolong, China) attached to an airflow meter (Key instrument FR 2000 series, Rhomberg instruments, Cape Town, South Africa) at 80 mL/min until 82 mL of foam was generated. The foam volume (measured using graduated cylinder) was recorded against time using a stopwatch (foam volume generation was recorded at 40sec intervals). The foaming behaviour was compared using foaming tendency (FT) and the foam reduction efficiency (FRE) and foam collapse rate (FCR) – see Equation 3.1 and 3.2. This method was used without modification as reported elsewhere (Kougias et al., 2014).

$$FT = \frac{Foam\ genererated\ immediately\ after\ aeration\ (mL)}{Rate\ at\ which\ air\ is\ sparged\ into\ the\ sample\ (\ ^{mL}/_{min}\ )} \quad (3.1)$$

$$FRE\ (\%) = \frac{(1-FT\ of\ a\ sample\ with\ defoamer)}{FT\ sample\ without\ defoamer} \times 100 \quad (3.2)$$

3.2.5.2 Foam collapse (decay) rate

For the foam collapse rate (FCR) (Equation 3.3), a method by Mangundu (2017) was used with minor modifications. A volume (100 mL) of PSW and mixed liquor suspended solids (MLSS) at a ratio of 1:2 was used as in the previous section (3.2.5.1). This mixture was placed in a foaming reactor (250 mL graduated cylinder). The height of the mixture was measured before the generation of foam. To thoroughly mix the PSW and MLSS, 40 mL/min of air was sparged through a porous air diffuser. The foam was generated by sparging air at a flow rate of 80 mL/min until a foam height of 13 cm was generated. Foam height collapse rate in the graduated cylinder was measured as a function of time using a stopwatch. The air pump (Resun Ac 9906, Shenzhen Xing Risheng Industrial Co. Ltd., Baolong, China) was switched off for 40 sec such that the foam and liquid layer were distinguishable. A 4 % (v/v) of synthetic defoamer, i.e., active silicone polymer antifoam A (A6582, Sigma Aldrich, Unit 16/17 Lake Site, Industrial Park, Jet Park, SA), determined to be an efficient defoamer for WWTPs, was used at different pH and defoamer concentrations that were generated by the RSM in combination with the PSW/MLSS mixture. Thereafter, 40 mL/min of air was sparged through the samples again for mixing and the foam collapse rate was measured every 10 sec until the foam had decayed. If not, the foam height was regenerated in repeat tests. These tests were performed using triplicate samples and an average of the samples was used to generate experimental data.

$$FCR(^{mm}/_{s}) = \frac{foam\ in\ the\ column\ after\ sparging}{time\ taken\ to\ collapse\ the\ entire\ foam} \quad (3.3)$$

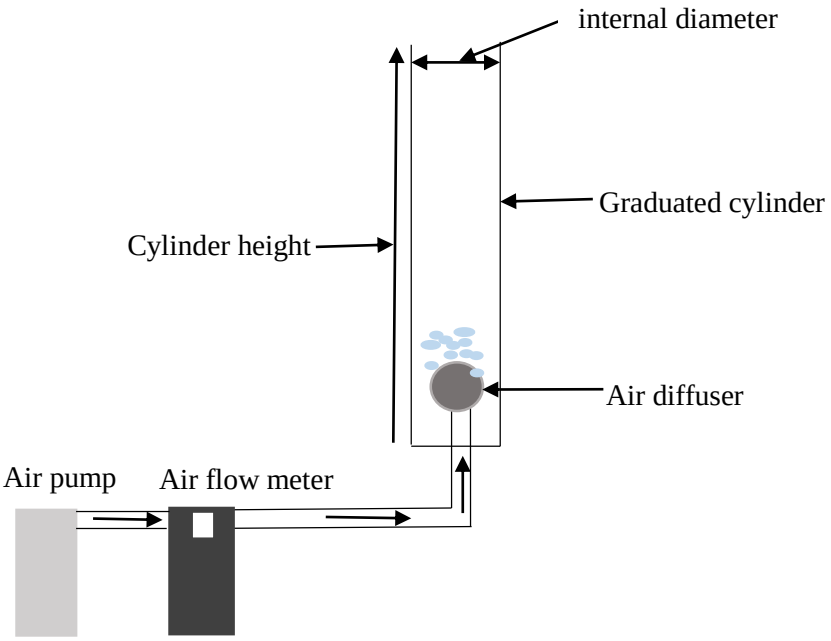

Figure 3.1: Aeration column reactor set-up

Table 3.1: Foaming assessment specifications

Dimensions	**Specifications**
Cylinder	
Material	Polypropylene
Height	24.5 cm
Diameter	3 cm
Air flow rate	80 mL/min
Diffusers	
Porous length	2.32 cm
Porous diameter	1.2 cm
Media grade	40
Porous material	316LSS

3.2.6 Microscopic analysis of sludge agglomeration in the presence and absence of bio- and synthetic-defoamers

AS samples were collected from a WWTP (Cape Town, South Africa) using 4 L polypropylene bottles. The sludge samples were taken from the aeration tank, and they were transported to the laboratory. To ensure aerobic conditions, the sampling polypropylene bottles were partly filled (one-third) and tightly closed subsequent to refrigeration at 4°C. Prior to experimental tests, the bottles were swirled to mix the sludge, and the agglomerated biomass was analysed according to Eikelboom et al. (2000). The filamentous microorganisms observed were compared with the images that were depicted in the method, and a filamentous index (FI) (the size of filamentous bacteria population observed using a microscope, 0-5 non-numerous filaments) was quantified. An experiment was conducted to observe the effect of the biodefoamer and synthetic defoamer on the AS filamentous bacteria. To observe this effect, a 96 well tissue culture plate (Corning® 96 well clear polystyrene microplates, Merck, New Jersey, United States of America) was used, with 4 wells serving as a control. The experiment was conducted such that 200 µL of the MLSS was mixed with160 µL of sterile PSW that was filtered through a 0.22 µm membrane filter and added to the 4 wells. Thereafter, a volume (245.6 µL) of the MLSS was added to each well after which 100 µL of the sterile PSW was added in the subsequent wells (n = 8). Out of the 8 wells, 4 wells were supplemented with 14.4 µL of the biodefoamer whereas the other 4 were supplemented with 14.4 µL of the synthetic defoamer. This was followed by incubation at 37°C for 10 days. Thereafter, 25 µL of each of the samples was extracted from each well on days 0, 5, and 10. The samples were gram stained and viewed under a light microscope (Olympus CX21FS1 microscope, Olympus Corporation, Tokyo, Japan) at 1000X. The microscope was connected to a computer running Dino Capture 2.0 software using a 4000 µm and 10 µm scale bar. This was to observe the effect of each defoamer on the MLSS microbial population.

3.2.7 Characterisation of the biodefoamers

The consortia were further cultured in the aforementioned biodefoamer production media and incubated for 48 h at 120 rpm at an optimum pH and temperature determined using RSM. Thereafter, the consortia were put on ice and centrifuged at 10000 rpm for 30 min, with the supernatant being collected for processing using ethanol (4°C) at a ratio of 2:1 (v/v), that is, alcohol: supernatant, followed by shaking the mixture at 121 rpm at 4°C overnight to produce a precipitate. The precipitate was then collected and re-centrifuged using a benchtop centrifuge at 15 000 rpm for 30 min. This procedure was repeated (n = 3 times) to collect a substantial quantity of the precipitate for each sample, after which the precipitate was washed using sterile distilled water and dialysed against the water overnight prior to vacuum drying in a desiccator for 24 h. The dried precipitate was analysed using

a Fourier transform infrared spectrophotometer (FTIR) (Spectrum Two, PerkinElmer, Waltham Massachusetts, United States of America). Additionally, nuclear magnetic resonance spectroscopy analysis was conducted using the purified and dried precipitate by dissolving it in 1 mL of deuterium oxide (D_2O) followed by swirling for 5 min and left overnight at ambient temperature. The swirled solution was then transferred into a 5 mL tube which was then capped and analysed using ^1H NMR (Bruker 400, Bruker Nano GmbH, Berlin, Germany) at a frequency resonance of 400 MHz.

3.3 Phase 2: Assessment of the compatibility of existing mathematical models to assess biodefoamer performance

This phase was aimed at comparing existing mathematical models and their ability to predict biofoam defoamation. Firstly, by generating data for foaming potential, foam stability including destabilisation and secondly thereafter, using the data to determine kinetic model parameters, i.e., rate constants which were applied to reproduce the profile of the phenomena under assessment.

3.3.1 Batch culture experiments

Isolates n=4 that were growing on nutrient agar plates were inoculated as a consortium into a 50 mL that was containedn a 250 mL conical flask as inin which was incubated at at 37°C for 24 h at 120 rpm (Labwit ZWYR-240 shaking incubator, Labwit Scientific, Burwood East, Vic., Australia) to produce a seed culture.. Thereafter 96 mL of nutrient broth media was inoculated with 4 mL of the seed culture and incubated at 37 °C overnight and the microbial growth was determined using a spectrophotometer (Jenway 7305 uv-visible spectrophotometer, Jenway®, Staffordshire, United Kingdom) at a wavelength of 660 nm. The cell concentration was calculated using Equation 3.4.

$$OD_{660} = 0.0086(CFU) - 0{,}448 \quad (3.4)$$

Thereafter, the consortium was tested for its foamability using a method developed by Collivignarelli et al. (2020) with minor modifications.

3.3.2 Foamability and foam stability in MLSS

A 5 L of MLSS was collected using a 10 L polypropylene bottles from a municipal activated sludge WWTP near Cape Town, South Africa. The experiments were conducted using a laboratory scale reactor as shown in Figure 3.1, i.e., using a similar configuration to that of the aeration system, although they differed in the diameter and height (3 cm diameter and 24.5 cm height, 4.6 cm diameter, and 29.4 cm height as well as 6.2 cm diameter and 49 cm height). This was done to determine the

effect of the reactor design on foamability and foam stability. To generate foam, the air was sparged at various flow rates listed in Table 3.3 through an air stone using an aeration pump coupled with an air flowmeter as described in previous sections, i.e., section 3.2.5.1.

Table 3.2: Foaming potential operational conditions and evaluated values adopted from Collivignarelli, 2020, with minor modifications.

Parameters	Evaluated values
Sample volumes (mL)	50, 100, 250
Aeration time (s)	10, 20,30
Air-flow rate (L/min)	14, 7, 3.5, 0.9

3.3.3 Foaming potential test

The following equation (3.5) was used to calculate the foaming potential (FP).

$$FP\ (mL.L^{-1}) = \frac{(H_0 - H_t) \times S}{Q \times \Delta T} \quad (3.5)$$

Were, H_0 was the initial liquid height before aeration (cm), H_t Was foam-liquid interface post aeration (cm)S was the cylinder area (cm^2), Q was the air flow rate L_{air}/ min, ΔT was the aeration time (min).

The half-life time ($H_{1/2t}$, min) of foam collapse after discontinuation of air sparging, was used to determine foam stability (min) – see Equation 3.6 whereby k is the rate constant (min^{-1}).

$$H_{(1/2t)} = H_0 \times e^{(-k.t)} \quad (3.6)$$

3.3.4 Foam destabilisation test

For foam destabilisation tests, a combine volume (1.8 L) PSW and MLSS (Filament Index of 4-5), in the ratio 1:2 were added into a 2L bioreactor (schott bottle). Biodefoamers were produced as in section 3.3.1; however, the time was elongated to 48 h. For each 2L mixture of the collected PSW and MLSS 4% v/v of the biodefoamer producing culture was added into the mixture was swirled and stored at room temperature for 10 days and sampling was done every 24 h. Before sampling the mixture was swirled for 5 min, after which a volume of 200 mL was added into the (500 mL) foaming column. For mixing the sample air was sparged at 40 mL/min after which foam was generated by sparging air

through an air diffuser at a flow rate of 900 mL/min until foam volume of 50 mL was generated an the air pump was switched off for 40 s; additionally, foam destabilisation (foam collapse and foam drainage) was determined using Ross-Miles method with minor modifications (Miles & Ross1944).

.

3.3.5 Kinetic models assessed

In the presence of microorganisms that produce a biodefoamer consisting of multiple charged functional groups, the sessile microbial cells that trail nutrients adsorb into the biodefoamer to form aggregates and collide due to electrostatic forces, including Van der Waals forces (Chen et al., 2021). These collisions are governed by turbulence and aeration, leading to the growth of the nutrient-rich aggregates (de Morais et al., 2020; Zhao et al., 2020). The biodefoamer produced by the cells might contain both hydrophilic and hydrophobic attachment sites, although this has to be confirmed, which act as a biological adhesive site that enhances the attachment of the filamentous bacteria into the flocs (Kozhukhova et al., 2020). This mechanism might deprive foam formers of the lipids required for their growth, meaning that the number of filaments can be reduced and biofoam lessened.

In this study, several kinetic models were used to elucidate foam destabilisation in the presence of a biodefoamer in comparison to a synthetic defoamer. All the experiments were conducted in an aeration column (500 mL). The foam destabilisation rate can be described as in Equation 3.7.

$$-\frac{dh}{dt} = r_a = k_i h^n \tag{3.7}$$

Where r_a is the rate of foam destabilisation, k_i is the kinetic defoamation constant, h is the foam height or liquid height obtained by calculating foam overrun and n is model fitting constant, when n is 0, it means the rate of the reaction does not depend on the concentration of the reactant, whereas when n increases to 1 or 2, foam destabilisation will solely depend on the defoamer concentration. Monod's proposed kinetic model was also used in Equation 3.8 where k_m, is the maximum specific foam defoamation rate, and h is the foam height.

$$-\frac{dh}{dt} = \frac{k_m.h}{k_i + h} \tag{3.8}$$

An exponential decay model (Equation 3.9) was also used since foam destabilisation usually occurs due to foam decay and drainage.

$$\frac{dh}{dt} = -k.h \tag{3.9}$$

Where, k is an exponential decay constant.

3.3.6 Regression and statistical analysis

Mathematical models that described foam decay and drainage were fitted into the experimental data and a non-linear regression function in Polymath v6.0 (Polymath 6.0, Polymath®, New Jersey, USA) and was used for simulation; moreover, the simulated data contained estimated kinetic parameters which were used to compare the generated data to experimental data. A comparison was then done and analysed on Microsoft excel v2016. The mean was calculated using Equation 3.10. Additionally, polymath software (Polymath 6.0, Polymath®, New jersey, USA) was used to estimate the value of the kinetic parameters in Equations 3.7-3.9 with the generated data from Polymath v6.0 being plotted against experimental data using Microsoft excel v2016.

$$Mean = \frac{\sum X}{n} \tag{3.10}$$

Where $\sum x$ is the sum of data points, while n is the number of experiments conducted.

3.4 Phase 3: Antimicrobial activity of the crude biodefoamer against the MLSS and PSW microbial community

The aim of this phase was to assess the ability of the produced biodefoamer to inhibit the biofoamers growth, i.e., proliferation.

3.4.1 Media and inoculum preparation

A 1:1 ratio of PSW and MLSS was centrifuged at 15 000 rpm for 15 min to remove the solids, and the supernatant was filtered through a 0.22 µm cellulose syringe filter (Merck Millipore, Burlington, Massachusetts, USA) to remove microorganisms from the mixture. The filtrate contained a concentration of 196 mg/L protein and 672 mg/L lipids, and the pH of the media was adjusted to 7. A volume (99 mL) of the mixture was inoculated with 1 mL of the consortium and incubated at 37°C for 24 h. This was to assess whether the consortium could grow in the presence of the constituents of the wastewater which it would treat, and the microorganisms were removed from the media to avoid production of the biodefoamers by the PSW and MLSS microbial community.

3.4.2 Biodefoamer production

Biodefoamer production experiments were carried out as in section 3.2.3. The only difference was that biological media (sterile PSW and MLSS) was used, and this experiment was carried out for 5 days

and 2 mL samples were withdrawn every 24 h to determine microbial growth, biodelipidation and deproteination. For biodefoamer production, a further 2 mL was withdrawn and processed as in section 3.2.3 and the foam collapse rate was determined using Equation 3.3.

3.4.3 Biofoamer inhibition using cell-free defoamers

On day 5, 2 mL of the incubated media was centrifuged at 15 000 rpm for 15 min to obtain cell-free biodefoamer aliquots which were then assessed for their ability to inhibit MLSS and PSW microbial community growth by adding 20 µL of the cell-free biodefoamers. Mueller-Hinton agar plates were incubated at 37°C, and microbial growth was observed every 24 h for 5 days, i.e., assessing the volumetric zone of inhibition (VZI) as described by Mewa-Ngongang et al. (2019).

3.5 Phase 4: Bench-scale biodefoamer supported activated sludge reactor design and performance assessment

The aim of this phase was to design and assess the performance efficiency of the AS for the removal of FOG, proteins, TSS and COD. Furthermore, to compare its efficiency against Synthetic defoamer activated sludge (Syn-AS) and conventional activated sludge system (CAS).

3.5.1 Activated sludge system design and operation

The AS treatment system used in this part of the study comprised a feed tank, an aerobic tank and a secondary clarifier, which were constructed using clear polyvinyl chloride sheets. The feed tank height was 28.3 cm, with a diameter of 18 cm. The aerobic tank and secondary clarifier systems had the same height and diameter of 28.5 and 15 cm respectively; however, the clarification tank had a cone with a height of 11 cm. The feed tank had a carrying capacity of 6 L, while the aerobic tank had a carrying capacity of 4.2 L and the secondary clarifier had a 5 L carrying capacity. The air was sparged using a Resun air pump (Ac9906) through silicon tubing connected to 3 air diffusers into the aerobic tank for efficient air supply. The air was pumped at a flow rate of 7 L/min. A 26-day-old AS which was used was collected from a municipal WWTP near Cape Town, South Africa. The PSW was pumped in the system using a Gilson® Minipuls Evolution peristaltic pump (Gilson Inc., Middleton,Wisconsin, USA) at a flow rate of 3.4 mL/min at a hydraulic retention time (HRT) of 24 h. The AS overflow was recycled from the secondary clarifier back into the AS tank using the Gilson® Minipuls Evolution peristaltic pump at a flow rate of 3.2 mL/min, and an AS retention time (SRT) of 10 days was maintained. This experiment was carried out for 10 days. The effluent from the aeration tank was pumped into the secondary clarifier at the same rate as the influent and the HRT of the secondary clarifier was similar to that of the aerobic tank. The effluent from the secondary clarifier was pumped out at the same rate

as the influent to the aeration tank to maintain a steady state operation for the whole system. Figure 3.2 diagrammatically illustrates the activated sludge treatment system that was used in this study.

.

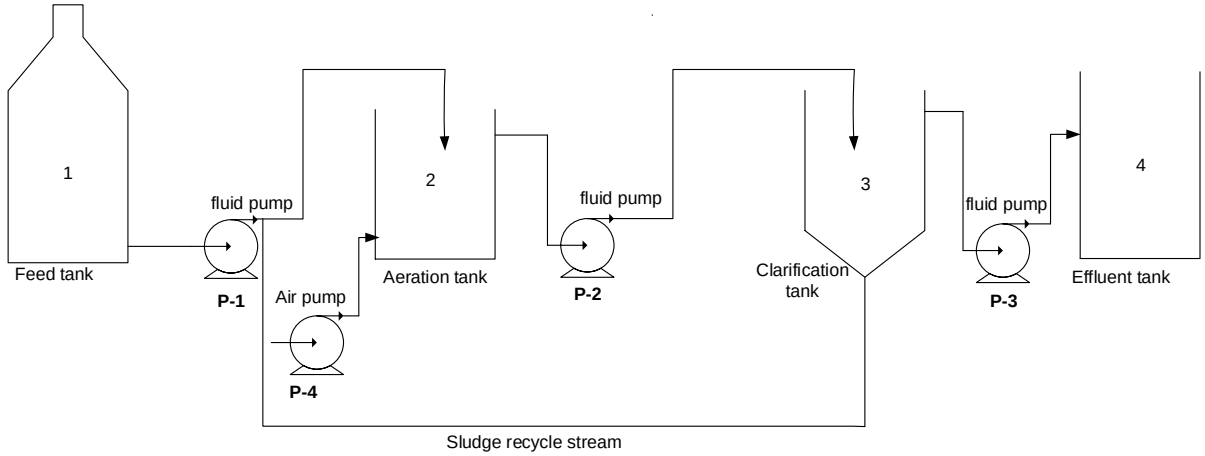

Figure 3.2: Design of the bench scale activated sludge treatment system

3.5.2 Activated sludge-supported poultry slaughterhouse wastewater treatment system start-up

Subsequent to the addition of PSW to the AS system, the aeration tank was inoculated with 0.16 L of a 26-day-old AS that was collected from a municipal wastewater treatment system near Cape Town, South Africa. For every 5 L of PSW, 4% (v/v) of biodefoamers, i.e., that were produced by a consortium of *Bacillus subtilis* (GCA_000009045.1), *Aeromonas veronii* (GCA_000204115.1), *Klebsiella grimontii* (UGJQ01000001.1) and *Comamonas testosteroni* (GCA_900461225.1), were added into the AS aeration tank after which the air pump was switched on. Air supplied by the air pump thoroughly mixed the MLSS, PSW, and the biodefoamers. This system was acclimated for 48 h before the actual experimental runs. The samples from the feed tank, aeration tank, and the secondary clarifier were collected periodically at 24 h intervals and immediately analysed. To maintain a steady state operation, flow rates as elucidated in section 3.5.1 were used. The AS systems was operated using a biodefoamer, synthetic defoamer (positive control) and a non-defoamer supplemented system (negative control) to determine the efficiency of individual defoamer-AS systems. The systems were operated under unsteady (0-2 days), transition (3 days) and steady state (4-10 days).

3.5.3 Analytical methods for wastewater quality characteristics

The 100 L of PSW collected biweekly using sterile 25 L polypropylene bottles from a poultry slaughterhouse near Cape Town, South Africa, was analysed for pH, temperature, turbidity, total suspended solids (TSS), COD, BOD_5, proteins, FOG, ammonium nitrogen (NH_4-N). Temperature and pH were analysed using PSCTestr 35 multi-parameter (Wirsam Scientific and Precision Equipment

(Pty) Ltd, Johannesburg, South Africa), turbidity was quantified using Oakton Turbidmeter TN 100 (Eutech Instruments Pte Ltd, Paisley, United Kingdom), while the TSS was quantified using EPA method 160.2, the COD was analysed using method EPA method 410.4, BOD5 was analysed by using EPA method 405.1 and FOG was analysed by EPA method 10056. The NH_4^+-N was analysed using tesk kits from Merck SA a franchise of Merck & Co., New Jersey, USA and the Merck Nova 60 spectroquant was used to quantify its concentration. The protein concentration was determined using the Bradford assay (see appendix B).

CHAPTER 4

Production, application, and efficacy of biodefoamers from a *Bacillus*, *Aeromonas*, *Klebsiella*, *Comamonas* spp. consortium for the defoamation of poultry slaughterhouse wastewater

Submitted as: **Cynthia Dlangamandla**, Seteno K.O. Ntwampe, Moses Basitere, Boredi S. Chidi, Benjamin I. Okeleye, Melody R. Mukandi. Production, application, and efficacy of biodefoamers from *Bacillus*, *Aeromonas*, *Klebsiella*, *Comamonas* spp. consortia for the defoamation of poultry slaughterhouse wastewater. *MDPI Water*, 15(4): 655. https://doi.org/10.3390/w15040655.

CHAPTER 4

PRODUCTION, APPLICATION AND EFFICACY OF BIODEFOAMERS FROM A *BACILLUS, AEROMONAS, KLEBSIELLA, COMAMONAS* SPP. CONSORTIUM FOR THE DEFOAMATION OF POULTRY SLAUGHTERHOUSE WASTEWATER

4.1 Introduction

The activated sludge process (ASP) microbiome is a significant constituent that influences the performance of biological wastewater treatment plants (WWTPs). ASP converts or absorbs organics, ammonium nitrogen, and some phosphorous, including suspended or dissolved solids, among many other contaminants(Burger et al., 2017). The efficiency of the AS system depends on organisms' ability to form active conglomerates in an aerated environment. This process is influenced by many factors, such as environmental conditions (pH, temperature, dissolved oxygen (DO)) and climate change. Climate change results in increased rainfall and this increases the influent flow rate by 15–25% as compared to dry weather. It also reduces total suspended solids (TSS), chemical oxygen demand (COD) and ammonium nitrogen ($N\text{-}NH_4^+$) concentration due to its dilution effect in the sewer and WWTP. Although these systems are designed to carry over capacity during increased precipitation, sludge washout can be encountered, leading to the inefficiency of the system in the long term as well as high energy consumption and will require increased operational costs(Borzooei et al., 2020; Gemza et al., 2022; Zhou et al., 2022). To curb this problem, storm overflow and combined sewer overflow tanks are used. However, during wet weather flow, the combined sewer may overflow into receiving water bodies and contaminate it; hence, these are short-term solutions. Therefore, an implementable research for long-term solutions is required(Gemza et al., 2022).

When treating wastewater that contains high concentrations of proteins, fat oil and grease (FOG), the system efficiency becomes a challenge because proteins are surface active and they reduce foam drainage, whereas FOG solidifies at lower temperatures, which results in the clogging of pipes and membrane fouling. Furthermore, it enhances filamentous bacteria growth which results in foam formation (Deepnarain et al., 2019), herein referred to as biofoam. The generation of

biofoam at the surface of an AS aeration tank is a nuisance and is thus considered undesirable. Mycolic acid-containing filamentous bacteria are significant contributors to this biofoam (Dlamini, et al., 2020). Furthermore, surfactants present in wastewater from various sources, including biosurfactants produced by numerous microorganisms in the AS in combination with aeration, culminate in foam formation. In most instances, biofoam producers result in foam stabilization within WWTPs (Dlangamandla et al., 2021). The excessive growth of these organisms leads to the production of biosurfactants and sludge deflocculants, which in turn lead to poor sludge settleability and excessive foaming. This increases WWTPs operational costs associated with defoaming operations, culminating in the deterioration of the effluent quality, requiring further treatment and the extension of sludge retention time, which is energy intensive (Borzooei *et al.*, 2020). Periodically, this results in the loss of essential microbiological cells in the AS. This necessitates efficient biological methods that are less energy intensive, which will shorten the sludge retention time and aeration time.

Numerous strategies have been employed to reduce biofoam formation. These strategies include those termed non-specific and specific strategies. Non-specific strategies include using chemical (synthetic) defoamers and physical techniques (water sprays and the adjustment of operational conditions) to remove or reduce foam. In contrast, specific strategies include the use of biological techniques that target the cause of biofoam formation (Dehestaniathar *et al.*, 2021).

Using chemical defoamers such as polyaluminum chloride results in sludge disintegration, which inhibits nitrification and increases soluble chemical oxygen demand (COD) concentration, while oil-based defoamers result in overgrowth of the biofoam-producing filamentous bacteria (Guo *et al.*, 2015). Furthermore, using chemical defoamers results in their bioaccumulation downstream, whereas applying physical methods requires adjustment or the design of new bioreactors. This necessitates the need to develop new environmentally benign, energy efficient and economic strategies that will use the water constituents to be treated to reduce the excessive growth of biofoamers rather than treating the symptoms, i.e., biofoam.

The literature reviewed reveals that several biological methods have been used successfully to reduce foam-forming filamentous bacteria such that foam formation is minute in AS systems. These methods include the use of biological reactors, such as up-flow packed bed bioreactors, to enhance nitrogen removal and biofilm granulation, as well as aerobic sludge granulation that produces granular sludge that results in nutrient removal and enhanced settling properties and reduces biofoam (Guo *et al.*, 2015; Dehestaniathar *et al.*, 2021; Shi & Liu, 2021). Bacteriophages that can be produced from various organisms isolated from various wastewaters have also been used, and these bacteriophages were previously determined to improve sludge settleability (Guo *et al.*, 2015). A study by Pajdak-Stós et al., 2017 elsewhere highlighted that *Lecane inermis* rotifers

were observed to "ingest" and decrease the number of branched filamentous bacteria in AS.

This study focused on producing a biodefoamer from poultry slaughterhouse (PSW) consortia isolates for use in PSW biofoam reduction compared to a commonly used synthetic defoamer. This was assessed using foam reduction efficiency and foam collapse rate. Furthermore, AS floc integrity and maintenance were also assessed microscopically to ascertain agglomeration, and thus settleability, when the produced biodefoamers were used.

4.2 Objectives

The objectives of this section were to:

- Isolate and identify microorganisms that can produce biodefoamers,
- Apply the biodefoamers produced by the microbial consortium and assess them for their activity in MLSS foam reduction.
- To assess the biodefoamers for their foam reduction efficiency in comparison with chemical/ synthetic defoamers.

4.3. Results and discussion

4.3.1 Microbial isolation and identification of biodefoamer-producing isolates

Amongst the microorganisms that were isolated from the PSW discharge spout, four isolates, i.e., *Bacillus subtilis* (GCA_000009045.1), *Aeromonas veronii* (GCA_000204115.1), *Klebsiella grimontii* (UGJQ01000001.1) and *Comamonas testosteroni* (GCA_900461225.1) were selected for biodefoamer production based on their rapid efficiency in foam decay, moderate pH and lower concentration. The *Bacillus* sp. colonies were rod-shaped and off-white, and when they were viewed under a microscope, their gram staining depicted that they were gram-positive. *Aeromonas veronii* was also off-white, albeit gram-negative. *Klebsiella grimontii*'s gram reaction was negative, with rod-shaped, slimy and white colonies. Similarly, *Comamonas testosteroni*'s gram reaction was negative, exhibiting slightly curved rods with mucoid colonies, which were also white. The consortium produced biodefoamers under various environmental conditions (pH and concentration) as determined using response surface methodology (RSM) (see section 4.3.2). This was the first study to use a consortium isolated from poultry slaughterhouse wastewater discharge spout to produce biodefoamers.

4.3.2 Mixed liquor suspended solids (MLSS) metagenomics analysis

The AS microorganism sequences were generated using metagenomics, indicating that the dominant foam formers in the AS samples were *Nostocoida limicola*, *Gordonia kroppenstedtii*, *Candidatus Microthrix parvicella*, *Nocardioides insulae* and *Bacteroides nordii*. These biofoamers are

hydrophobic actinobacteria that contain mycolic acids and produce biosurfactants to break down FOG so that they uptake it as a carbon source. These characteristics enhance biofoamation in AS systems (Garg *et alet al.*, 2020; Tsilo *et alet al.*, 2021).

4.3.3 Biodefoamer production, reactor conditions optimization and characterization

Two independent variables, pH (range 7–14) and concentration (range 1–4%*v/v*), were used to evaluate the defoamer (synthetic and biodefoamer) activity (foam reduction efficiency and foam decay rate). The efficiency of biodefoamers produced from a competitive consortium was compared to that of the synthetic defoamer. The results in Table 4 showed that pH 7 at a concentration of 4% (*v/v*) positively affected biodefoamer production, which inculcated rapid foam decay and suppression rate. The results depicted that the biodefoamer effect became less effective as the pH increased. This was because the microorganisms preferred a neutral pH to produce the biodefoamers with high activity. Overall, biodefoamers have a different electrical state at different pHs. A change in pH not only alters the defoamer's charge, it also alters the charge of the suspended solids, which affects the settleability of the MLSS and the PSW SS, which in turn affects the foaming behavior of the wastewater (Tsilo *et alet al.*, 2021). The concentration of the biodefoamer is also crucial. Low concentration affects the bridging mechanism. Higher concentration leads to sludge deflocculation and high viscosity, which further results in foam formation; hence, lower and higher concentrations produce minimal biodefoamer activity (Biswas *et al.*, 2020) . According to the synthetic defoamer specification, it is effective at a concentration of 1–100 ppm and stable at pH 5–9. According to this study, it was more effective at pH 7 and 1% (*v/v*), and this falls in the specific ranges of the defoamer specification. This defoamer's effectiveness also deteriorated at higher pH, albeit at a lower concentration, because silicone-based defoamers are sensitive to pH. They lose their activity at acidic pH and pH more significant than 10 (Lee, et al., 2021). These results highlight that the defoamers are not universal because their activity depends on the ever-changing environmental condition of the CAS. Table 2 lists the ANOVA quadratic model used to optimize biodefoamer production. Table 4.1 lists the ANOVA quadratic model that was used to optimize biodefoamer production.

Table 4.1: Experimental design table for the independent variables pH (A) and defoamer concentration (B); and for the dependent variables (foam reduction efficiency and foam collapse rate of the biodefoamer and synthetic defoamer (AB))

Run	pH	Concentration (%v/v)	Foam reduction efficiency (%v/v)		Foam collapse rate mm/s	
			Synthetic defoamer	Biodefoamer	Synthetic defoamer	Biodefoamer
1	8.5	0.38	93	73	0.83	0.5

2	10	1	2.9	73	0.55	0.55
3	8.5	2.5	83	82	0.42	0.5
4	8.5	2.5	83	82	0.42	0.5
5	8.5	4.6	15	15	0.5	0.5
6	6.38	2.5	96	42	1	0.5
7	8.5	2.5	83	82	0.42	0.5
8	8.5	2.5	83	82	0.42	0.5
9	10.6	2.5	87	73	0.45	0.45
10	8.5	2.5	83	82	0.42	0.5
11	7	1	90	73	1.25	0.83
12	7	4	96	96	1.7	2.5
13	10	4	95	78	0.42	0.42

The RSM was used to optimize the environmental conditions of the bioreactor such that an optimum response was achieved. The effect of the two independent variables (pH and concentration) on the foam reduction efficiency as well as foam decay rate, which were used to determine biodefoamer production, are graphically illustrated in Fig. 4.2A for the biodefoamer and in Fig. 4.2B for the synthetic defoamer. It was observed that both pH and concentration significantly impacted the efficacy of both defoamers. Wongsamuth and Doran also reported that pH and defoamer concentration significantly impact a defoamer's effectiveness. The optimal biodefoamer production was observed at pH 7 and a concentration of 4% (*v*/*v*), where the highest foam reduction efficiency was 96% at a faster foam decay rate of 1.7 mm/s. The biodefoamer results are similar to the results Mamais, 2011 obtained when a polyaluminum chloride (PAX-14) concentration of 6.6 to 11.5 g Al^{3+}/kg MLSS reduced foam by 75 to 100%, improving the sludge flocculation. However, PAX could only eliminate *Gordonia amarae* and *Microthrix parvicella* cells, and using chlorine-based chemicals can be detrimental to the microbial communities because it can break down the microbial cell walls.

The lowest biodefoamer production was observed at pH 8.5 and at a higher defoamer concentration of 4.6 (*v*/*v*), with a foam reduction efficiency of 15% at a decay rate of 0.42 mm/s. This showed that the defoamer production was more affected by the pH than the defoamer concentration. Similarly, the biodefoamer obtained a minute foam collapse rate of 0.42 mm/s at alkaline conditions pH 10, even with a higher defoamer concentration of 4% (*v*/*v*); however, the foam reduction efficiency of 78% was observed. This was due to the deprotonation of the biodefoamer amino charges under alkaline

conditions. This increased electrostatic repulsion between the negatively charged defoamer and the activated sludge sample, leading to sludge disintegration and biofoam(Mohamed Hatta *et al.*, 2021).

The highest foam reduction efficiency for the synthetic defoamer was 96%, which corresponded with the highest foam collapse rate of 2.5 mm/s at a pH of 7 and a higher concentration of 4% (*v*/*v*). The lowest foam reduction efficiency of the synthetic defoamer was 2.9% at pH ten and a concentration of 1% (*v*/*v*). In contrast, the lowest foam decay rate of 0.42 mm/s was observed at pH 10 and a concentration of 4% (*v*/*v*). This indicated that the synthetic defoamer was ineffective at very alkaline pH, regardless of the defoamer concentration (Routledge, 2012). Overall, the synthetic defoamer had a higher foam collapse rate than the biodefoamer, although foam reduction efficiency was similar.

The ANOVA quadratic equations were generated to estimate optimum biodefoamer production. The mean was 0.4, and the standard deviation for the model was 0.3. Essential parameters in the model had $p < 0.05$; however, the parameters with a *p* value that was greater than the latter were negligible, thus indicating that the terms A and A^2 were of significance; hence, Equation; hence, Eq. 4.1 was simplified to Eq. 4.2

$$Y = 0.42 + 0.34A - 0.02B - 0.15AB - 0.22A^2 - 0.19B^2 \quad (4.1)$$

$$Y = 0.42 + 0.22A^2 \quad (4.2)$$

Eq. 4.3 was used to estimate the effectiveness of synthetic defoamers and foam collapse rate. This model was also deemed to be insignificant to adequately describe the foam reduction efficiency, with a mean of 71.7 as well as a standard deviation of 23.1, and an F-value that was more than 0.57; the *p* values for all the terms in the model were more significant than 0.05, showing this quadratic model to be insignificant in predicting the foam reduction efficacy of synthetic defoamers.

$$Y = 155 + 44A + 38B - 02AB - 2.2\,A^2 - 5B^2 \quad (4.3)$$

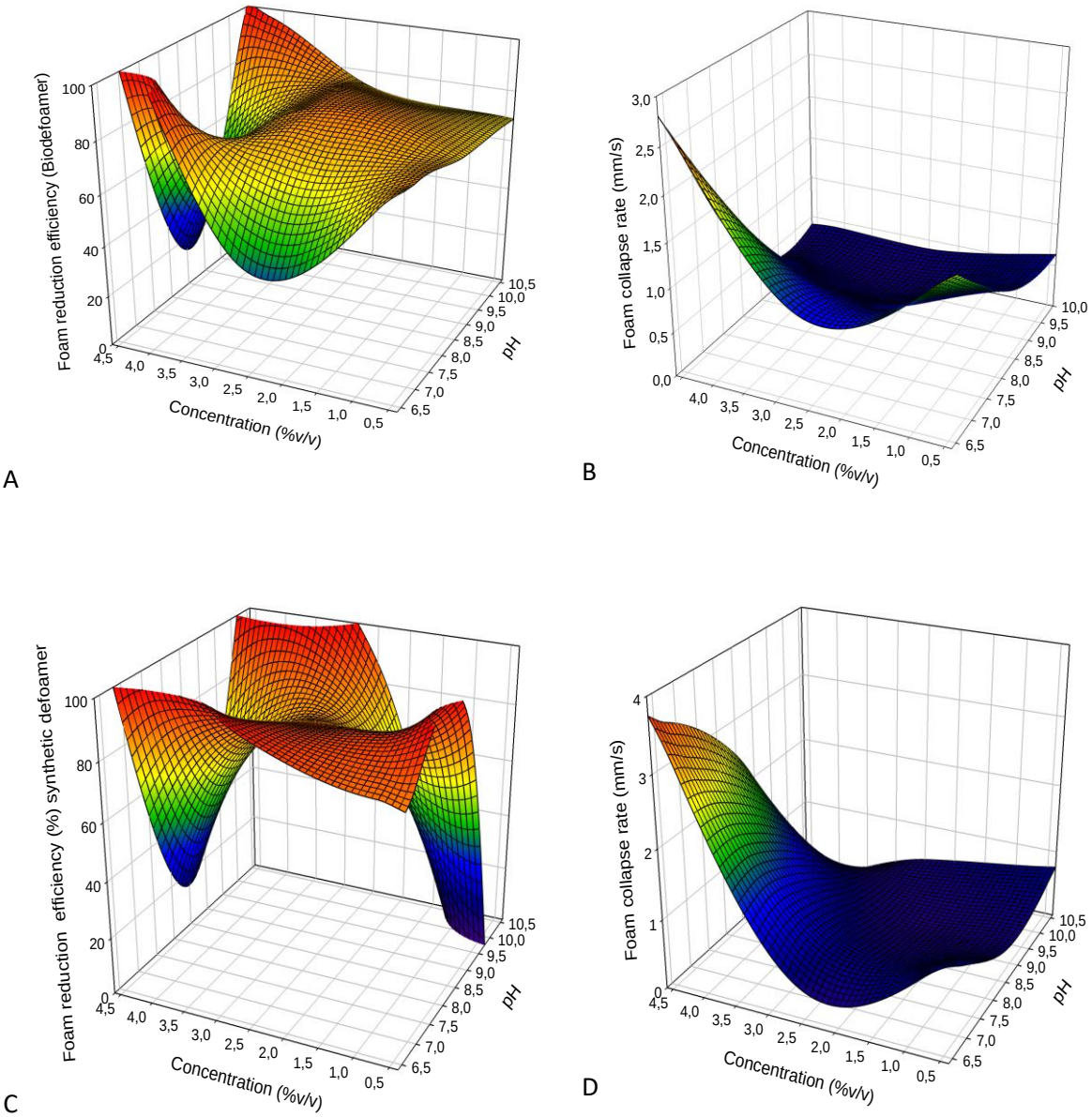

Figure 4.1: A graphical illustration showing the effect of pH and concentration on (A) and (C) foam reduction efficiency of the biodefoamer; and synthetic defoamer (B) and (D) foam collapse rate in the presence of a biodefoamer and a synthetic defoamer respectively

4.3.4 Dynamic foam decay test

The foam generation rate is usually faster than the foam collapse rate (Mamais et al., 2011). The foam height reduction over time was recorded in this study. The colour mash red (in this case dark orange) is the highest optimal colour and the blue is the lowest. Fig. 4.2 a and c mash colour is dark orang to red When pH is 7 and the concentration is 4 %*v/v* it indicates maximum foam reduction efficiency. It becomes blue at increased pH of up to 10. Fig. 4.2 b and d shows that the foam collapse rate is minimal at elevated pH, concentration

as well as pH below 7. Fig. 4.2 illustrates the foam behaviour in the absence and presence of both a bio- and synthetic defoamer (4% *v/v)* at pH 7. For both the bio- and synthetic defoamer, the foam decay rate was observed to be under 40 s. After that, there was minimal foam regeneration even with subsequent sparging, meaning that both defoamers were efficient in foam reduction. However, the biodefoamer reduced the foam height by 85.4% within 40 s, whereas the synthetic defoamer only reduced the foam height by 61.5%. Mangundu, 2017 assumed that the minimum threshold required for foam decay was above 30%; however, in this study, a defoamer concentration of 4% (*v/v*) was able to collapse and suppress the foam height significantly. The efficiency of a defoamer is determined by its potential to form a destabilizing bridge that stretches across the lamellae such that it ruptures individual foam bubbles, thus causing liquid drainage from the foam, causing the foam to collapse. Moreover, it was previously demonstrated that bubble coalescence occurs in such instances; therefore, both defoamers had a potential to be used in large-scale applications (Manyele, 2007). Overall, when no defoamers were applied, the foam height was slightly reduced for 210 s. The foam height was reduced by 23%. The constituents of the wastewater, such as dissolved solids, including the presence of microorganisms such as *Actinomycetes* sp. in the MLSS, which produce biosurfactants and reduce the surface tension, can increase the viscosity that stabilizes the lamellae, increasing foam surface elasticity. This can further increase bubble deflocculation, causing excessive foaming as minimal pressure will be applied on the gas–liquid interface, resulting in minute liquid drainage (Gao *et al.*, 2018). When such a thing occurs in a WWTP, excessive foam generation will ensue, causing a nuisance for operators and facility managers.

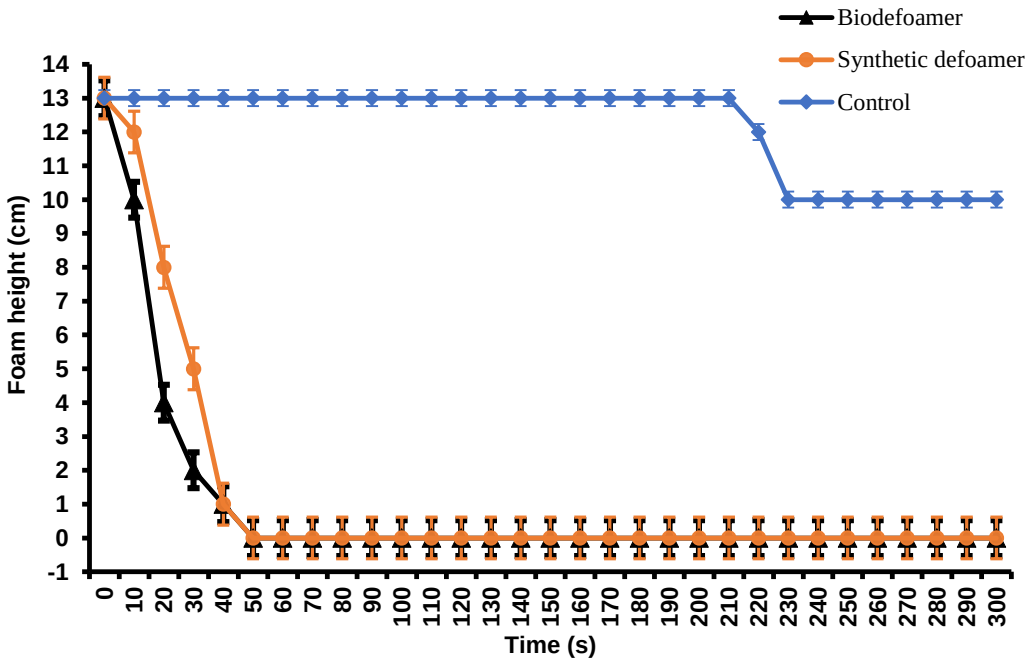

Figure 4.2: Graphical profile of foam behaviour in the presence of bio- and synthetic defoamer as well as in the presence of a defoamer

4.3.5 Microscopic analysis of recovered activated sludge in the presence and absence of bio- and synthetic-defoamers

Microscopic images of the AS with a filamentous index of 3–5 were observed over ten days when it was exposed to the 4% (*v/v*) of the bio- and/or synthetic defoamers (see Fig. 4.3). When the MLSS was exposed to a biodefoamer, minute floc formation was initially observed (day 0), with compacted (agglomerated) flocs forming on days 5 and 10. This showed that the biodefoamer could assist in floc formation, which can resolve challenges associated with sludge deflocculation, which results in the proliferation of filamentous bacteria. These filamentous bacteria prevalent within the flocs increase floc compaction strength, which is resistant to shearing and leads to good solid–liquid separation in AS (Wang et al., 2016). Through bridging, floc- and foam-formers can be bound together by extracellular polymeric substances (EPS). For this study, the biodefoamer was hypothesized to have a balanced protein and/or polysaccharide ratio with the MLSS to overcome deflocculation. This led to a balanced foam- and floc-formers growth reduction, resulting in stabilized form floc formation (Nilsson *et al.*, 2019).

The synthetic defoamer, however, had a negative effect on sludge compaction. The images showed oil droplets assumed to be from FOG, which significantly contributes to filamentous foam-forming bacterial growth. Observations indicated that on day 0, there was excessive filamentous bacterial growth. On day 5, although there was minute floc formation and visible oil droplets, the filaments protruded outside of individual flocs, leading to bridging and recalcitrant deflocculation on day 10, as observed elsewhere (Nilsson *et al.*, 2019). These results showed that the number of filamentous bacteria must not be excessive, as this will lead to weaker floc agglomeration. The synthetic defoamer favoured the proliferation of some, if not most, filamentous bacteria associated with WWTP (Omar et al., 2009). It was demonstrated that the non-application of a defoamer in the control experiments resulted in the MLSS showing a significant proliferation of filamentous bacteria throughout the experiment until day 10, with minute floc formation or agglomeration being observed. This was attributed to the changes in the quality characteristics of wastewater whereby aged sludge (>27 days) can be easily disintegrated with a weakened compaction attribute due to pH, organic and inorganic nutrients present therein (Pajdak-Stós *et al.*, 2017). Previously, it was observed that excessive filamentous growth leads to poor sludge sedimentation, the washout of microbial cells from the aeration tank/stage in the WWTP, and excessive biofoam formation (Pal & Paunikar, 2014; Pedrazzani *et al.*, 2016).

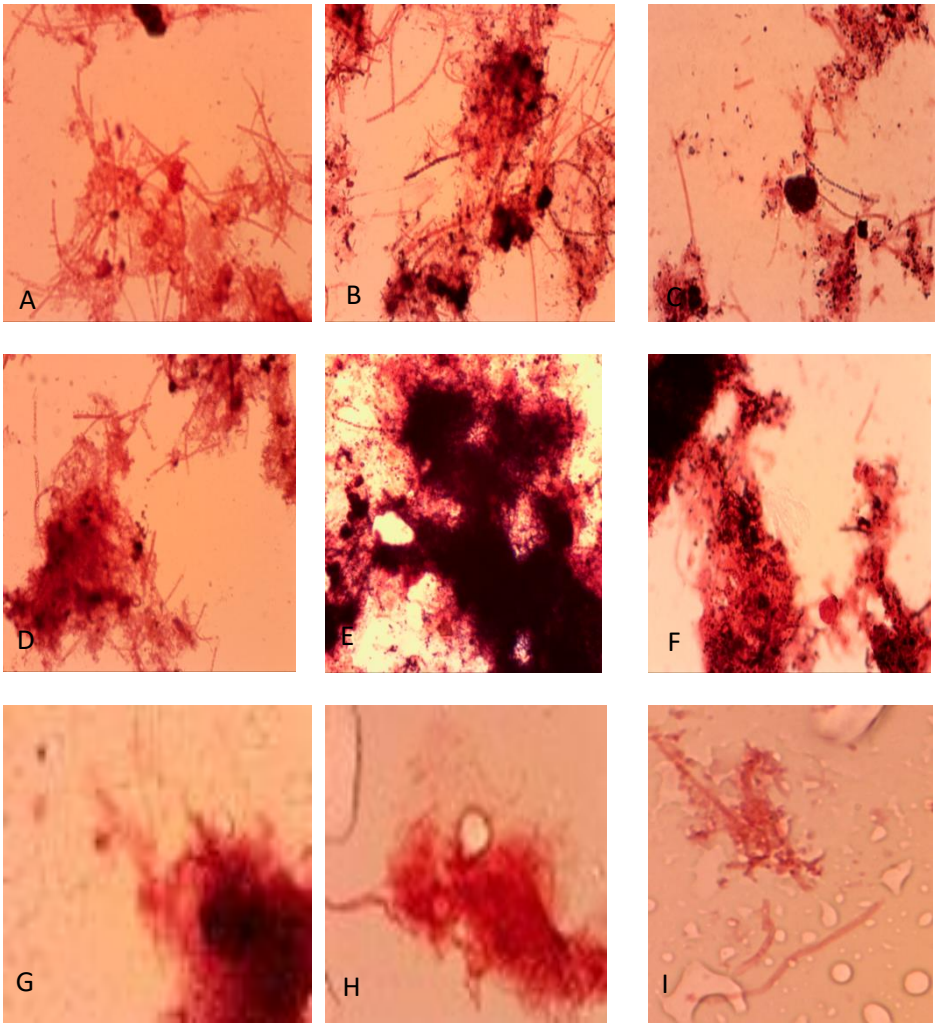

Figure 4.3: A micrograph representation of sludge: in the absence of a defoamer (A-C), in the presence of a biodefoamer (D-F), and when it was exposed to a synthetic defoamer (images G-I)

4.3.6 Biodefoamer FTIR and ^{1}H NMR characterisation

The Fourier infrared spectroscopy ((FTIR) of the biodefoamer that was produced by a PSW consortium in Fig. 4.4 was conducted to examine the correlation of the functional groups to biodefoamer activity. The peak at 3292 (49. 20%; 3292 cm^{-1}) indicated an OH- functional group (Petrovski *et al.*, 2011; Simjoo *et al.*, 2013), while the peak at 2112.25 (95.62%; 212.25 cm^{-1}) (Petrovski *et al.*, 2011; Simjoo *et al.*, 2013) indicated an aliphatic C-H stretching group (Simjoo *et al.*, 2013); the peak at 1634. Seventy-five (70.27%; 1634 cm^{-1}) indicated N-H- bending primary amines or carboxylic groups (Vanaja *et al.*, 2014; Subudhi *et al.*, 2016). These groups, i.e., carboxyl, alkane, amine and hydroxyl groups, confirmed that the biodefoamer was predominantly a polysaccharide. Although it was concluded that the biodefoamer was pH-sensitive, minute concentrations were required for its efficacy, imparting electrical neutrality to MLSS; however, the crude biodefoamer contained impurities, all of which resulted in foam decay.

The weak peaks at 410–439 (30.48–31.19%; 410-.46–439.18 cm^{-1}) were associated with azomethine

groups CH=N/C=N (Katritzky *et al.*, 2002). These groups, i.e., carboxyl, alkane, amine and hydroxyl groups, confirmed that the biodefoamer was predominantly a polysaccharide. The carboxyl functional groups contain multiple binding sites, ensuring compact attachment through charge neutralization and/or bridging (Shi & Liu, 2021). In charge neutralization, the negatively charge MLSS particulates will bind to the opposite charge in the defoamer, and this will reduce the repulsive electrostatic forces and increase attraction forces, meaning that the defoamer will adsorb and neutralize the charge of the MLSS particulate. Although it was concluded that the biodefoamer was pH-sensitive, minute concentrations were required for its efficacy, imparting MLSS foam electrical neutrality; however, the crude biodefoamer contained impurities, all of which resulted in foam decay.

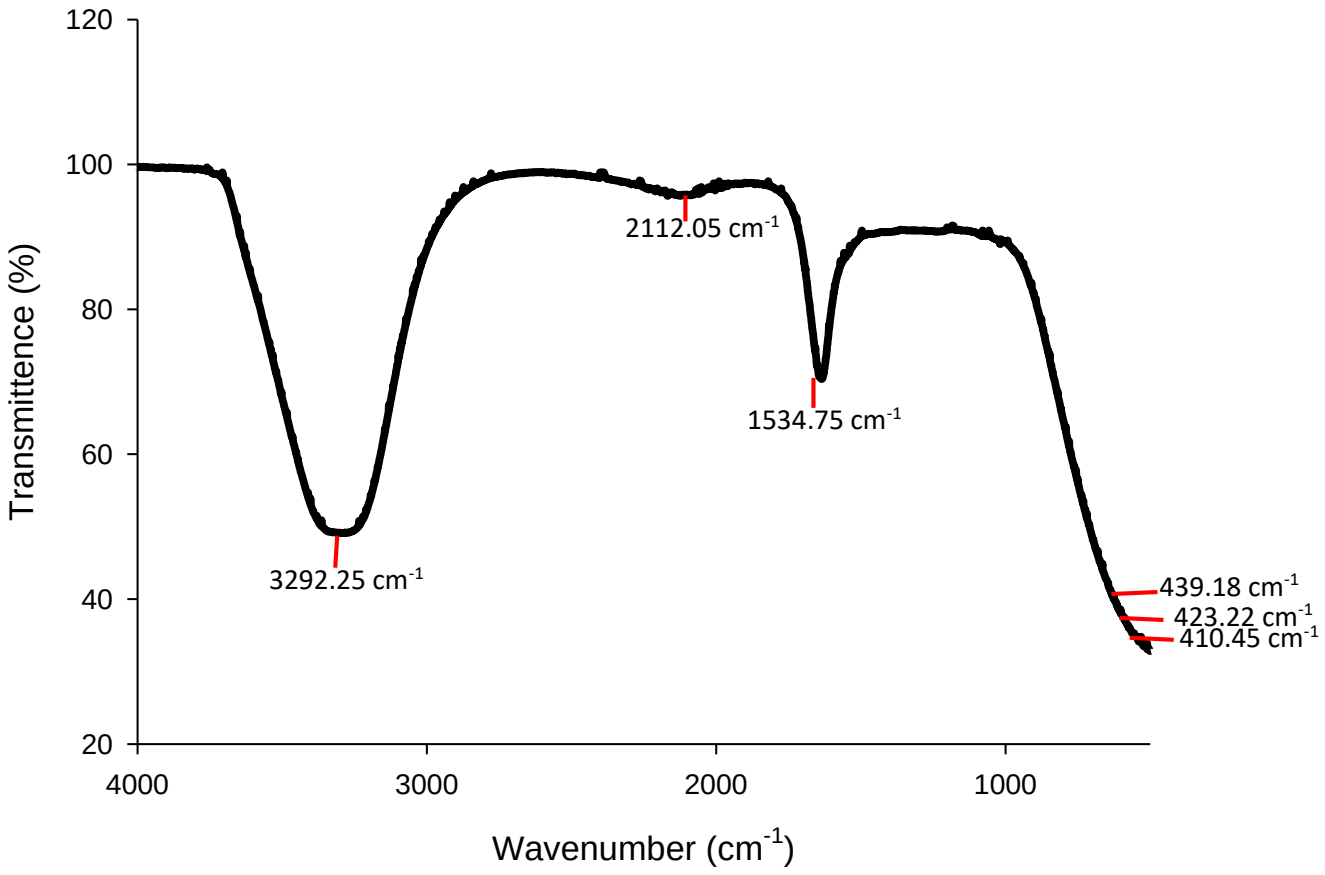

Figure 4.4: Fourier transform infrared spectroscopy (FTIR) spectrogram of the biodefoamers produced by a PSW consortium.

The ^{1}H NMR spectrum in Figure 6 revealed signals between δ 0.8–1.9 ppm, confirming the aliphatic stretches' presence and the signal at 1.9 ppm depicted a CH_2 proton. The chemical shifts from δ 2.0–2.92 ppm showed the presence of amines, whereas the signal at δ 2.0 ppm showed CH- protons that were bounded to a vinyl carbon the solvent peak appeared at δ 4.7 ppm, and the signal at δ 3.1 ppm

showed the presence of a hydroxyl group (Deval *et al.*, 2017). The concentrated conspicuous peaks revealed the presence of aromatic rings in the structure. The multiple signals between δ 3.5 and 4.0 ppm were carbohydrate attributes, whereas the signals from δ 0.8 to 3.5 ppm were similar to a polysaccharide structure. The chemical shifts between δ 3.5 to δ 4.0 revealed that the polysaccharide structure had an electro-negative oxygen that originated from an ester functional group attached to it, resulting in functional groups such as alkoxy and hydroxyl (Tsilo *et al.*, 2021). The carbohydrate signals usually resonated between δ 3.5 and 4.5 ppm; some carbohydrate peaks were observed from δ 4.4 to 5.5 ppm, and others appeared from δ 0 to 5 ppm. These are unique from the existing literature, and these peaks are affected by various factors, such as the type of solvent used to dissolve the sample (Mohamed Hatta *et al.*, 2021). The ^{1}H NMR spectra can be used to estimate the configuration of the glycosidic bonds of the polysaccharide structure. When the chemical signals of a proton are more significant than 5 ppm, the structure is predominantly α glycosidic linkage. However, if it is less than 5 ppm, the glycosidic bonds are mostly β. The biodefoamer used in this study is a carbohydrate with predominantly β glycosidic linkages. The carbohydrate structure of the biodefoamer will enhance MLSS flocculation due to its surface charges.

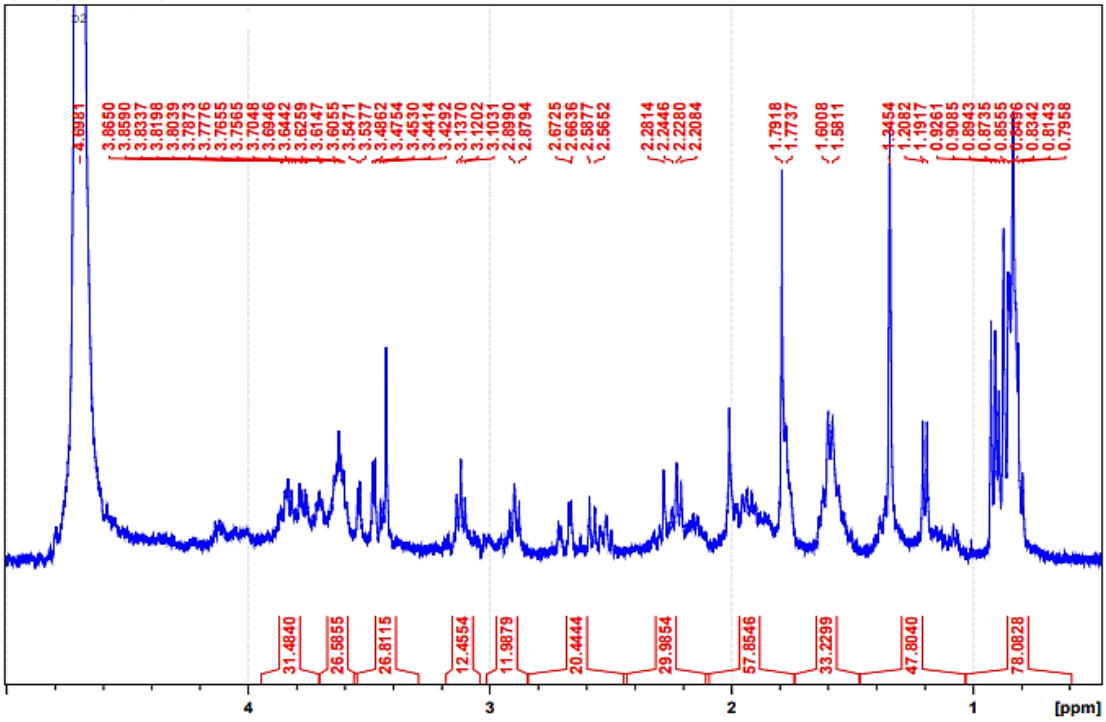

Figure 4.5**: ^{1}H NMR spectra of a biodefoamer4.5 Conclusion**

The isolated microbial consortium of *Bacillus*, *Aeromonas*, *Klebsiella* and *Comamonas* spp. produced biodefoamers with high biodefoamer efficacy and a foam decay rate suitable for WWTP application

when RSM optimized the application conditions. The highest synthetic and biodefoamer efficiency was 96% under these conditions, i.e., pH 7 and a concentration of 4% (*v*/*v*). When further foam collapse studies were carried out, i.e., using the RSM optimum conditions, the maximum foam decay rate for the synthetic and biodefoamer was determined to be 99% at 50 min, with total foam suppression at 190 min. The microscopic pictures indicated that the AS was impacted by the presence and absence of defoamers (synthetic and biodefoamers), with the absence of both defoamers resulting in excessive filamentous bacterial growth. The FTIR spectra indicated that the biodefoamer used in this study was a polysaccharide, and ^{1}H NMR confirmed that the defoamer was a carbohydrate constituent. These characteristics of the biodefoamers produced by *Bacillus, Aeromonas, Klebsiella* and *Commamonas* spp. consortia show that it is competent for activated sludge that contains biofoamers. The results that are portrayed in this paper show that the consortium was isolated from poultry slaughterhouse wastewater and it produced biodefoamers that were used for PSW and activated sludge defoamation. These biodefoamers' foam reduction efficiency and foam decay rate were comparable to that of a synthetic defoamer, and it did not just reduce foam but also flocculated the sludge to prevent continuous foam regeneration and dosing. The microscopic analysis that was carried out in this study revealed that the synthetic silicone defoamer left oil residues in the sludge that harnesses filamentous growth and foam regeneration, which will require continuous dosing. This was the first study to compare a biodefoamer that is produced by a microbial consortium with a synthetic defoamer.

CHAPTER 5

BIOKINETIC MODELLING OF BIOFOAM DESTABILISATION BY BIODEFOAMERS IN POULTRY SLAUGHTERHOUSE WASTEWATER TREATMENT.

Submitted as: Cynthia Dlangamandla, Seteno K.O. Ntwampe, Moses Basitere, Boredi S. Chidi, Benjamin I. Okeleye, Ncumisa Mpongwana, Melody R. Mukandi. Biodefoamer supported activated sludge for the treatment of poultry slaughterhouse wastewater. Submitted to *Bioengineering (under review)*

CHAPTER 5

BIOKINETIC MODELLING OF BIOFOAM DESTABILISATION BY BIODEFOAMERS IN POULTRY SLAUGHTERHOUSE WASTEWATER TREATMENT

5.1 Introduction

Foams in conventional activated sludge (CAS) systems are generated by forcing gas into the continuous aqueous phase that contains surface-active substances as well as biofoamers, suspended, and dissolved solids. Activated sludge (AS) foaming occurs due to the design of the system, operational conditions, as well as the attributes of the wastewater (Garg et al., 2021) Chemical foams, are usually related to the presence of surfactants, whereas, biological foams result from the presence of biofoamers such as *Nocardia amarae*, *Microthrix parvicella*, and their bioproducts (Alizad Oghyanous, Etemadi and Yegani, 2020). Excessive biofoamation in wastewater treatment plants (WWTPs) leads to poor performance of the system and degrades the quality of the effluent (Collivignarelli et al., 2020). This leads to increased operational costs and environmental pollution. In order to curb these negative impacts that are caused by the presence of biofoam, foam have to be destabilised.

Foams are usually unstable two-phased colloids that contain polyhedral bubbles (gas) that are separated by a thin liquid layer that is called lamella (Trybala et al., 2019). Foam destabilisation occurs due to intermittent gaseous phase, bubble coalescence and collapse, liquid drainage, lamellae breakage as well as Ostwald ripening (Panizzolo, Mussio and Aón, 2012). This destabilisation can be enhanced by using synthetic defoamers which are short-chain hydrophobic alkanes that enter into the lamellae and dehydrates them (Dlangamandla et al., 2020). Though these defoamers can be efficient in foam destabilisation, they focus on removing the symptom, which is foam, and they do not prevent the proliferation of filamentous bacteria. They are relatively expensive, and they produce unwanted by-products such as trihalomethanes which can damage the AS biomass. Mangundu (Mangundu, 2017) suggested that novel approaches are required to overcome the shortcomings of the existing strategies. Biokinetic modelling of biofoam destabilisation is required to understand the processes such as foam drainage and foam collapse that results in foam distability in the presence of a biodefoamer or a synthetic defoamer (Dlangamandla *et al*., 2020).

Liu et al. (2019) suggested the use of specific bacteriophages that have a monospectrum for the reduction of biofoamers and reported that the use of $GordTnk_2$, $Gmal_1$, $GordDuk_1$, and $Gsput_1$ reduced *Gordonia* in

wastewater tenfold. Dyson et al. (2016) isolated specifically targeting bacteriophage from the wastewater that it was going to be tested against, and this bacteriophage managed to reduce *Skermania piniformis* which is a foam-forming bacteria. Two polyvalent DNA bacteriophages GTE2 and GTE7 lysed multiple spectrums of biofoamers (Ji et al., 2021). Pajdak-Stos et al. (2017) used rotifers *Lecane tenuiseta, Lecane inermis* and *Lecane pyriformis* to reduce *M. parvicella* and Eikelboom type 0092 filaments. However, the use of biological cells or their bio-products (biodefoamers) that are isolated directly from the poultry slaughterhouse wastewater (PSW) and tested for their activities in this study have a restricted bio-defoamation coverage in the literature. Hence the objective of this paper was to develop a kinetic model that determines foam destabilisation in the presence of biodefoamer; additionally, to quantify factors that are involved in foam destabilisation.

5.2 Objectives

- To identify the municipal MLSS (mixed liquor of suspended solids) microbial community in order to assess the presence of biofoamers present.
- To assess the biodefoamer-producing microorganisms on their ability to biodegrade FOG and NH_4^+-N.
- To design a bench-scale aeration column to assess the effect of reactor design and specifications on foamability and foam stability.
- To assess mathematical models on their ability to predict biodefoamation.

5.3 Results and discussion

The biodefoamer-producing isolates were characterized by sequencing 16srRNA using 27F and 1492R primers to amplify the target region. The products were put on NCBI BLAST search, and their sequences indicated that these isolates were *Bacillus subtilis* (gene accession number GCA_000009045.1), *Aeromonas veronii* (GCA_000204115.1), *Klebsiella grimontii* (UGJQ01000001.1), and *Comamonas testosteroni* (GCA_900461225.1). *Bacillus subtilis* was a gram-positive rod-shaped bacteria that had slimy and mucoid colonies, whereas *Aeromonas veronii*, *Klebsiella grimontii*, and *Comamonas testosteroni* were gram-negative rod-shaped bacteria that were gram-negative (Guo and Zhang, 2012; Chen *et al.*, 2019); Hubbard et al., 2020; Orsini et al., 2014). All of these species were biofilm-forming species that produce polysaccharide (e.g. carbohydrates) extracellular polymeric substances which are beneficial for activated sludge agglomeration (Dih, Jamaluddin and Zulkeflee, 2019). The activated sludge microorganism sequences were generated using metagenomics, indicating that the dominant foam formers in the activated sludge sample were *Nostocoida limicola*, *Gordonia kroppenstedtii*, *Candidatus Microthrix parvicella*, *Nocardioides insulae,* and *Bacteroides nordii*. These biofoamers are hydrophobic

actinobacteria that contain mycolic acids and produce biosurfactants to break down FOG such that they uptake it as a carbon source, characteristics which enhance biofoamation in AS (Diao et al., 2019).

5.3.1 Biodelipidation and biodegradation of ammonium nitrogen (NH_4-N)

In an activated sludge system the biological removal of nutrients such as nitrogen through nitrification and aerobic denitrification is extremely crucial to avoid eutrophication in receiving water bodies and to deprive biofoamers of the nutrients that they require to flourish (Yao et al., 2013). Biodelipidation is also significant because the biofoamers solubilise FOG by producing biosurfactants that enhance biofoam formation; thereby, the less the FOG, the more proliferation of biofoamers declines (Dlangamandla et al., 2021). The presence of a high concentration of FOG and NH_4^+-N can result in saponification which also increases foaming in bioreactors. An experiment was conducted to assess the growth of a consortium in lipid-laden wastewater and to investigate the ability of the consortium to biodegrade total nitrogen and FOG.

Figure 5.1 illustrates that the consortium sequentially used FOG and NH_4^+-N as it grew. It also indicates that the consortium at 216 h assimilated NH_4^+-N from 49 mg/L to 15.8 mg/L, showing that nitrification occurred due to the production of ammonium monooxygenase enzyme (AMO) by the consortium (Ma et al., 2019). However, from 96 to 120 h NH_4^+-N increased from 38 mg/L to 47 mg/L, showing that the consortium also produced nitrite reductase to denitrify the wastewater, and then it decreased again at 144 h to 38 mg/L. These results proved that the consortium simultaneously nitrified and denitrified (SND) the lipid-laden wastewater. Joo et al. (2013) bioaugmented an aerobic reactor that contained piggery wastewater with *Alcaligenes faecalis* no. 4 that portrayed simultaneous nitrification and aerobic denitrification characteristics. The consortium also biodelipidated the lipid-laden wastewater. Figure 5.1 shows that FOG decreased from a concentration of 170 mg/L to 6 mg/L, which indicates that the consortium also produced lipases which broke down the covalent bonds that attached the lipids through hydrolysis/semi-hydrolysis, and hence, FOG concentration declined (Mbulawa et al., 2018). The consortium did not produce foam when it was evaluated for foamability.

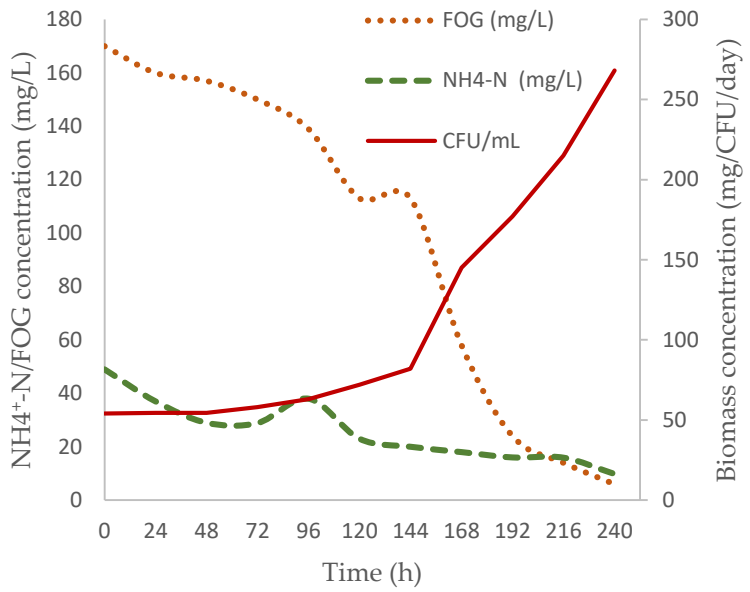

Figure 5.1: Consortium growth and biodegradation of $NH4^+$-N and FOG

5.3.2 Foamability/foam potential and foam stability of the MLSS

Foamability is the consumed sample volume from sparging 1 L of air (Nakajima and Mishima, 2005). It is crucial to determine the foamability/foam potential of a sample because it leads to foam stability (Dlangamandla et al., 2020), and it is an intrinsic factor of the wastewater to be tested (Collivignarelli et al., 2020). Figure 5.2 illustrates the foamability of the sample and the effect of MLSS concentration. For each of the tested samples, foamability increased as the concentration of MLSS increased, because MLSS contains planktonic EPS and protein material which led to increased foamability as the concentration increased. This was also due to sludge age – as the sludge grew older than 8 days, foaming occurred.

The MLSS used for this study was dominated by foam formers such as *N. limicola*, *G. kroppenstedtii*, *M. parvicella*, *N. insulae*, and *B. nordii*. These filamentous microorganisms are hydrophobic actinobacteria that contain mycolic acid which helps them to attach to the gas bubbles (Li et al., 2020). If they reach a critical micelle concentration beyond their level, they cause inter-floc deflocculation which leads to foaming and bulking of the activated sludge; moreover, their surface activity will increase (Blackall et al., 2000; Garg et al., 2020). The foaming of the activated sludge leads to the carrying over of suspended solids to the effluent, and this leads to the inefficiency of the system (Nierychlo et al., 2020). Hence, the foamability of the MLSS increased with an increase in concentration.

Foam stability was determined by using foam half-life tests using MLSS. These tests conveyed different results compared to the literature. Usually, foamability affects foam stability; however, in this study, these two were not interrelated. The highest foam stability of 5.1 cm was achieved using a 150 mL sample in a 250 mL foaming rector at 3080 mg/L MLSS concentration, which had a foaming potential of 51.3 mL/L. Meanwhile, the lowest foam stability of 0.94 cm was achieved when using a 250 mL sample with 4090 mg/L MLSS concentration in a 500 mL foaming reactor. This was the highest concentration of MLSS used in this study, with a foaming potential of 83.5 mL/L. So the reactor design specifications such as volume and diameters played a crucial role in the foam stability of the samples. Conventionally, foamability is portrayed as directly proportional to foam stability; however, this study proves that this is not always the case. Foamability in this study was not affected by the reactor designs; however, foam stability was.

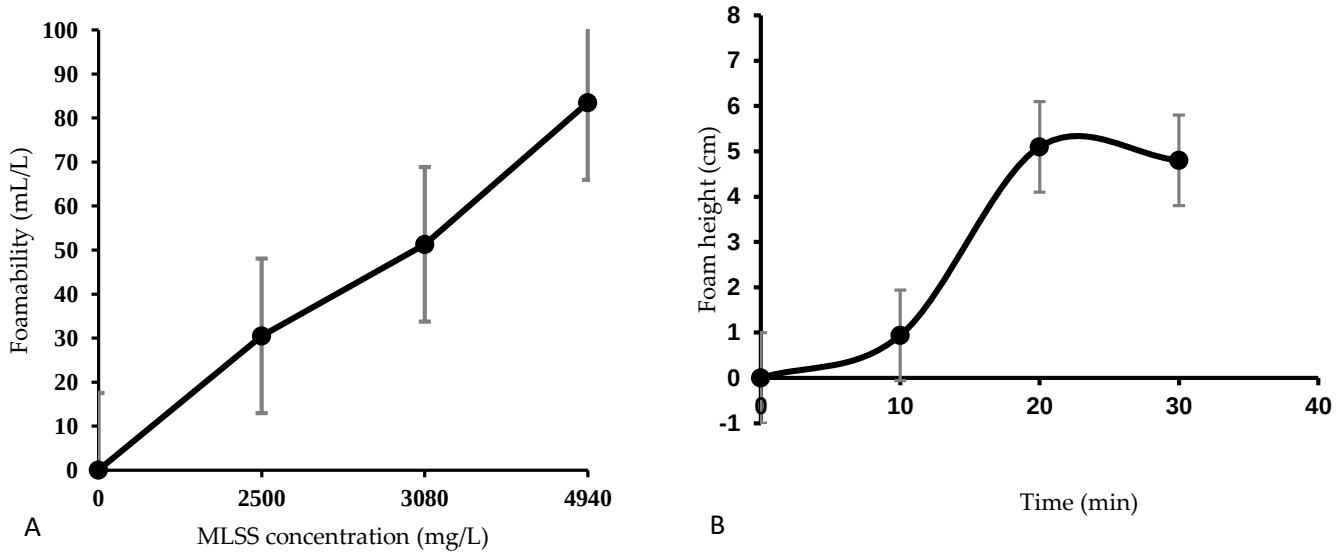

Figure 5.2: (A) shows the effect of MLSS concentration on foamability; (B) portrays the foam half-life of the biofoam

5.3.3 Foam drainage kinetics

Foamability and stability are immensely affected by foam drainage and collapse, which results from the pressure difference within the foam as well as the pressure gradients between plateau edges of the lamellae which result in lamellae rupture and foam destabilisation (Salager et al., 1999; Panizzolo, Mussio and Aón, 2012). Rate law, Monod's model, and exponential decay models were used to evaluate and estimate the foam drainage. This was observed by simulating the estimated model data in correlation with the experimental data using Polymath 6.0 software, which predicted the kinetic constants of each model,

moreover, by graphically illustrating the parity plots to determine the interrelation between the predicted and experimental values. The rate law and Monod's model had a better description of the foam drainage experimental data, with the determination co-efficients of (R^2) 1 and 0.99 respectively. Table 5.1 lists computed kinetic parameters for foam drainage.

Table 5. 1: Predicted kinetic parameters for foam drainage

Model	K_m	K_i	n	R^2	Variance
Rate law	-	9	-	1	6,99 E-19
$-\frac{dh}{dt} = r_a = k_i h^n$			14,62		
	-0.988	0.099	-	0.99	0.015
Monod's $-\frac{dh}{dt} = \frac{k_m * h}{k_i + h}$					
Exponential decay $-\frac{dh}{dt} = -k_i * h$	-	-0.014	-	-0.998	8.086

The adjusted R^2 for rate law, Monod's model, and exponential decay kinetics were 1, 0.99, and -0.99 respectively. The highest adjusted R^2 indicated that the rate law and Monod's models were significant in predicting the kinetic constants. The lowest variance of 6.99 E-19 and 0.015 shows that the estimated model produced using the predicted values indicated that they were similar to the experimental data. These models gave a better fit where R^2= 1 and 0.99, adj R^2= 1 and 0.99 and the standard deviation = 2.2 E-10 and 0.034 respectively. The exponential decay model had a poor estimation of foam drainage parameters (R^2= -0.99, adj R^2= -0.998, variance= 8.086 and standard deviation of 0.817). Ross, & Miles (Miles, 1944) studied foam drainage kinetics using a similar model to rate law, Pal et al. (2020)studied foam defoamation kinetics using a sonicator as a defoamer. Wang et al. (2016) also studied foam drainage kinetics.

5.3.4 Foam collapse kinetics

Foam collapse kinetics were analysed by using three models (generic rate law, Monod's, and exponential decay kinetics). This was achieved by simulating the predicted model and comparing it to the generated experimental data; additionally, plotting them together to determine the relationship between the model and the experimental data. The experimental data were fitted to the model such that kinetic constants can be predicted using Polymath 6.0 software. The generic rate law model was able to describe the experimental data of foam decay. The co-efficient R^2 was 0.98 (Table5.2).

Table 5. 2: Estimated kinetic parameters for foam decay rate models

Model	K_m	K_i	n	R^2	Variance
Rate law $-\frac{dh}{dt} = r_a = k_i h^n$	-	0.00011	0.781	0.98	0.0148
	5.96	0.439	-	0.62	0.038
Monod's $-\frac{dh}{dt} = \frac{k_m \times h}{k_i + h}$					
Exponential decay $-\frac{dh}{dt} = -k_i \times h$	-	0.0367	-	0.64	0.032

The adjusted R^2 for rate law, Monod's, and exponential decay kinetics were 0.98, 0.58, and 0.64 respectively. The highest adjusted R^2 indicates the significance of the model and its predicted kinetic constants. The significant model for this study was the rate law model. The minute variance 0f 0,0148 for the rate law model depicted that the estimated model produced, using the predicted parameters, was similar to the experimental data and it also gave a better fit (R^2= 0.98, adj R^2= 0.98, variance= 0,0148 and the standard deviation= 0.001). Monod's model had poor estimation of foam decay parameters (R^2= 0.62, adj R^2= 0.58, variance= 0.038 and standard deviation 0f 0.0053).

Polyuzhyn et al. (2016) studied the effect of a silicone deformer on foam destabilisation using an exponential decay model; in this study the rate at which the foam decayed/collapsed was proportional to foam height; hence volume and height in this equation can be used interchangeably. Polydzhyn et al. (2016) obtained R^2= 0.99, adj R^2= 0.98, variance= 0.021 and standard deviation of 0.00011, whereas when using the exponential decay model in this study R^2= 0.64, adj R^2= 0.64, variance= 0.032 and standard deviation of 0.051, which was insignificant. The foam collapse rate resembled a second-order degradation response (Verma, Chauhan and Ojha, 2018). In Fig. 5.3 (a), the R^2 of Monod's equation was 0.77, which was higher than the 0.62 obtained when data were assimilated into the experimental values. Since the model does not show consistency, it was not a better fit for the experimental data used in this study. However, the R^2 for the generic rate law was consistent with the assimilation plot; hence it was a better fit for foam decay. The mathematical model that had the ability to predict biodefoamation was the generic rate law model.

Models

Monod's

$$-\frac{dh}{dt} = \frac{k_m \times h}{k_i + h}$$

Rate law

$$-\frac{dh}{dt} = r_a = k_i h^n$$

Consistency plots

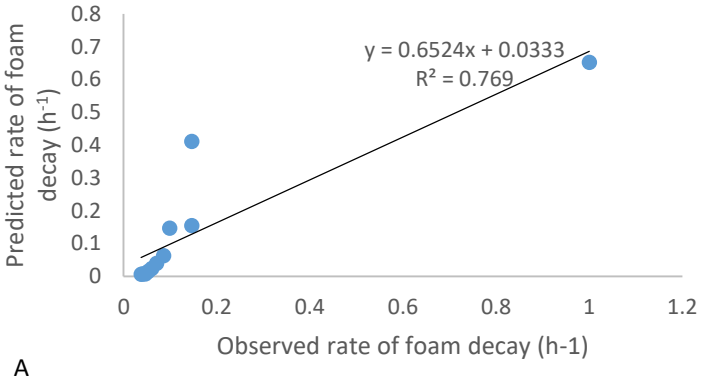

A

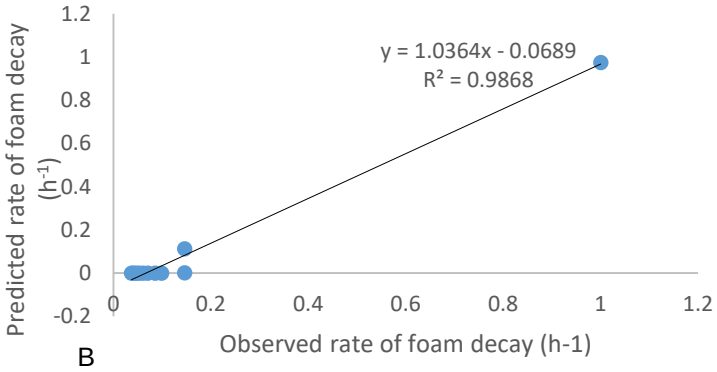

B

Incorporation of models into experimental data

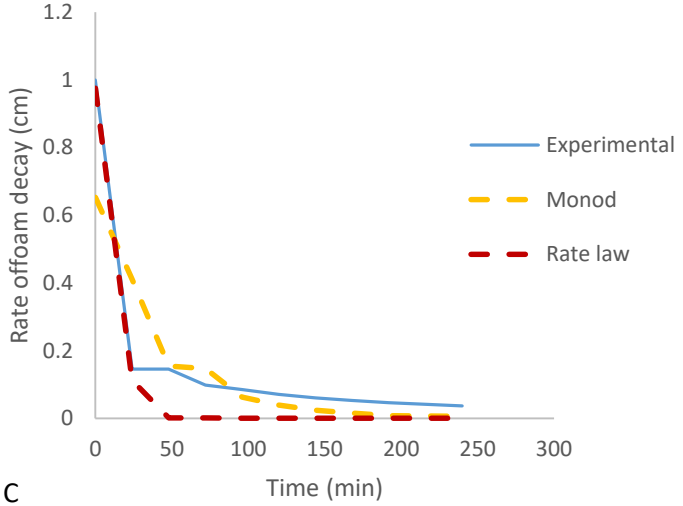

C

Figure 5.3: : Consistency plots of predicted data versus (a) Monod's model, (b) Rate law. (c) Incorporation of model values into foam decay experimental data (Monod's and Rate law)

5.5 Conclusion

The MLSS community was identified using metagenomics to assess the presence of bioamers and the results depicted that it did contained the biofoamers *Nostocoida limicola*, *Gordonia kroppenstedtii*, Candidatus *Microthrix parvicella*, *Nocardioides insulae*, and *Bacteroides nordii* which resulted in high foamability and stability and produced stable foams. The growth of *Bacillus subtilis* (gene accession number GCA_000009045.1), *Aeromonas veronii* (GCA_000204115.1), *Klebsiella grimontii* (UGJQ01000001.1), and *Comamonas testosteroni* (GCA_900461225.1) consortium was unaffected by a high concentration of NH_4^+-N and high lipid content of the PSW. This consortium proved that it could biodegrade NH_4^+-N and FOG. This revealed that the biodefoamer producing microorganisms were able to degrade FOG and NH_4^+-N. The highest foam stability of 5.1 cm was achieved using 250 mL and low foaming potential of 51.3 mL/L; whereas, the lowest foam stability of 0.94 cm was achieved when using 500 mL and with a highest foaming potential of 83.5 mL/L. So, the reactor specifications played a huge role in both foamability and foam stability. The mathematical model that could predict biodefoamation both foam drainage and collapse better than the other ones used in this study was the rate law model. This modelcould predict both foam drainage and collapse with high R^2 and adjacent R^2 values. Moreover, it had low values for variance and standard deviation and these aspects are a requirement for a good predictive model. Although this consortium's capability to destabilize biofoam is high, its biological and physicochemical attributes require more exploration for a better understanding of the mechanism that is used by these microbes for biodefoamation and to optimise the biofoam destabilisation efficiency. All the objectives for this chapter were achieved.

.

CHAPTER 6

ANTAGONISTIC CHARACTERISTICS OF BIODEFOARMERS AGAINST BIOFOAM FORMERS IN POULTRY SLAUGHTERHOUSE WASTEWATER

***Submitted as*: Cynthia Dlangamandla**, Seteno K.O. Ntwampe, Moses Basitere, Boredi S. Chidi, Benjamin I. Okeleye, Ncumisa Mpongwana, Melody R. Mukandi. Antagonistic characteristics of biodefoamers against biofoam formers in poultry slaughterhouse wastewater. Submitted to *Bioengineering (under review)*

CHAPTER 6

ANTAGONISTIC CHARACTERISTICS OF BIODEFOARMERS AGAINST BIOFOAM FORMERS IN POULTRY SLAUGHTERHOUSE WASTEWATER

6.1 Introduction

Foaming in conventional activated sludge (CAS) wastewater treatment systems is a complex phenomenon that can be influenced by various factors such as certain microorganisms and their byproducts whose growth is influenced by environmental factors, nutrients, and the inorganic and organic makeup of the wastewater, such as fats, oil and grease as well as proteins (Collivignarelli et al., 2017). The overgrowth of foam formers occurs due to poor operational conditions, which leads to poor sludge settleability, and this results in blockage of pipes reduces oxygen transfer efficiency, and leads to the presence of suspended solids that appear in the influent; moreover, this results in increased operational costs (Deepnarin et al., 2019). The common foam formers are filamentous mycolic acid-producing microorganisms (Rosso et al., 2018). The current methods that are used for biofoam removal are synthetic methods that are toxic to people and the environment; therefore, there is a need for the development of new methods that are environmentally friendly, less harmful to people, and economical.

Poultry slaughterhouse wastewater contains biological characteristics such as fats, grease, proteins, scum, suspended solids, nitrogen, phosphorous, and high chemical and biochemical oxygen demand concentrations, which indicates that this wastewater is toxic but amenable to biological treatment. Its constituents favour filamentous growth; hence, when it is discharged to a municipal wastewater treatment plant (WWTP) that utilizes CAS, it disrupts the mixed liquor suspended solids (MLSS) as well as the floc-formers, which leads to biofoaming and the requirement of a synthetic defoamer that will further disrupt the biological makeup of the activated sludge. This necessitates the use of biological

treatment before disposal of the wastewater. Biodefoamers are biodegradable and economically friendly biopolymers that are produced intra- and extra-cellularly by bacteria during cell growth and cell lysis, and which act as a bioadhesive to enhance floc formation and simultaneously eliminate biofoam.

The biodefoamers improve defoaming efficacy, improve drainage, reduce the use of chemicals, have energy-saving potential, and improve flocculation (Bajpai, 2015). Whitey et al. (2015) and Khairnar et al. (2014 used specific bacteriophages that targeted certain mycolata species that decreased the number of filaments, thereby reducing biofoam formation, whereas Petrovski et al. (2017) used multispectrum bacteriophages which reduced the number of filaments. Pajak-Stos et al. (2017) used rotifers that ingested the filaments and reduced their excessive growth, which then decreased foam formation and enhanced sludge flocculation. This study focused mainly on the ability of the microorganisms to produce biodefoamer in the presence of PSW and activated sludge microbial communities. The microorganisms that can produce biodefoamers in the presence of these communities are deemed appropriate for biodefoamer-supported activated sludge systems.

6.2 Objectives

- To assess biodefoamer-producing microorganisms for their ability to grow and degrade high FOG and protein concentrations.
- To test these microorganisms on their ability to produce biodefoamers that can reduce foam efficiently.
- To assess the biodefoamer antimicrobial activity in terms of volumetric zones of inhibition (VZI) against the PSW and MLSS microbial community.

6.3 Results and discussion

6.3.1 Microbial and MLSS amplicon identification

The biodefoamer-producing isolates were characterized by sequencing 16srRNA using 27F and 1492R primers to amplify the target region. The products were put on NCBI BLAST search and their sequences indicated that these isolates were *Bacillus subtilis* (gene accession number GCA_000009045.1), *Aeromonas veronii* (GCA_000204115.1), *Klebsiella grimontii*

(UGJQ01000001.1), and *Comamonas testosteroni. Bacillus subtilis* was a gram-positive rod shape bacteria which had slimy and mucoid colonies, whereas *Aeromonas veronii, Klebsiella grimontii and Comamonas testosteroni* were *gram-negative rod shaped bacteria* (Guo and Zhang, 2012; Orsini *et al.*, 2014; Chen *et al.*, 2019; Hubbard *et al.*, 2020). All of these species were biofilm-forming species that produce polysaccharides (e.g. carbohydrates), extracellular polymeric substances which are beneficial for activated sludge agglomeration (Dih, Jamaluddin and Zulkeflee, 2019). The activated sludge microorganism sequences were generated using metagenomics indicating that the dominant foam formers in the activated sludge sample were *Nostocoida limicola, Gordonia kroppenstedtii, Candidatus Microthrix parvicella, Nocardioides insulae,* and *Bacteroide nordii*. These biofoamers are hydrophobic actinobacteria that contain mycolic acids and produce biosurfactants to break down FOG such that they uptake it as a carbon source, characteristics that enhance biofoamation in AS (Diao *et al.*, 2019).

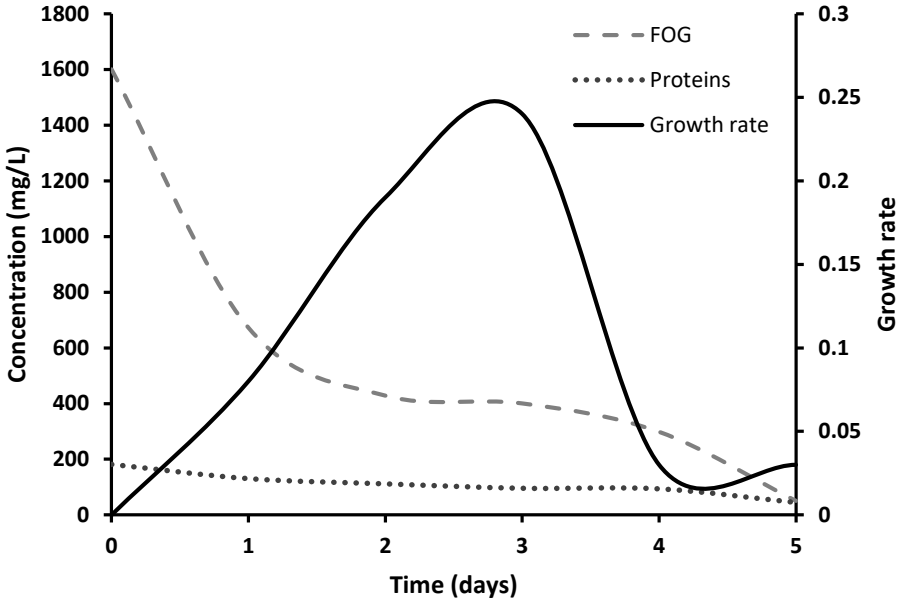

Figure 6.1: Microbial growth rate and biodefoamer production in the presence of PSW and MLSS microbial community

Poultry slaughterhouse wastewater is made up of high protein and lipid content which may lead to the inefficiency of the biological wastewater treatment system (Dlangamandla, Ntwampe and Basitere, 2018; Dyosile et al., 2021). Proteins contribute 30-60% of activated sludge EPS and they are made up of nitrogen, hydrogen carbon, and oxygen. They contribute about 29–49 % of total organic carbon (TOC) and they are the major constituents of organic nitrogen (Westgate, 2009). The inorganic nitrogen can be reduced in the process of nitrification and denitrification; however, organic nitrogen is complex and it results in high oxygen demand that leads to eutrophication, lysis of aerobes which are critically required for the efficiency of AS, and they deteriorate the secondary treatment (Bai and

Liao, 2019; Miao et al., 2019). However, FOG-laden wastewater like PSW results in the accumulation of actinomycetes which contains hydrophobic cells, produce surfactant to breakdown FOG molecules and can float onto the surface of the aeration which results in foam formation(Ifeoluwa et al., 2021).

In this study, microbial growth rate (μ_g) concerning the biodegradation of FOG and protein in the presence of PSW and MLSS nutrients was assessed (see Figure 6.1). During the lag phase on day 0, there was minimal growth rate and minute removal of FOG and protein concentration. This was because the microorganisms were still adjusting to the new environmental conditions (Bertrand, no date). Log phase or exponential phase began on day 1 when microbial community and cells were doubled in number through cell division that was caused by adaptation of the cells to the growth media as well as the environmental growth conditions; the highest growth rate was observed on day 3 (Rolfe et al., no date). During this phase there was also an exponential reduction of FOG (from 672 mg/L on day 1 to 400 mg/L on day 3). This reduction was due to escalation in biomass, adsorption of the lipids into activated sludge flocs by the DLVO forces, microbial hydrolysis of lipids by the biodefoamers that produced lipases as well biosynthesis through active transport that was facilitated by specialized proteins and direct diffusion into the cells (Chipasa and Mdrzycka, 2008). Chipasa and Mdrzycka (2008) carried out a study where an influent with 2000 mg/L of lipids was treated in the activated sludge system and this concentration of FOG was reduced up to 300 mg/L in the permeate, which suggested that lipids in activated sludge cannot be reduced below this concentration. The proteins were also reduced (from 130,8 mg/L on day 1 to 96 mg/L on day 3), which was also influenced by adsorption. The death phase was initiated on day 4 and continued until day 5. During this period there was nutrient depletion, which resulted in a high accumulation of toxins that were produced by the microorganisms to survive. This led to cell lysis, during which microorganisms produce EPS and IPS which contain enzymes that lead to a high reduction of proteins and FOG. The biodefoamer activity in term of foam reduction efficiency over time in days (0-5) was assessed and calculated using equation 3.1 and 3.2 (see Figure 6.2).

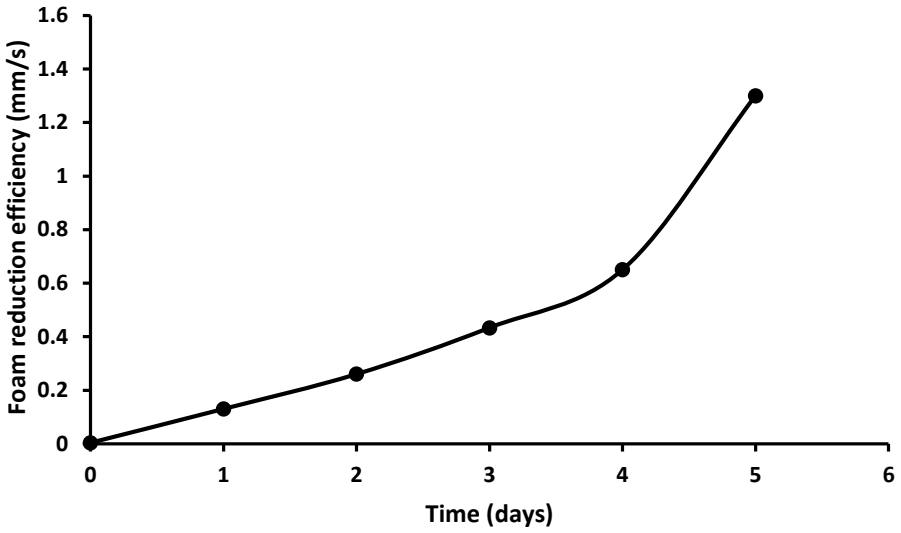

Figure 6.2: Foam reduction efficiency

Biodefoamer activity was also examined in terms of foam reduction efficiency (Figure 6.2). The lowest foam reduction occurred on day 0, which was influenced by high protein and FOG concentration. Proteins are detersive, decrease surface tension, adsorb in the gas-liquid interface and stabilize it, lower surface tension, increase viscosity and elasticity, and decrease foam drainage, which results in stable foams (Ifeoluwa et al., 2021). Whereas a high concentration of FOG also contributed to the low foam reduction since the long-chain fatty acids entered the lamellae and stabilized the foam, FOG was also biodegraded and solubilized by actinomycetes through the production of biosurfactants that further stabilized the foam (Cisterna-osorio and Arancibia-avila, 2019). The highest foam reduction efficiency of 1.3 mm/s was achieved on day 5. This was due to fact that the biodefoamers' bacterial cells and EPS adsorbed into the MLSS and enhanced sludge flocculation(Shi et al., 2017). This graph showed that biodefoamer production did not occur during microbial growth only, it also occurred during cell lysis on days 4 and 5. This was attributed to the fact that these microorganism's cells produced intracellular polymeric structures, biodefoamers that were able to defoam.

6.3.2 Volumetric zones of inhibition

It is of great importance to test the biodefoamers' ability to inhibit the growth of PSW and MLSS communities in order to assess the compatibility of the defoamer against these microbial communities. This enables the consortium to develop survival mechanisms in the presence of the resident bacteria, this will enhance their activity, growth, and help them to adapt to the environmental stressors. The highest growth inhibition of 1.39 L/mL was observed when the consortium was used (see Figure 6.3). This reveals that the consortium survived in the presence of PSW and MLSS community due to

destruction, neutralisation as well as inactivation (Chen et al., 2018; Kang et al., 2017; Li et al., 2020) The literature reviewed showed that growth inhibition commonly occurs due to toxin production (Ejaz et al., 2020). The lowest growth inhibition of 1.32 L/mL was noticed when a biodefoamer produced by *Aeromonas veronii* and *Klebsiella grimontii* was used. This shows that the microorganisms survive better as a consortium than as co-cultures, meaning that the consortium grew competitively as compared to the resident microbial community and this shows that the consortium can be able to survive in biodefoamer activated sludge and produce biodefoamer.

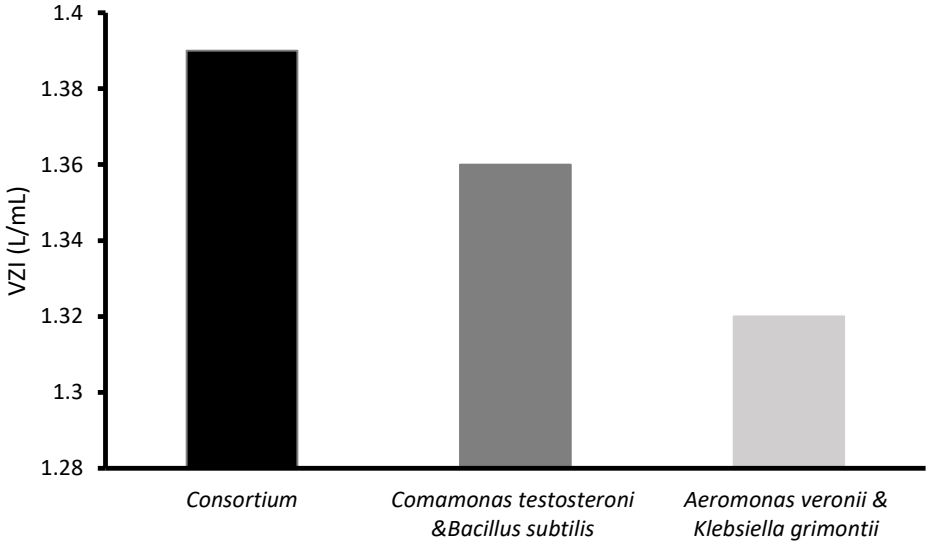

Figure 6.3: Volumetric zones of inhibition of crude biodefoamer that was produced by the consortium in comparison to biodefoamers produced by co-cultures

6.4 Conclusion

The biodefoamer producing microorganisms were able to grow exponentially to a growth rate of 0.44 on day 3. It was concluded that the biodefoamer-producing microorganisms can grow and degrade FOG from 1600 mg/L on day 0 to 400 mg/L on day 3. FOG from 1600 mg/L on day 0 to 400 mg/L on day 3. FOG from 1600 mg/L on day 0 to 400 mg/L on day 3. It was also observed that it can reduce proteins from 182 mg/L on day 0 to 96 mg/L on its exponential growth phase on day 3. Furthermore, when these microorganisms were tested for their ability to produce biodefoamers that can reduce foam efficiently they had the highest foam reduction efficiency of 1.3 mm/s on day 5, this depicted that these defoamers were not only produced during cell exponential growth phase; however, they were also be produced intracellularly during cell lysis. The biodefoamer that was produced from the culture also had antimicrobial activity against PSW and MLSS microbial communities. The biodefoamers were assessed for their antimicrobial activity in terms of volumetric zones of inhibition, the lowest VZI of 1.32 L/mLwas observed when the co-culture of *Aeromonas veronii* and *Klebsiella grimontii* was used and the highest VZI of 1.39 L/mL was achieved when the consortium was used meaning that the

microorganisms were more competent as a community than as co-cultures. All the objectives of this section were achieved.

CHAPTER 7

BIODEFOAMER SUPPORTED ACTIVATED SLUDGE FOR THE TREATMENT OF POULTRY SLAUGHTERHOUSE WASTEWATER

Submitted as: Cynthia Dlangamandla, Melody R. Mukandi, Ncumisa Mpongwana, Seteno K.O. Ntwampe, Moses Basitere, Boredi S. Chidi and Benjamin I. Okeleye. Biodefoamer supported activated sludge for the treatment of poultry slaughterhouse wastewater. Submitted to *Bioengineering (under review).*

CHAPTER 7

BIODEFOAMER SUPPORTED ACTIVATED SLUDGE FOR THE TREATMENT OF POULTRY SLAUGHTERHOUSE WASTEWATER

7.1 Introduction

Wastewater treatment, management, and reuse is a promising solution to improving the water crisis, especially in semi-arid countries such as South Africa (Meyo et al., 2021). To protect the environment and aquatic life, it is necessary to treat wastewater before discharging it into fresh water (Rinquest et al., 2019). Various methods such as physical, mechanical, chemical, and biological methods can be used, depending on the type of wastewater generated, depending on the constituents of the wastewater to be treated (Dlangamandla et al., 2018). Poultry slaughterhouse wastewater (PSW) is toxic and decreases in dissolved oxygen concentration, which leads to eutrophication if it is discharged untreated into the environment (Dlangamandla et al., 2016). It contains high chemical oxygen demand (COD), biochemical oxygen demand (BOD_5), nitrogen, phosphorous, pathogenic microorganisms, blood, faecal matter, soluble proteins, FOG as well as suspended solids. These characteristics make PSW amenable to biological treatment (Basitere et al., 2016). The high lipid content of the PSW leads to biofoamation and excessive growth of filamentous bacteria which leads to sludge floatation (Affes et al., 2017). There is a need to treat such wastewater to protect aquatic life, prevent environmental pollution, and prevent the poultry slaughterhouses from paying extra levies for disposing of their untreated wastewater to the municipal wastewater treatment system (Meyo et al., 2021).

Biological wastewater treatment systems involve aerobic, anaerobic and wetland systems; all of these systems use biological cells for bio-augmentation (Kim et al., 2020). The anaerobic systems require the use of simple systems, require less energy, have high BOD_5 removal efficiency, and produce biogas; however, high-strength wastewater (which contains a high concentration of FOG, proteins, TSS, and

COD) harms the treatment efficiency of these systems; moreover, it requires an aerobic post-treatment system to enhance microbial community contact time to improve COD and BOD_5 by 91%, as well as to remove total phosphorous (TP), total nitrogen (TN) as well as pathogenic microorganisms ((Meiramkulova *et al.*, 2020; Baker *et al.*, 2021; Njoya *et al.*, 2021). The aerobic and anaerobic systems can be integrated to improve the performance of the system e.g. integrated aerobic/anaerobic sequential batch reactor (IAASBR) and anaerobic fluid bed reactor (AFBR), etc. (Rajab et al., 2017; Ardestani & Abbasi, 2019). However, the aerobic systems such as sequential batch reactors, granular aerobic sludge (GAS), activated sludge (AS) and biodefoamer-supported dissolved air flotation use aerobic microorganisms to flocculate the microbial cells and to improve the flocculation of suspended solids as well as FOG (Aziz et al., 2018; Dlangamandla et al., 2018; Septiana et al., 2019). The oxygen concentration can be adjusted depending on the wastewater strength. This system improves ammonia oxidation, reduces TP, TN, COD, BOD_5 suspended solids (SS), biomass is recycled, and it increases microbial density. This enhances biodegradation of organic matter and it is cost-effective and efficient (Baker et al., 2021).

AS systems are largely used in municipal wastewater treatment systems, and for livestock and poultry slaughterhouse wastewater treatment (Masoumi et al., 2015). The disadvantage of this treatment system especially in poultry slaughterhouse wastewater treatment systems (PSWWTs) is the prevalence of biofoam, which occurs due to the presence of protein and FOG in the wastewater. To overcome this problem, synthetic defoamers have been in use, however, reports have shown that they are toxic to humans and the environment; hence there is a need to produce biodefoamers (Mangundu, 2017; Dlangamandla et al., 2021). Biodefoamers are produced by microbial cells during growth and cell lysis, and enhance the removal of FOG, thereby depriving the biofoamers of the nutrients that they require to grow. This improves the bioflocculation of the wastewater, biodegradation of organic matter, and the quality of the wastewater. They also prevent foam formation that is caused by biofoamers, especially the nuisance actinomycetes that cause sludge deflocculation, thereby improving the efficiency of an activated sludge treatment system (Dlangamandla et al., 2021). This study aimed to apply biodefoamers that were produced by a PSW consortium in an activated sludge designed bench scale in the treatment of PSWW and assess its efficiency in the removal of FOG suspended solids, proteins, and COD in PSW,

which are the main cause of foam in activated sludge; and further to compare this system (a) to synthetic defoamer-supported activated sludge (Syn-AS) and (b) to a control system that did not contain any defoamer (CAS).

7.2 Objectives

- To isolate, identify and asses biodefoamer-producing microorganisms from PSW.
- To design a bench-scale activated sludge system.
- To assess the design for the removal of FOG, proteins, TSS, and COD when supported by biodefoamers (Bio-AS), when supported by chemical or synthetic defoamers (Syn-AS), and when operated conventionally (CAS).

7.3 Results and discussion

7.3.1 Bacterial identification

The biodefoamer-producing isolates were characterized by sequencing 16srRNA using 27F and 1492R primers to amplify the target region. The NCBI BLAST search and their sequences indicated that these isolates were *Bacillus subtilis* (gene accession number GCA_000009045.1), *Aeromonas veronii* (GCA_000204115.1), *Klebsiella grimontii* (UGJQ01000001.1), and *Comamonas testosteroni* (GCA_900461225.1). They were found to produce defoamers with high foam removal efficiency and high foam decay rate; in chapter 4 and they were assed for their antimicrobial activity in chapter 6 and they were deemed appropriate to be used for the designed AS; hence they were used in the designed biodefoamer-supported activated sludge system see Fig. 4.2.2; hence, they were used in the designed biodefoamer-supported activated sludge system (see Fig. 7.1).

7.3.2 Activated sludge treatment performance

Lipids are determined as fats, oil, and grease which are long-chain fatty acids that are the constituents of the PSW (Dlangamandla et al., 2018). A high concentration of FOG results in the removal of dissolved oxygen (DO), pipe blockages, and deflocculation of sludge in the secondary clarifier. They are degraded at a lower rate compared to sugars, and their accumulation enhances the growth of filamentous bacteria that results in biofoaming in the activated sludge treatment system (Collin et al., 2020). Fig. 7.2 (a, d, g, j) represent the characteristics of the PSW (FOG, protein, TSS, and COD) that

was fed into the activated sludge aeration tank. These attributes fluctuated over time, and they depict the higher concentration of FOG, TSS, and COD. These characteristics were influenced by various factors such as sampling time (slaughtering time) as well as external factors such as temperature.

Figure 7.2(c) illustrates that during unsteady state, FOG removal was between 53.3% and 85.3% in Bio-AS as compared to 29.6% and 74% achieved in the Syn-AS. During the transition, state FOG was removed by 84.2% in the Bio-AS, whereas only 73% was removed in the Syn-AS. In the course of the steady state FOG, removal increased from 82,3 to 94% at steady state (day 10) for the Bio-AS, in contrast to Syn-AS which acquired 74% and 50% during steady state (on days 4 and 10). Moreover, during the steady state, CAS acquired 72.3% and 62.5% FOG removal (days 4 and 10). The removal of lipids in the Bio-AS was facilitated by the presence of the competitive 48 h acclimated consortium that produced polysaccharide biodefoamers during their growth, which contained multiple charges that attracted the charge of the amphiphilic lipid and facilitated sludge agglomeration. These biopolymers were less affected by environmental conditions, hence an increase in lipid removal was observed (Pu et al., 2020). Furthermore, their presence destabilized the covalent bonds of the lipids and enhanced hydrolyzation (Mbulawa et al., 2018). In the Syn-AS system, the FOG removal decreased as the days increased (day 5-10) and this was subjected to the fact that the biomass in the activated sludge was still adjusting to the presence of the synthetic defoamer. Additionally, as the days increased, the oily defoamer resulted in sludge bed congestion, which led to an inactive microbial community and subsequent reduction in biodegradation of FOG. Furthermore, this revealed that the FOG adsorbed into the sludge resulting in overgrowth of saponified hydrophobic microorganisms that cause major problems downstream, such as sludge deflocculation, biofoaming, and suspended biomass, which also contributes to increased suspended solids concentration in the reactor (Chipasa and Mdrzycka, 2008; Damasceno et al., 2018). FOG also results in an increased organic load that requires additional energy consumption due to increased aeration demand in the secondary clarifier, hence 35% of COD is in FOG form (Dehghani et al., 2014; Collin et al., 2020).

In this study, the protein removal was quantified to assess the design efficiency of Bio-AS, Syn-AS, and CAS on the removal of protein that causes biofoamation. Figure 7.2 (d) shows that initially, the raw PSW that was fed into the Bio-AS contained 96 mg/L of protein. During days 0 to 2, the Bio-AS

aeration tank removed protein between 50,2% and 51%. During day 3, protein depreciation was 51.5% and the highest average protein removal obtained during days 4 to 10 was 99%. The PSW that was fed into the Syn-AS contained 29.4 mg/L of soluble proteins and the protein removal observed was between 5% and 57% during the unsteady state, while the highest removal during the steady state was 92% on day 5. The CAS was fed with a concentration of 31 mg/L soluble protein and the highest protein removal achieved during the steady state was 72%. These systems can reduce the soluble proteins; however, Bio-AS achieved the highest protein removal due to the presence of a biodefoamer that also enhanced sludge flocculation in the presence of oxygen.

A high concentration of TSS affects the turbidity of the treated wastewater and harms water quality as well as aquatic life (Sadeddin et al., 2011). Figure 7.2 (h, i) graphically illustrates the removal of TSS by Bio-AS, Syn-AS, and CAS at unsteady, transitional, and steady state. At an unsteady state (days 0-2), the Bio-AS removed 55.3% of TSS. During the transition state (day 3), 39% of the TSS was decreased; during the steady state (day 10), the highest TSS reduction was 88%. This indicated the effectiveness of biodefoamer-producing microorganisms against PSW and activated sludge microorganisms. The 48 h acclimated biodefoamer-producing culture was added to enhance the attachment of the planktonic colloids into the sludge; this was due to charge neutralization of the surface charge of the solids and the biodefoamer. The synthetic defoamer (Antifoam A concentrate) used in the Syn-As contained active silicon. Solubility and hydrophobicity of a defoamer are important for the effectiveness of the defoamer; however, these conditions are not favourable for the activated sludge microbial culture (Mohamad Pauzi *et al.*, 2019). Throughout the unsteady state, TSS removal in Syn-AS ranged between 5.2% and 86%, whereas through the transition state it increased to 34% %; during steady state, the highest TSS removal obtained was 59% in the aeration tank.

A high concentration of COD in wastewater is an indication of high oxidizable organic and inorganic matter that leads to a decrease in DO, and this creates an anaerobic environment which deteriorates the efficiency of an aerobic treatment system. As depicted in figure 7.2 (k and l), during steady state (day 10) the Bio-AS, achieved the highest COD removal of 60.2 % achieved on day 10. Syn-AS attained 24.4 % removal during unsteady state (day 1) but reached a maximum of 41.2% later on during steady state (day 6). Though the aeration tank can decrease the organic contaminants that are present in the

wastewater a secondary clarifier is necessary to further improve the quality of the wastewater by settling down the aggregates and clarifying the wastewater.

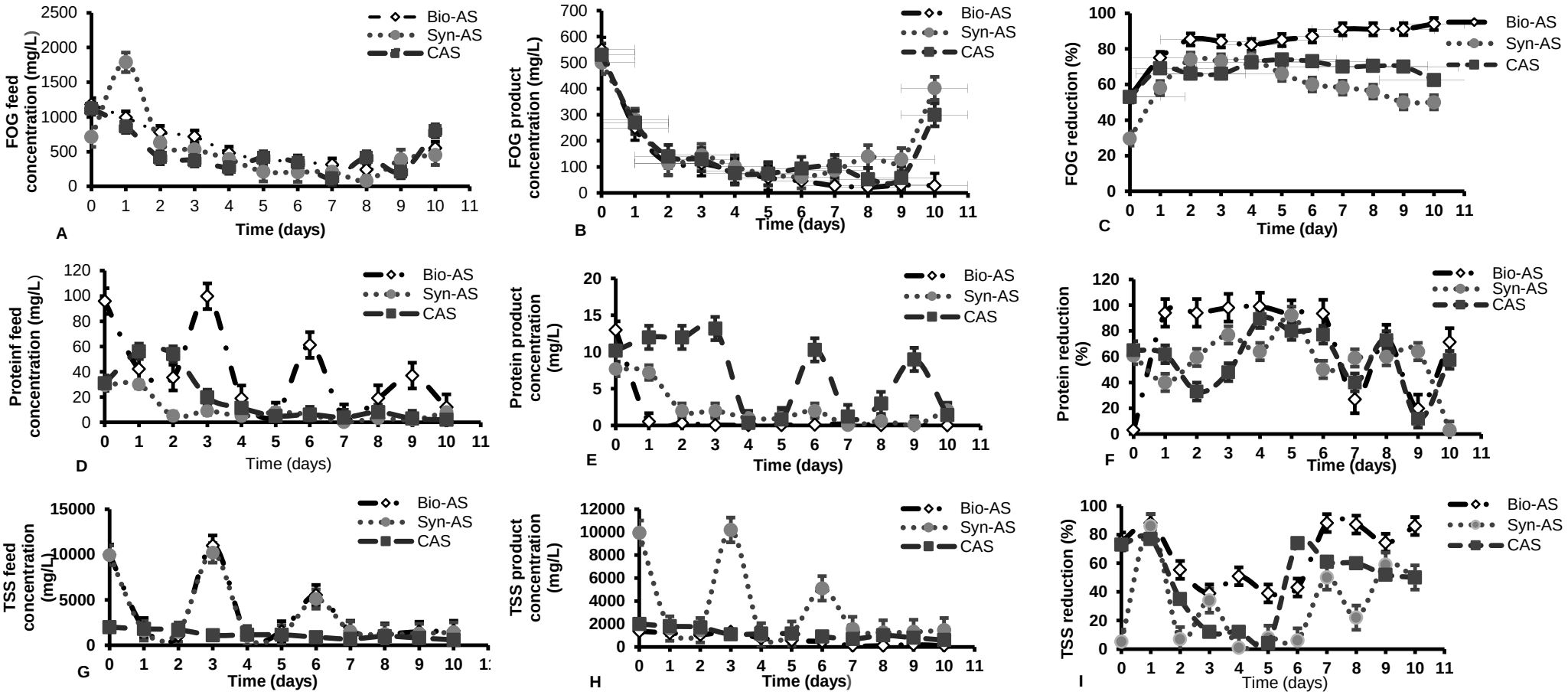
FOG feed concentration (mg/L)
Time (days)
A
Bio-AS
Syn-AS
CAS
FOG product concentration (mg/L)
Time (days)
B
FOG reduction (%)
Time (day)
C
Proteinf feed concentration (mg/L)
Time (days)
D
Protein product concentration (mg/L)
Time (days)
E
Protein reduction (%)
Time (days)
F
TSS feed concentration (mg/L)
Time (days)
G
TSS product concentration (mg/L)
Time (days)
H
TSS reduction (%)
Time (days)
I

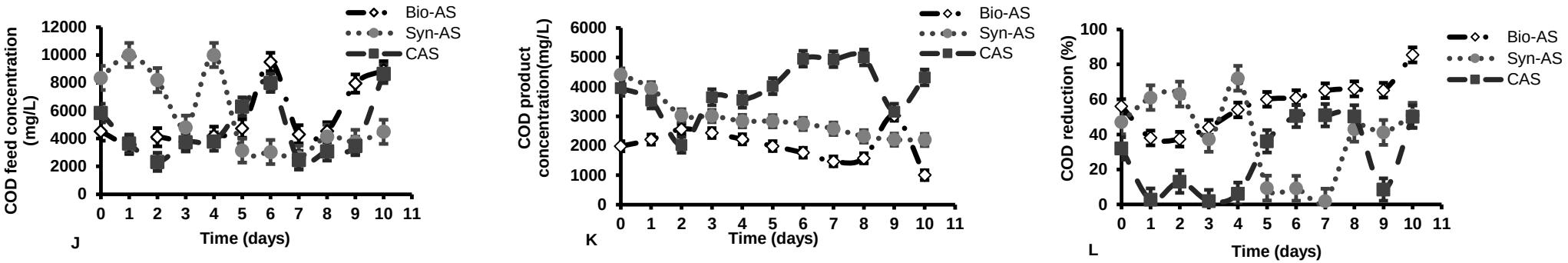

Figure 7.1: FOG Feed (a), aerobic tank FOG product concentration (b), and (c) reduction profiles. (c). Protein feed concentration (d), aerobic tank protein product concentration (e) protein concentration reduction profile (f), TSS feed (g), product concentration (h) reduction profile (i), COD feed (j), product concentration (k) and reduction profile (l). All of the above profiles were operated under Bio-AS, Syn-AS and CAS.

7.4.3 Secondary clarifier performance

In the secondary clarifier, the processed raw wastewater from the aeration tank was held in a tank such that the aggregated biological flocs settled at the bottom of the tank due to gravity and density dissimilarities that were adequate to subdue suspension due to turbulence. The aeration tank product was fed into the sedimentation tank or secondary clarifier, where further FOG removal took place. The highest FOG removal observed during steady state in Figure 7.2 (c), for Bio-AS, Syn-AS and CAS were 64.3%, 64%, and 63.3% respectively. Despite the decrease in Bio-AS FOG removal on day 2, days 5 to 8, the Bio-AS secondary clarifier efficacy improved. The secondary clarifier FOG influent concentration was relatively low, hence, the decrease in FOG concentration reduction.

Figure 7.3(f) graphically illustrates the reduction of soluble protein reduction when the AS was operated under the Bio-AS conditions. During steady state (day 4), the Bio-AS achieved a maximum of 99% protein reduction, whereas during steady state (day 5), the Syn-AS removed a maximum of 92.2%; moreover, the CAS minimized soluble protein concentration by 89.3% during steady state (day 4). Furthermore, liquid-solid separation was noted due to TSS concentration removal. The highest TSS removal for the Bio-AS of 88% was obtained during steady state (day 7), which shows that the macroflocs with higher density than the wastewater were created by the presence of the biodefoamer, and the sludge flocculation occurred, which ensured good solid-liquid separation. During unsteady state (day1), the Bio-AS obtained the highest protein reduction of 88%, whereas the Syn-AS achieved the highest removal of 86% and the CAS attained 77%. The Bio-AS removed COD concentration by 67% during steady state (day9), whereas the Syn-AS achieve the highest COD removal of 44.1 % during unsteady state (day 1), and the CAS achieved COD removal of 43,2% during steady state (day 7). It can be observed that the Bio-AS was consistent in the removal of FOG, protein, and TSS, as it removed FOG up to 10 mg FOG/L in the final effluent, which was less than 400 mg FOG/L. It minimized TSS concentration up to 100 mg TSS/L in comparison to the discharge standard concentration of 100 mg TSS/L and depreciated COD concentration up to 400 mg/L that was less compared to the ≤5000 mg COD/L according to the City of Cape Town (CoCT) discharge standards.

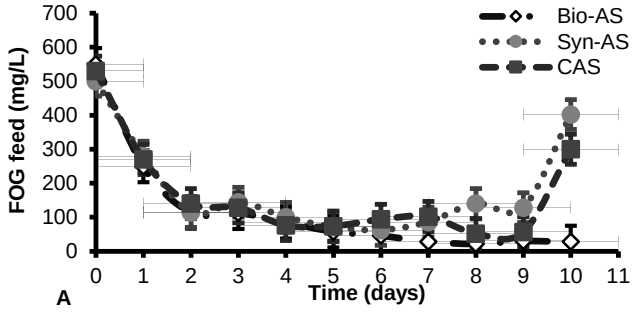
FOG feed (mg/L)
Time (days)
Bio-AS
Syn-AS
CAS
A

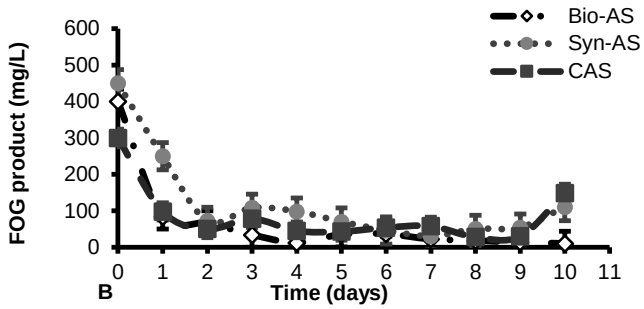
FOG product (mg/L)
Time (days)
Bio-AS
Syn-AS
CAS
B

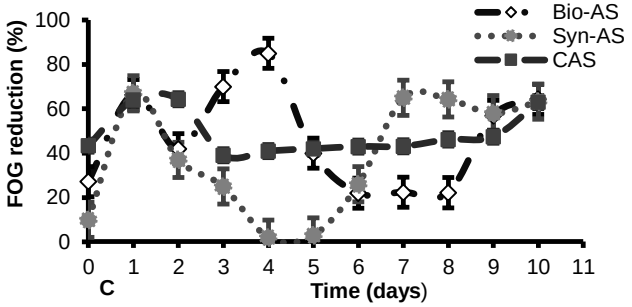
FOG reduction (%)
Time (days)
Bio-AS
Syn-AS
CAS
C

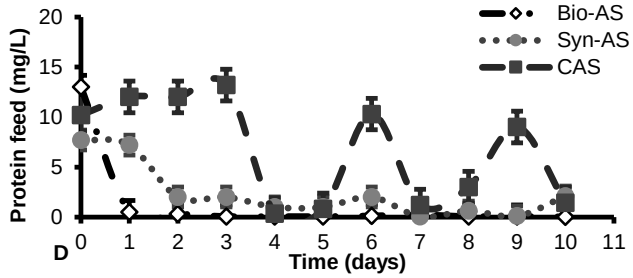
Protein feed (mg/L)
Time (days)
Bio-AS
Syn-AS
CAS
D

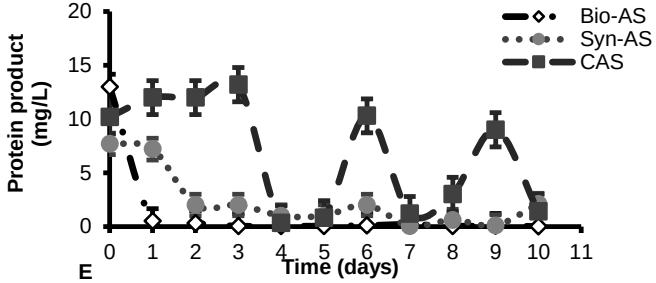
Protein product (mg/L)
Time (days)
Bio-AS
Syn-AS
CAS
E

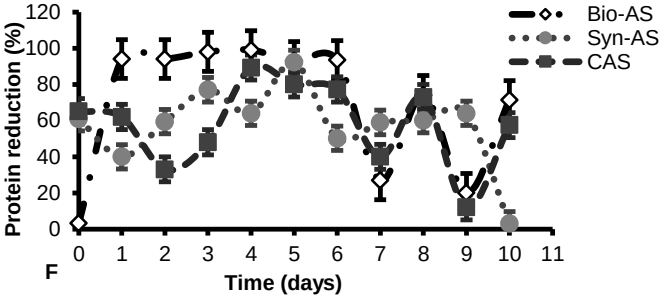
Protein reduction (%)
Time (days)
Bio-AS
Syn-AS
CAS
F

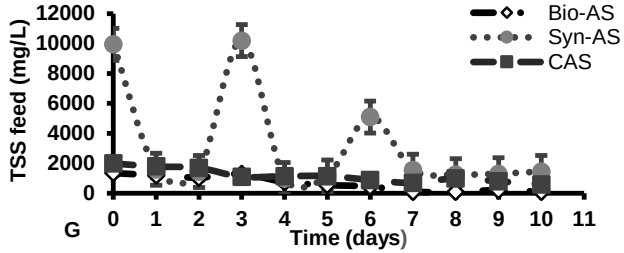
TSS feed (mg/L)
Time (days)
Bio-AS
Syn-AS
CAS
G

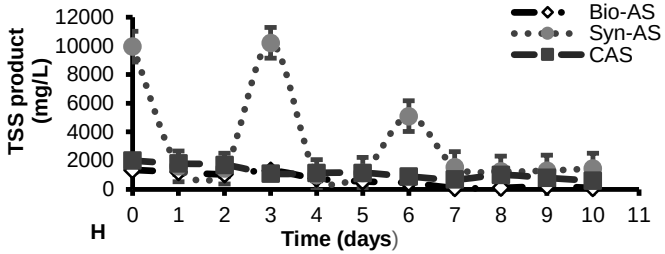
TSS product (mg/L)
Time (days)
Bio-AS
Syn-AS
CAS
H

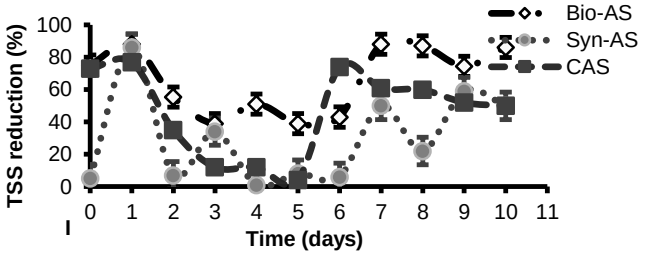
TSS reduction (%)
Time (days)
Bio-AS
Syn-AS
CAS
I

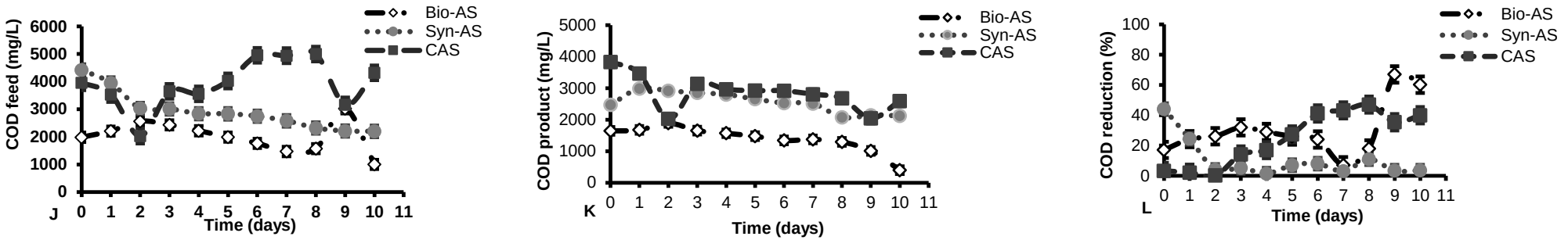

Figure 7.2: FOG (feed-a, product concentration-b, reduction-c); protein (feed-d, concentration product-e, reduction-f; TSS (feed-g, product-h, reduction-i; COD (feed-j, product concentration-k, reduction-L) – profiles carried out under Bio-AS, Syn-AS and CAS.

7.5 Conclusion

The microorganisms were isolated, identified and assessed for their ability to produce biodefoamers and the AS system was designed as in Figure 3.2 and it was used to remove contaminants from PSW, but this technology has the disadvantage of biofoaming and sludge disintegration, which is mainly caused by the FOG and proteins in the PSW. To improve the performance of such systems, synthetic defoamers were applied; however, their major drawback is that they reduce foam for a short period, and they damage the sludge because they are mainly oil-based products; hence, they enhance biofoamer growth. This study focused on the efficacy of biodefoamer-supported activated sludge (Bio-AS), in comparison to the Syn-AS and CAS for the removal of FOG, soluble proteins, TSS, and COD. The results illustrated that the BIO-AS aeration tank can remove up to 94% FOG, 99% soluble proteins, 93.3% TSS, and 85.4% COD; whereas the Syn-AS removed 74% FOG, 79% soluble proteins, 83.2% TSS as well as 61% COD; moreover, the CAS achieved removal of up to 72.3 % FOG, 68% soluble proteins, 87% TSS and 50.5% COD. The contaminants were further removed in the secondary clarifier where solid-liquid separation by gravity was observed. Bio-AS was able to remove FOG, soluble protein, TSS as well as COD by 85%, 99%, 86%, and 67% respectively. The Syn-A removed 67% FOG, 92.2% soluble proteins, 86% TSS and 44.1% COD, in contrast with CAS that removed 64.3% FOG, 89.3% soluble proteins, and 77% TSS, including 47% COD. This indicates that the Bio-AS performed better compared to Syn-AS and CAS. The objectives of this chapter were all achieved.

CHAPTER 8

OVERALL CONCLUSION AND RECOMMENDATIONS

CHAPTER 8
OVERALL CONCLUSION AND RECOMMENDATIONS

8.1 Overall conclusions

It was concluded that the biodefoamers that were produced by the isolated microbial consortium of *Bacillus subtilis, Aeromonas veronii, Klebsiella grimontii,* and *Comamonas testosteroni* produced biodefoamers with high biodefoamer efficiency and a foam decay rate that were suitable for WWTP application when the conditions of application were optimized by RSM. The highest synthetic- and bio-defoamer efficiency was 96% under the following conditions: pH 7 and a concentration of 4% (v/v). When further foam collapse studies were carried out, i.e., using the RSM optimum conditions, the maximum foam decay rate for the synthetic defoamer and biodefoamer were determined to be 96% at 50 s, with total foam suppression occurring at 190 s. The microscopic pictures obtained indicated that the AS was impacted by the presence and absence of defoamers (bio- and synthetic), with the absence of both defoamers resulting in excessive filamentous bacterial growth**.** The FTIR spectra indicated the biodefoamer used in this study was a polysaccharide and ^{1}H NMR confirmed that the defoamer was a carbohydrate constituent. Overall, this study reports for the first time that the production of a biodefoamer is comparable to a common synthetic defoamer.

The metagenomics of the MLSS confirmed that it contained the biofoamers *Nostocoida limicola*, *Gordonia kroppenstedtii*, *Candidatus Microthrix parvicella*, *Nocardioides insulae,* and *Bacteroides nordii.* All of these microorganisms were biofoamers that resulted in high foamability and stability and produced stable foams. The growth of the biodefoamer-producing microorganisms was unaffected by the high concentration of NH_4^+-N and the high lipid content of the PSW. This consortium proved that it could biodegrade NH_4^+-N and FOG. The rate law model could predict both foam drainage and collapse with high R^2 and adjacent R^2 values, and moreover, it had low values for variance and standard deviation, and these aspects are a requirement for a good predictive model. Although this consortium's capability to destabilise biofoam is high, its biological and physicochemical attributes require more exploration for a better understanding of the mechanism that is used by these microbes for biodefoamation and to optimise the biofoam destabilisation efficiency.

Furthermore, the biodefoamer-producing microorganisms proliferated and were able to biodegrade FOG from 672 to 400 mg/L on day 3. It was also observed that they could reduce proteins from 130.8 to 96 mg/L in its exponential growth phase. The crude biodefoamer could reduce foam by 1.33 mm/s.

It was discovered that the biodefoamer-producing microorganisms did not only produce active biodefoamers during cell growth only but also during cell lysis. It also had antimicrobial activity against PSW and MLSS microbial communities.

The designed AS system was able to remove contaminants from PSW when it was operated as biodefoamer-supported activated sludge (Bio-AS), in comparison to Syn-AS and CAS for the removal of FOG, soluble proteins, TSS and COD. The results illustrated that the BIO-AS aeration tank can remove up to 94% FOG, 99% soluble proteins, 93.3% TSS, and 85.4% COD; whereas the Syn-AS removed 74% FOG, 79% soluble proteins, 83.2% TSS as well as 61% COD; moreover, the CAS achieved removal of up to 72.3 % FOG, 68% soluble proteins, 87% TSS and 50.5% COD. The contaminants were further removed in the secondary clarifier where solid-liquid separation by gravity was observed, and the Bio-AS was able to remove FOG, soluble protein, TSS as well as COD by 85%, 99%, 86%, and 67% respectively. The Syn-A removed 67% FOG, 92.2% soluble proteins, 86% TSS and 44.1 COD, in contrast to CAS that removed 64.3% FOG, 89.3% soluble proteins, and 77% TSS including 47% COD. This indicates that the Bio-AS performed better compared to Syn-AS and CAS.

It was concluded that the consortium that was isolated from PSW was able to produce sufficient biodefoamers with high foam reduction efficiency and foam collapse rate, which made it eligible for use in an activated sludge system. Furthermore, the biodefoamers' functional groups affected foam reduction and flocculation of bulking sludge and they were effective on biodefoamation. The Rate law model was able to predict foam drainage and foam collapse that was induced by the biodefoamers. Additionally, the crude biodefoamers were able to inhibit the growth of PSW and MLSS and this gave it a competitive advantage over AS biodefoamation. Moreover, the biodefoamer-supported activated sludge was more efficient in the removal of nutrients compared to the Syn-AS and CAS. It was recommended that the Bio-AS should be mathematically modelled and the impact of spargers should be explored.

8.2 Recommendations for future studies

- The consortium that was used in this study was able to produce biodefoamers, therefore, it is recommended that single isolates be applied to assess their efficacy in comparison with the consortium.
- Biological and physicochemical attributes of the consortium require more exploration for better understanding of the mechanism that it uses to produce the biodefoamers.
- Mathematical modelling of the biodefoamer-supported activated sludge should be explored.
- The impact of spargers should also be studied in depth.

REFERENCES

REFERENCES

Affes, M., Aloui, F., Hadrich, F., Loukil, S. & Sayadi, S. 2017. Effect of bacterial lipase on anaerobic co-digestion of slaughterhouse wastewater and grease in batch condition and continuous fixed-bed reactor. *Lipids in Health and Disease*, 16(1): 1–8.

Ardestani, F. & Abbasi, M. 2019. Poultry slaughterhouse wastewater treatment using anaerobic fluid bed reactor and aerobic mobile-bed biological reactor. *International Journal of Engineering, Transactions B: Applications*, 32(5): 634–640.

Aziz, H.A., Puat, N.N.A., Alazaiza, M.Y.D. & Hung, Y.T. 2018. Poultry slaughterhouse wastewater treatment using submerged fibers in an attached growth sequential batch reactor. *International Journal of Environmental Research and Public Health*, 15(8): 1–12.

Bai, H. & Liao, S. 2019. Bioresource Technology high-efficiency inorganic nitrogen removal by newly isolated Pannonibacter phragmitetus B1. *Bioresource Technology*, 271(September 2018): 91–99.

Baker, B.R., Mohamed, R., Al-Gheethi, A. & Aziz, H.A. 2021. Advanced technologies for poultry slaughterhouse wastewater treatment: A systematic review. *Journal of Dispersion Science and Technology*, 42(6): 880–899. https://doi.org/10.1080/01932691.2020.1721007.

Basitere, M., Williams, Y., Sheldon, M.S., Ntwampe, S.K.O., De Jager, D. & Dlangamandla, C. 2016. Performance of an expanded granular sludge bed (EGSB) reactor coupled with anoxic and aerobic bioreactors for treating poultry slaughterhouse wastewater. *Water Practice and Technology*, 11(1): 86-92.

Bertrand, R.L., 2019. Lag phase is a dynamic, organized, adaptive, and evolvable period that prepares bacteria for cell division. *Journal of bacteriology*, *201*(7): 00697-18. Beye, M., Fahsi, N., Raoult, D. & Fournier, P.E. 2018. Careful use of 16S rRNA gene sequence similarity values for the identification of Mycobacterium species. *New Microbes and New Infections*, 22: 24–29. https://doi.org/10.1016/j.nmni.2017.12.009.

Biswas, J.K., Banerjee, A., Sarkar, B., Sarkar, D., Sarkar, S.K., Rai, M. & Vithanage, M. 2020. Exploration of an extracellular polymeric substance from earthworm gut bacterium (Bacillus licheniformis) for bioflocculation and heavy metal removal potential. *Applied Sciences (Switzerland)*, 10(1).

Blackall, L.L., Seviour, E.M., Bradford, D., Rossetti, S., Tandoi, V. & Seviour, R.J. 2000. 'Candidatus Nostocoida limicola', a filamentous bacterium from activated sludge. *International Journal of*

Systematic and Evolutionary Microbiology, 50(2): 703–709.

Borzooei, S., Miranda, G.H.B., Abolfathi, S., Scibilia, G., Meucci, L. & Zanetti, M.C. 2020. Application of unsupervised learning and process simulation for energy optimization of a WWTP under various weather conditions. *Water Science and Technology*, 81(8): 1541–1551.

Borzooei, S., Amerlinck, Y., Panepinto, D., Abolfathi, S., Nopens, I., Scibilia, G., Meucci, L. & Zanetti, M.C. 2020. Energy optimization of a wastewater treatment plant based on energy audit data: small investment with high return. *Environmental Science and Pollution Research*, 27(15): 17972–17985.

Bukhari, N.A., Loh, S.K., Nasrin, A.B. & Jahim, J.M. 2020. Enzymatic hydrolysate of palm oil mill effluent as potential substrate for bioflocculant BM-8 production. *Waste and Biomass Valorization*, 11(1): 17–29. http://dx.doi.org/10.1007/s12649-018-0421-8.

Burger, W., Krysiak-Baltyn, K., Scales, P.J., Martin, G.J.O., Stickland, A.D. & Gras, S.L. 2017. The influence of protruding filamentous bacteria on floc stability and solid-liquid separation in the activated sludge process. *Water Research*, 123: 578–585. http://dx.doi.org/10.1016/j.watres.2017.06.063

Chen, C., Liu, C.H., Cai, J., Zhang, W., Qi, W.L., Wang, Z., Liu, Z. Bin & Yang, Y. 2018. Broad-spectrum antimicrobial activity, chemical composition and mechanism of action of garlic (Allium sativum) extracts. *Food Control*, 86: 117–125. https://doi.org/10.1016/j.foodcont.2017.11.015.

Chen, F., Sun, J., Han, Z., Yang, X., Xian, J.A.A., Lv, A., Hu, X. & Shi, H. 2019. Isolation, identification and characteristics of Aeromonas veronii from diseased Crucian Carp (Carassius auratus gibelio). *Frontiers in Microbiology*, 10(November): 1–10.

Chen, Z., Chen, C., Luo, X., Liu, J. & Huang, Z. 2021. Flocculation of polystyrene nanoplastics in water using Mg/Al layered double hydroxides via heteroaggregation. *Applied Clay Science*, 213(August): 106264. https://doi.org/10.1016/j.clay.2021.106264.

Chipasa, K.B. & Mdrzycka, K. 2008. Characterization of the fate of lipids in activated sludge. *Journal of Environmental Sciences*, 20(5): 536–542.

Collin, T.D., Cunningham, R., Asghar, M.Q., Villa, R., MacAdam, J. & Jefferson, B. 2020. Assessing the potential of enhanced primary clarification to manage fats, oils and grease (FOG) at wastewater treatment works. *Science of the Total Environment*, 728: 138415. https://doi.org/10.1016/j.scitotenv.2020.138415.

Collivignarelli, M.C., Carnevale Miino, M., Caccamo, F.M. & Baldi, M. 2020. Evaluation of foaming potential for water treatment: Limits and developments. *Environmental Science and Pollution*

Research, 27(22): 27952–27960.

Damasceno, F.R.C., Cavalcanti-Oliveira, E.D., Kookos, I.K., Koutinas, A.A., Cammarota, M.C. & Freire, D.M.G. 2018. Treatment of wastewater with high fat content employing an enzyme pool and biosurfactant: Technical and economic feasibility. *Brazilian Journal of Chemical Engineering*, 35(2): 531–542.

Deepnarain, N., Nasr, M., Kumari, S., Stenström, T.A., Reddy, P., Pillay, K. & Bux, F. 2019. Decision tree for identification and prediction of filamentous bulking at full-scale activated sludge wastewater treatment plant. *Process Safety and Environmental Protection*, 126: 25–34. https://doi.org/10.1016/j.psep.2019.02.023.

Dehghani, M., Sadatjo, H., Maleknia, H. & Shamsedini, N. 2014. A Survey on the Removal Efficiency of Fat, Oil and Grease in Shiraz Municipal Wastewater Treatment Plant. *Jentashapir Journal of Health Research*, 5(6): 10–13.

de Morais, A.P.M., Abreu, P.C., Wasielesky, W. & Krummenauer, D. 2020. Effect of aeration intensity on the biofilm nitrification process during the production of the white shrimp Litopenaeus vannamei (Boone, 1931) in biofloc and clear water systems. *Aquaculture*, 514: 734516.

Deval, A.S., Parikh, H.A., Kadier, A., Chandrasekhar, K., Bhagwat, A.M. & Dikshit, A.K. 2017. Sequential microbial activities mediated bioelectricity production from distillery wastewater using bio-electrochemical system with simultaneous waste remediation. *International Journal of Hydrogen Energy*, 42(2): 1130–1141.

Dehestaniathar, S., Nesari, S., Borzooei, S. & Abolfathi, S. 2021. Application of natural biodegradable fiber as biofilm medium and carbon source in DEnitrifying AMmonium OXidation (DEAMOX) process for nitrogen removal from wastewater. *Journal of the Taiwan Institute of Chemical Engineers*, 119(3): 108–114. https://doi.org/10.1016/j.jtice.2021.01.030.

Diao, H., Li, L., Liang, J., Lu, C., Ding, X. & Guo, W. 2019. Optimized extraction process and compositional analysis of bioflocculant produced by Klebsiella M1. *BioResources*, 14(2): 3146–3167.

Dih, C.C., Jamaluddin, N.A. & Zulkeflee, Z. 2019. Removal of heavy metals in lake water using bioflocculant produced by bacillus subtilis. *Pertanika Journal of Tropical Agricultural Science*, 42(1): 89–101.

Dlamini, N.G., Basson, A.K. & Pullabhotla, R.V.S.R. 2020. Wastewater treatment by a polymeric bioflocculant and iron nanoparticles synthesized from a bioflocculant. *Polymers*, 12(7): 1618.

Dlangamandla, C., Dyantyi, S.A., Mpentshu, Y.P., Ntwampe, S.K.O. & Basitere, M. 2016.

Optimisation of bioflocculant production by a biofilm forming microorganism from poultry slaughterhouse wastewater for use in poultry wastewater treatment. *Water Science and Technology*, 73(8): 1963–1968.

Dlangamandla, C., Ntwampe, S.K.O. & Basitere, M. 2018. A bioflocculant-supported dissolved air flotation system. *Water Science and Technology*, 78(2): 452 –458.

Dlangamandla, C., Basitere, M., Okeleye, B.I., Chidi, B.S. & Ntwampe, S.K.O. 2021. Biofoam formation and defoamation in global wastewater treatment systems. *Water Practice and Technology*, 16(1): 1–18.

Dyosile, P.A., Mdladla, C., Njoya, M., Basitere, M., Karabo, S., Ntwampe, O. & Kaskote, E. 2021. Assessment of an integrated and sustainable multistage system for the treatment of poultry slaughterhouse wastewater. *Membranes*, 11(8): 582.

Ejaz, S., Ihsan, A., Noor, T., Shabbir, S. & Imran, M. 2020. Mannose functionalized chitosan nanosystems for enhanced antimicrobial activity against multidrug resistant pathogens. *Polymer Testing*, 91(August): 106814. https://doi.org/10.1016/j.polymertesting.2020.106814.

Gao, N., Xia, M., Dai, J., Yu, D., An, W., Li, S., Liu, S., He, P., Zhang, L., Wu, Z., Bi, X., Chen, S., Haft, D.H. & Qiu, D. 2018. Both widespread PEP-CTERM proteins and exopolysaccharides are required for floc formation of Zoogloea resiniphila and other activated sludge bacteria. *Environmental Microbiology*, 20(5): 1677–1692.

Garg, A., Stensel, H.D., Bucher, B., Sukapanpotharam, P. & Winkler, M.K.H. 2021. Effect of waste activated sludge pretreatment methods to mitigate Gordonia foaming potential in anaerobic digestion. *Water and Environment Journal*, 35(1): 381–389.

Garg, A., Stensel, H.D., Bucher, B., Sukapanpotharam, P. & Winkler, M.K.H. 2020. Effect of waste activated sludge pretreatment methods to mitigate Gordonia foaming potential in anaerobic digestion. *Water and Environment Journal*, 35(1): 381–389.

Garg, A., Stensel, H.D., Bucher, B., Sukapanpotharam, P. & Winkler, M.K.H. 2021. Effect of waste activated sludge pretreatment methods to mitigate Gordonia foaming potential in anaerobic digestion. *Water and Environment Journal*, 35(1): 381–389. doi: 10.1111/wej.12636.

Gemza, N., Janiak, K., Zięba, B., Przyszlak, J. & Kuśnierz, M. 2022. Long-term effects of hydrocyclone operation on activated sludge morphology and full-scale secondary settling tank wet-weather operation in long sludge age WWTP. *Science of the Total Environment*, 845(April).. doi: 10.1016/j.scitotenv.2022.157224.

Guo, F., Wang, Z.P., Yu, K. & Zhang, T. 2015. Detailed investigation of the microbial community in foaming activated sludge reveals novel foam formers. *Scientific Reports*, 5: 1–9. doi:

10.1038/srep07637.

Guo, F. and Zhang, T. (2012) 'Profiling bulking and foaming bacteria in activated sludge by high throughput sequencing', *Water Research*, 46(8), pp. 2772–2782. doi: 10.1016/j.watres.2012.02.039.

Hubbard, A.T.M., Newire, E., Botelho, J., Reiné, J., Wright, E., Murphy, E.A., Hutton, W. & Roberts, A.P. 2020. Isolation of an antimicrobial-resistant, biofilm-forming, Klebsiella grimontii isolate from a reusable water bottle. *MicrobiologyOpen*, 9(6): 1128–1134.doi: 10.1002/mbo3.1023.

Ji, M., Liu, Z., Sun, K., Li, Z., Fan, X. & Li, Q. 2021. Bacteriophages in water pollution control: Advantages and limitations. *Frontiers of Environmental Science and Engineering*, 15(5).doi: 10.1007/s11783-020-1378-y.

Katritzky, A.R., Akhmedov, N.G., Denisenko, S.N. & Denisko, O. V. 2002. 1H NMR spectroscopic characterization of solutions of Sepia melanin, Sepia melanin free acid and human hair melanin. *Pigment Cell Research*, 15(2): 93–97. doi: 10.1034/j.1600-0749.2002.1o062.x.

Kim, K., Hur, J.W., Kim, S., Jung, J.Y. & Han, H.S. 2020. Biological wastewater treatment: Comparison of heterotrophs (BFT) with autotrophs (ABFT) in aquaculture systems. *Bioresource Technology*, 296(September 2019): 122293. https://doi.org/10.1016/j.biortech.2019.122293.

Kougias, P.G., Boe, K., Tsapekos, P. & Angelidaki, I. 2014. Foam suppression in overloaded manure-based biogas reactors using antifoaming agents. *Bioresource Technology*, 153: 198–205. http://dx.doi.org/10.1016/j.biortech.2013.11.083.

Kozhukhova, E., Litvinova, M., Makarevich, E. & Malaeva, A. 2020. Biodegradation of petroleum hydrocarbons by bioflocculant-producing microorganisms of the aquatic ecosystems in the Arctic region. IOP Conference Series: Earth and Environmental Science, 539(1).doi: 10.1088/1755-1315/539/1/012192.

Lee, S., Lee, J. & Hwang, N. 2021. Effect of the dispersion state in Y5O4F7 suspension on YOF coating deposited by suspension plasma spray *Coatings*, 11(7). doi: 10.3390/coatings11070831.

Li, B.B., Peng, Z.Y., Zhi, L.L., Li, H.B., Zheng, K.K. & Li, J. 2020. Distribution and diversity of filamentous bacteria in wastewater treatment plants exhibiting foaming of Taihu Lake Basin, China. *Environmental Pollution*, 267. doi: 10.1016/j.envpol.2020.115644.

Ma, B., Li, Z., Wang, S., Liu, Z., Li, S., She, Z., Yu, N., Zhao, C., Jin, C., Zhao, Y., Guo, L. & Gao, M. 2019. Insights into the effect of nickel (Ni(II))on the performance, microbial enzymatic activity and extracellular polymeric substances of activated sludge. *Environmental Pollution*, 251: 81–89. doi: 10.1016/j.envpol.2019.04.094.

Mamais, D., Kalaitzi, E. and Andreadakis, A. (2011) Foaming control in activated sludge treatment plants by coagulants addition, *Global Nest Journal*, 13(3), 237–245. doi: 10.30955/gnj.000751.

Mangundu, J. (2017) Optimisation of Defoamer in a Bio-Reactor.

Manyele, S. V (2007) FOAMING CHARACTERISTICS OF THE FOOD-INDUSTRY, 30(1).

Masoumi, Z., Shokohi, R., Atashzaban, Z., Ghobadi, N. & Rahmani, A.R. 2015. Stabilization of Excess Sludge From Poultry Slaughterhouse Wastewater Treatment Plant by the Fenton Process. Avicenna, *Journal of Environmental Health Engineering*, 2(1): 1–5.2(1), pp. 1–5. doi: 10.17795/ajehe3239.

Mbulawa, S., Ntwampe, S.K.O., Basitere, M. & Mpentshu, Y.P. 2018. Bio-Delipidation of Dissolved Air Flotation Pre-Treated Poultry Slaughterhouse Wastewater. ,November).Slaughterhouse Wastewater', (November). doi: 10.17758/eares4.eap1118213.

Meiramkulova, K., Zorpas, A.A., Orynbekov, D., Zhumagulov, M., Saspugayeva, G., Kydyrbekova, A., Mkilima, T. & Inglezakis, V.J. 2020. The effect of scale on the performance of an integrated poultry slaughterhouse wastewater treatment process. *Sustainability* (Switzerland), 12(11). doi: 10.3390/su12114679.

Meyo, H.B., Njoya, M., Basitere, M., Ntwampe, S.K.O. & Kaskote, E. 2021. Treatment of poultry slaughterhouse wastewater (Psw) using a pretreatment stage, an expanded granular sludge bed reactor (egsb), and a membrane bioreactor (mbr). *Membranes*, 11(5). 11(5). doi: 10.3390/membranes11050345.

Miao, L., Yang, G., Tao, T. & Peng, Y. 2019. Recent advances in nitrogen removal from land fi ll leachate using biological treatments – A review. *Journal of Environmental Management*, 235(November 2018): 178–185.. doi: 10.1016/j.jenvman.2019.01.057.

Miles, G. D. (1944) 'OF PURE FATTY ACIDS'.

Mohamad Pauzi, S., Anak Halbert, D., Azizi, S., Ahmad, N.A.A., Ahmad, N. & Marpani, F. 2019. Effect of organic antifoam's concentrations on filtration performance. *Journal of Physics: Conference Series*, 1349(1). doi: 10.1088/1742-6596/1349/1/012141.

Mohamed Hatta, N.S., Lau, S.W., Takeo, M., Chua, H.B., Baranwal, P., Mubarak, N.M. & Khalid, M. 2021. Novel cationic chitosan-like bioflocculant from Citrobacter youngae GTC 01314 for the treatment of kaolin suspension and activated sludge. , *Journal of Environmental Chemical Engineering*, 9(4). doi: 10.1016/j.jece.2021.105297.

de Morais, A.P.M., Abreu, P.C., Wasielesky, W. & Krummenauer, D. 2020. Effect of aeration intensity on the biofilm nitrification process during the production of the white shrimp Litopenaeus vannamei (Boone, 1931) in Biofloc and clear water systems. *Aquaculture*, 514(July 2019).doi:

10.1016/j.aquaculture.2019.734516.

Nakajima, J. & Mishima, I. 2005. Measurement of foam quality of activated sludge in MBR process. *Acta Hydrochimica et Hydrobiologica*, 33(3): 232–239.. doi: 10.1002/aheh.200400575.

Nierychlo, M., Andersen, K.S., Xu, Y., Green, N., Jiang, C., Albertsen, M., Dueholm, M.S. & Nielsen, P.H. 2020. MiDAS 3: An ecosystem-specific reference database, taxonomy and knowledge platform for activated sludge and anaerobic digesters reveals species-level microbiome composition of activated sludge. *Water Research*, 182: 115955. https://doi.org/10.1016/j.watres.2020.115955.

Nilsson, F., Davidsson, Å., Falås, P., Bengtsson, S., Bester, K. & Jönsson, K. 2019. Impact of activated sludge ozonation on filamentous bacteria viability and possible added benefits. *Environmental Technology* (United Kingdom), 40(20): 2601–2607. doi: 10.1080/09593330.2018.1447023.

Njoya, M., Basitere, M., Ntwampe, S.K.O. & Lim, J.W. 2021. Performance evaluation and kinetic modeling of down-flow high-rate anaerobic bioreactors for poultry slaughterhouse wastewater treatment. *Environmental Science and Pollution Research*, 28(8): 9529–9541.. 9529–9541. doi: 10.1007/s11356-020-11397-5.

Omar, M.M., Mohamed, G.G. & Ibrahim, A.A. 2009. Spectroscopic characterization of metal complexes of novel Schiff base. Synthesis, thermal and biological activity studies. Spectrochimica Acta - Part A: *Molecular and Biomolecular Spectroscopy*, 73(2): 358–369. doi: 10.1016/j.saa.2009.02.043.

Orsini, J., Tam, E., Hauser, N. & Rajayer, S. 2014. Polymicrobial bacteremia involving comamonas testosteroni. *Case Reports in Medicine*, 2014: 15–18.. doi: 10.1155/2014/578127.

Pajdak-Stós, A., Kocerba-Soroka, W., Fyda, J., Sobczyk, M. & Fiałkowska, E. 2017. Foam-forming bacteria in activated sludge effectively reduced by rotifers in laboratory- and real-scale wastewater treatment plant experiments. *Environmental Science and Pollution Research*, 24(14): 13004–13011. doi: 10.1007/s11356-017-8890-z.

Pal, P., Khairnar, K. and Paunikar, W. (2014) Causes and remedies of activated sludge foaming, *Global NEST*, 16(1):1–11.

Panizzolo, L. A., Mussio, L. E. and Aón, M. C. (2012) A kinetic description for the destabilization process of protein foams, *International Journal of Food Properties*, 15(1):60–68. doi: 10.1080/10942911003687264.

Pedrazzani, R., Menoni, L., Nembrini, S., Manili, L. & Bertanza, G. 2016. Suitability of Sludge Biotic Index (SBI), Sludge Index (SI) and filamentous bacteria analysis for assessing activated sludge process performance: the case of piggery slaughterhouse wastewater. *Journal of Industrial*

Microbiology and Biotechnology, 43(7): 953–964.. doi: 10.1007/s10295-016-1767-1.

Petrovski, S., Dyson, Z.A., Quill, E.S., McIlroy, S.J., Tillett, D. & Seviour, R.J. 2011. An examination of the mechanisms for stable foam formation in activated sludge systems. *Water Research*, 45(5): 2146–2154. http://dx.doi.org/10.1016/j.watres.2010.12.026.

Pu, L., Zeng, Y.J., Xu, P., Li, F.Z., Zong, M.H., Yang, J.G. & Lou, W.Y. 2020. Using a novel polysaccharide BM2 produced by Bacillus megaterium strain PL8 as an efficient bioflocculant for wastewater treatment. *International Journal of Biological Macromolecules*, 162: 374–384. https://doi.org/10.1016/j.ijbiomac.2020.06.167.

Rajab, A.R., Salim, M.R., Sohaili, J., Anuar, A.N., Salmiati & Lakkaboyana, S.K. 2017. Performance of integrated anaerobic/aerobic sequencing batch reactor treating poultry slaughterhouse wastewater. *Chemical Engineering Journal*, 313: 967–974. http://dx.doi.org/10.1016/j.cej.2016.10.144. .doi: 10.1016/j.cej.2016.10.144.

Rinquest, Z., Basitere, M., Ntwampe, S.K.O. & Njoya, M. 2019. Poultry slaughterhouse wastewater treatment using a static granular bed reactor coupled with single stage nitrification-denitrification and ultrafiltration systems. *Journal of Water Process Engineering*, 29(April 2018): 100778.doi: 10.1016/j.jwpe.2019.02.018.

Rolfe, M.D., Rice, C.J., Lucchini, S., Pin, C., Thompson, A., Cameron, A.D.S., Alston, M., Stringer, M.F., Betts, R.P., Baranyi, J., Peck, M.W. & Hinton, J.C.D. Lag Phase Is a Distinct Growth Phase That Prepares Bacteria for Exponential Growth and Involves Transient Metal Accumulation. doi: 10.1128/JB.06112-11.

Routledge, S. J. (2012) 'Beyond de-foaming: The effects of antifoams on bioprocess productivity', *Computational and Structural Biotechnology Journal*, 3(4), p. e201210001. doi: 10.5936/csbj.201210014.

Sadeddin, K., Naser, A. and Firas, A. (2011) 'Removal of turbidity and suspended solids by electro-coagulation to improve feed water quality of reverse osmosis plant', *Desalination*, 268(1–3), pp. 204–207. doi: 10.1016/j.desal.2010.10.027.

Salager, J.-L., Antón, R., Bracho, C.L., Briceño, M.I., Peña, a., Rondón, M. & Salager, S. 1999. Attainment of emulsion properties on design, a typical case of formulation engineering. *Second European Congress of Chemical Engineering*, (May 2014): 1–8.

Septiana, I., Siami, L., Tazkiaturrizki, T., Hadisoebroto, R. & Ratnaningsih, R. 2019. Analysis of load variation on chicken slaughterhouse waste water treatment using GAS-SBR. *Journal of Physics: Conference Series*, 1402(2). doi: 10.1088/1742-6596/1402/2/022109.

Shi, Y., Huang, J., Zeng, G., Gu, Y. & Chen, Y. 2017. Chemosphere Exploiting extracellular polymeric

substances (EPS) controlling strategies for performance enhancement of biological wastewater treatments : An overview. , 180: 396–411. doi: 10.1016/j.chemosphere.2017.04.042.

Shi, Y. and Liu, Y. (2021) Evolution of extracellular polymeric substances (EPS) in aerobic sludge granulation: Composition, adherence and viscoelastic properties, *Chemosphere*, 262: 128033. doi: 10.1016/j.chemosphere.2020.128033.

Simjoo, M., Rezaei, T., Andrianov, A. & Zitha, P.L.J. 2013. Foam stability in the presence of oil: Effect of surfactant concentration and oil type. *Colloids and Surfaces A: Physicochemical and Engineering Aspects*, 438: 148–158.

Subudhi, S., Bisht, V., Batta, N., Pathak, M., Devi, A. & Lal, B. 2016. Purification and characterization of exopolysaccharide bioflocculant produced by heavy metal resistant Achromobacter xylosoxidans. , 137: 441–451.

Trybala, A., Koursari, N., Johnson, P., Arjmandi-Tash, O. & Starov, V. 2019. Interaction of liquid foams with porous substrates. *Current Opinion in Colloid and Interface Science*, 39: 212–219. https://doi.org/10.1016/j.cocis.2019.01.011.

Tsilo, P.H., Basson, A.K., Ntombela, Z.G., Maliehe, T.S. & Pullabhotla, R.V.S.R. 2021. Isolation and Optimization of Culture Conditions of a Bioflocculant-Producing Fungi from Kombucha Tea SCOBY. *Microbiology Research*, 12(4): 950–966.

Vanaja, M., Paulkumar, K., Baburaja, M., Rajeshkumar, S., Gnanajobitha, G., Malarkodi, C., Sivakavinesan, M. & Annadurai, G. 2014. Degradation of methylene blue using biologically synthesized silver nanoparticles. *Bioinorganic Chemistry and Applications*, 2014.

Verma, A., Chauhan, G. and Ojha, K. (2018) 'Characterization of α-olefin sulfonate foam in presence of cosurfactants: Stability, foamability and drainage kinetic study', *Journal of Molecular Liquids*, 264, pp. 458–469. doi: 10.1016/j.molliq.2018.05.061.

Wang, J., Nguyen, A. V. and Farrokhpay, S. (2016) 'Foamability of sodium dodecyl sulfate solutions: Anomalous effect of dodecanol unexplained by conventional theories', *Colloids and Surfaces A: Physicochemical and Engineering Aspects*, 495, pp. 110–117. doi: 10.1016/j.colsurfa.2016.02.001.

Westgate, P. J. (2009) 'Characterization of Proteins in Effluents from Three Wastewater Treatment Plants that Discharge to the Connecticut River', *Environmental & Water Resources Engineering Masters Projects*, 42, pp. 1–56.

Yao, S., Ni, J., Ma, T. & Li, C. 2013. Heterotrophic nitrification and aerobic denitrification at low temperature by a newly isolated bacterium, Acinetobacter sp. HA2. *Bioresource Technology*, 139: 80–86.

Zhao, K., Vowinckel, B., Hsu, T.J., Köllner, T., Bai, B. & Meiburg, E. 2020. An efficient cellular flow model for cohesive particle flocculation in turbulence. *Journal of Fluid Mechanics*, 889: 1–11.

Zhou, S., Liu, M., Chen, B., Sun, L. & Lu, H. 2022. Microbubble- and nanobubble-aeration for upgrading conventional activated sludge process: A review. *Bioresource Technology*, 362(August): 127826. https://doi.org/10.1016/j.biortech.2022.127826.

Yekeen, N., Idris, A., Manan, M. & Samin, A. 2016 Experimental study of the influence of silica nanoparticles on the bulk stability of SDS-foam in the presence of oil. *Journal of Dispersion Science Technology*, 38(3): 416-424.

Zayas, J.F. 1997 Foaming properties of Proteins. In Zayas, J.F. *Functionality of proteins in food*. Berlin: Springer, 260-309.

Zhao, K., Vowinckel, B., Hsu, T.J., Köllner, T., Bai, B. & Meiburg, E. 2020. An efficient cellular flow model for cohesive particle flocculation in turbulence. *Journal of Fluid Mechanics*, 889: 1–11.

Zhang, W., Alvarez-Gaitan, J., Dastyar, W., Saint, C., Zhao, M. & Short, M. 2018. Value-added products derived from waste activated sludge: A biorefinery perspective. *Water*, 10(5): 545.

APPENDICES

APPENDICES

APPENDIX A: Phylogenetic tree generation and analysis

Appendix A1 Methods and materials

The query sequence used in in this study was sequenced at Inqaba. It was opened using Bioedit 7.2 software and it was deposited on NCBI nucleotide BLAST to view similar sequences from the gene bank that were closely related to this sequence (95-99% sequence identity) and out of 100 nucleotide sequences that were obtained on NCBI blast gene bank database, only 20 sequences were used and their accession numbers appears in Fig. 4.3.1. The query sequence and 20 sequences (95-99% identity) that were on FASTA format were deposited on Mega 11 software and they were aligned using muscle, after which, they were converted to Mega format and a neighbor joining tree was created using 1000 bootstrap and an evolutionary distance of 0.005.

Appendix A2: Results and discussion

The close relationship among species in the genus on Fig. 4.3.1 (a) *Aeromonas*, (b) *Bacillus*, (c) *Comamonas* and (d) *Klebsilla* were confirmed based on gene sequencing, however, the phylogenetic trees revealed that the isolates in these genus were divided into subgroup based on their genetic similarities. 16S rRNA is used for Characterisation of bacteria species; hence it was used in this study to generate phylogenetic trees. The tree on Fig. 4.3.1 (a) showed that the genus *Aeromonas* contains

many species that are closely related with various percentage identities from 95-98%. The query sequence had 98% identity to *A. veronii* 97.5% with *A. hydrophila*, 96% similarity with *A. allosacchorophila* and 95% with *A. dhakins*. Although this specie had highest percentage similarity with *A. veronii*, it formed a clade with *A. hydrophilla* and the bootstrap of the node was 100% this was due to intragenomic heterogeneity that is due to evolution divergence as well as lateral transfer (Chen et al. 2015; Espejo & Plazza, 2018;). The *Bacillus* BE 3 sequence was deposited on blast and it showed maximum similarity of 99% to *B. subtilis* and the phylogenetic tree shows that it was also closely related to other B. spizizeni. *C. testestoroni* BW5 had 98% specie identity to *C. testestoroni*, however it formed a clade with *C. thiooxidans*. Additionally, *K. grimontii* BS5 formed a clade with *K. michiganesis* though its percentage identity was 98% similar to *K. grimontii* this is due to the fact that 2 strains that belong to different species can share 16S rRNA sequence similarity of up to 97% (Beye et al. 2017.

The microorganisms were isolated from PSW, for the treatment of PSW in activated sludge and the results depicted that intrinsic wastewater microorganisms have the potential to bioremediate the wastewater in which they were isolated from, provided, that they are cultured in a nutrient media that enhances their growth, so that they can be competitive above the other microbial community that is present in the wastewater. The results suggested that (strains) are potential novel biodefoamer with excellent bioflocculation and they were effective when applied in activated sludge defoamation this reveals a promising application of the consortium and other bacterial isolates as biodefoamer in wastewater treatment systems. Further investigation on the polymer chemistry of this novel consortium is required since it influence the aggregation of sludge which the decreases biofoaming

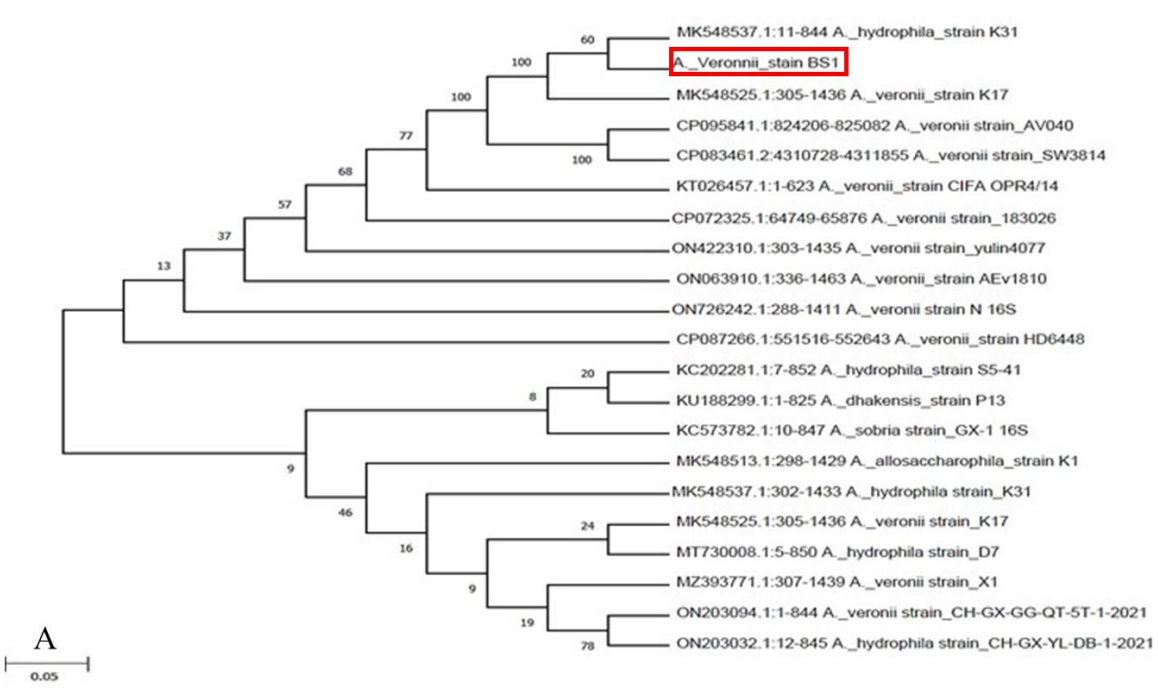
MK548537.1:11-844 A._hydrophila_strain K31
A._Veronnii_stain BS1
MK548525.1:305-1436 A._veronii_strain K17
CP095841.1:824206-825082 A._veronii strain_AV040
CP083461.2:4310728-4311855 A._veronii strain_SW3814
KT026457.1:1-623 A._veronii_strain CIFA OPR4/14
CP072325.1:64749-65876 A._veronii strain_183026
ON422310.1:303-1435 A._veronii strain_yulin4077
ON063910.1:336-1463 A._veronii_strain AEv1810
ON726242.1:288-1411 A._veronii strain N 16S
CP087266.1:551516-552643 A._veronii_strain HD6448
KC202281.1:7-852 A._hydrophila_strain S5-41
KU188299.1:1-825 A._dhakensis_strain P13
KC573782.1:10-847 A._sobria strain_GX-1 16S
MK548513.1:298-1429 A._allosaccharophila_strain K1
MK548537.1:302-1433 A._hydrophila strain_K31
MK548525.1:305-1436 A._veronii strain_K17
MT730008.1:5-850 A._hydrophila strain_D7
MZ393771.1:307-1439 A._veronii strain_X1
ON203094.1:1-844 A._veronii strain_CH-GX-GG-QT-5T-1-2021
ON203032.1:12-845 A._hydrophila strain_CH-GX-YL-DB-1-2021
A
0.05

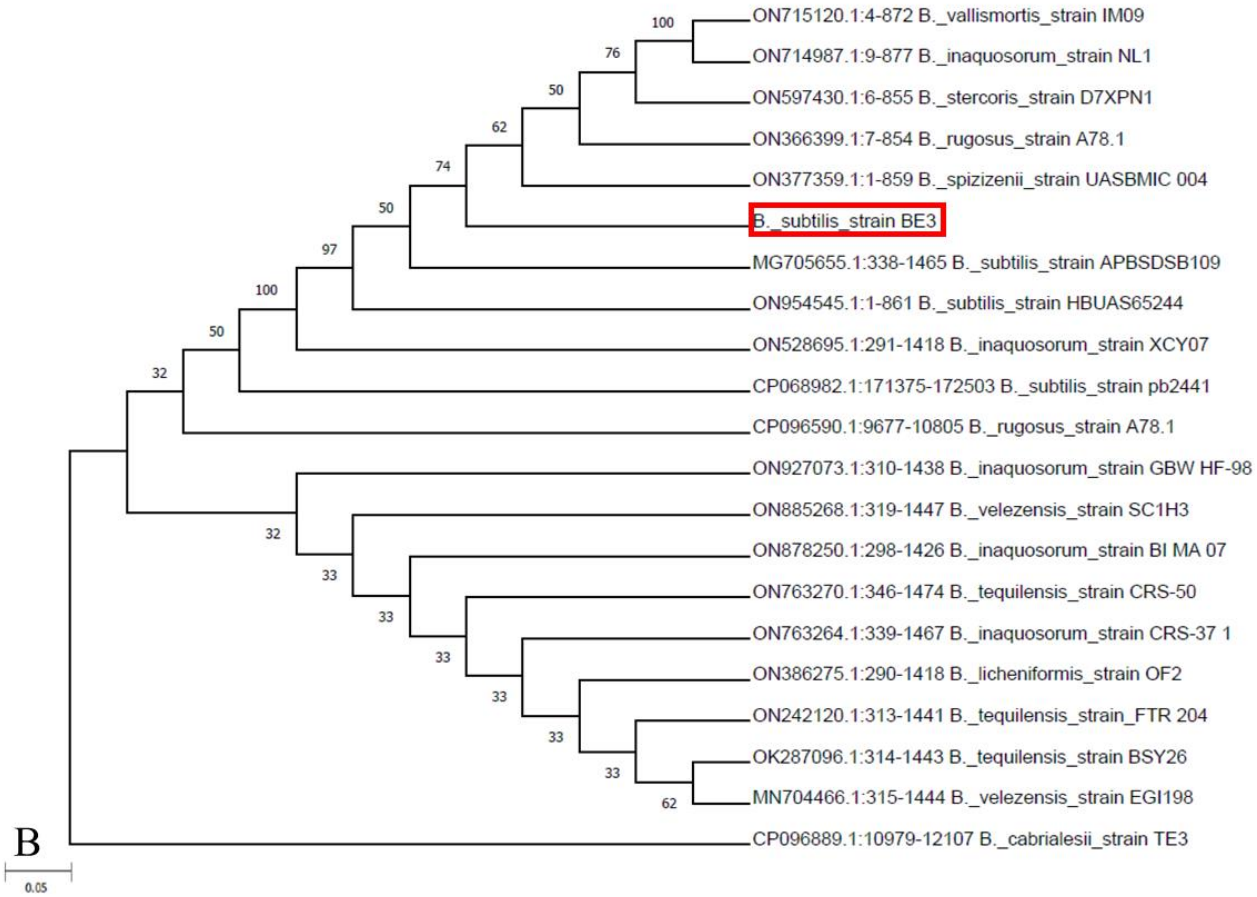
ON715120.1:4-872 B._vallismortis_strain IM09
ON714987.1:9-877 B._inaquosorum_strain NL1
ON597430.1:6-855 B._stercoris_strain D7XPN1
ON366399.1:7-854 B._rugosus_strain A78.1
ON377359.1:1-859 B._spizizenii_strain UASBMIC 004
B._subtilis_strain BE3
MG705655.1:338-1465 B._subtilis_strain APBSDSB109
ON954545.1:1-861 B._subtilis_strain HBUAS65244
ON528695.1:291-1418 B._inaquosorum_strain XCY07
CP068982.1:171375-172503 B._subtilis_strain pb2441
CP096590.1:9677-10805 B._rugosus_strain A78.1
ON927073.1:310-1438 B._inaquosorum_strain GBW HF-98
ON885268.1:319-1447 B._velezensis_strain SC1H3
ON878250.1:298-1426 B._inaquosorum_strain BI MA 07
ON763270.1:346-1474 B._tequilensis_strain CRS-50
ON763264.1:339-1467 B._inaquosorum_strain CRS-37 1
ON386275.1:290-1418 B._licheniformis_strain OF2
ON242120.1:313-1441 B._tequilensis_strain_FTR 204
OK287096.1:314-1443 B._tequilensis_strain BSY26
MN704466.1:315-1444 B._velezensis_strain EGI198
CP096889.1:10979-12107 B._cabrialesii_strain TE3
B
0.05

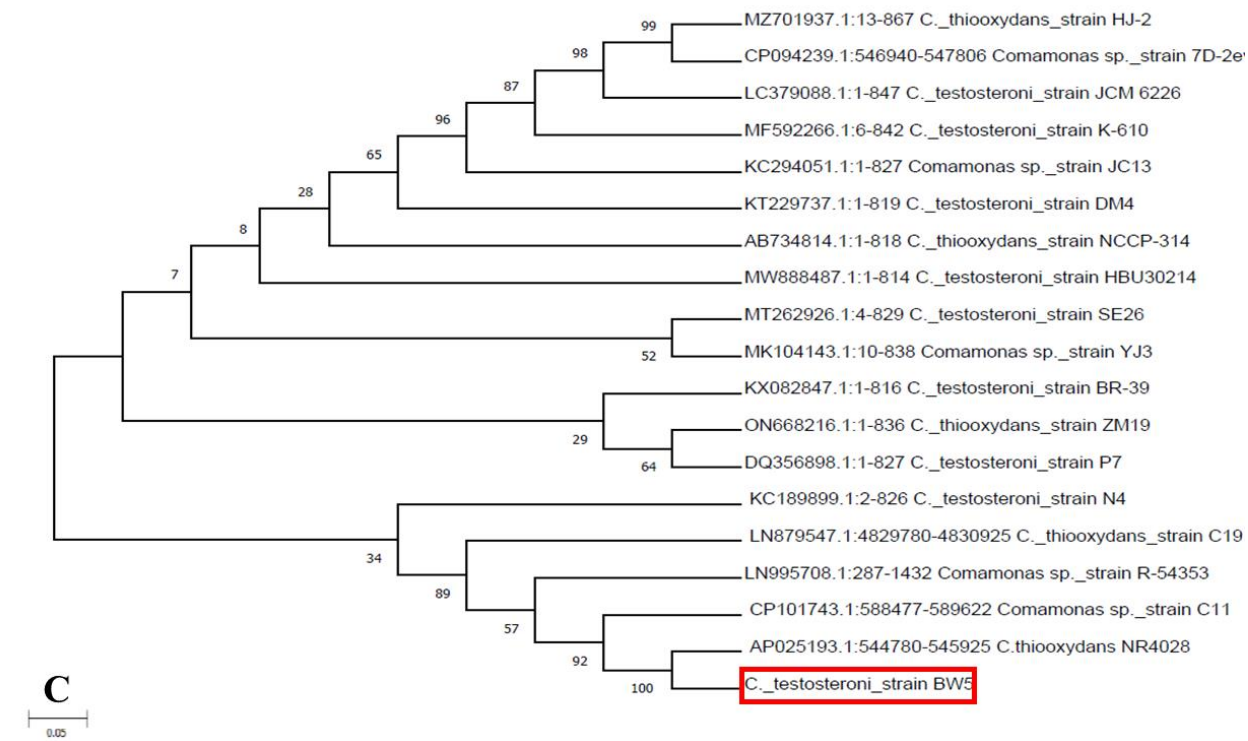

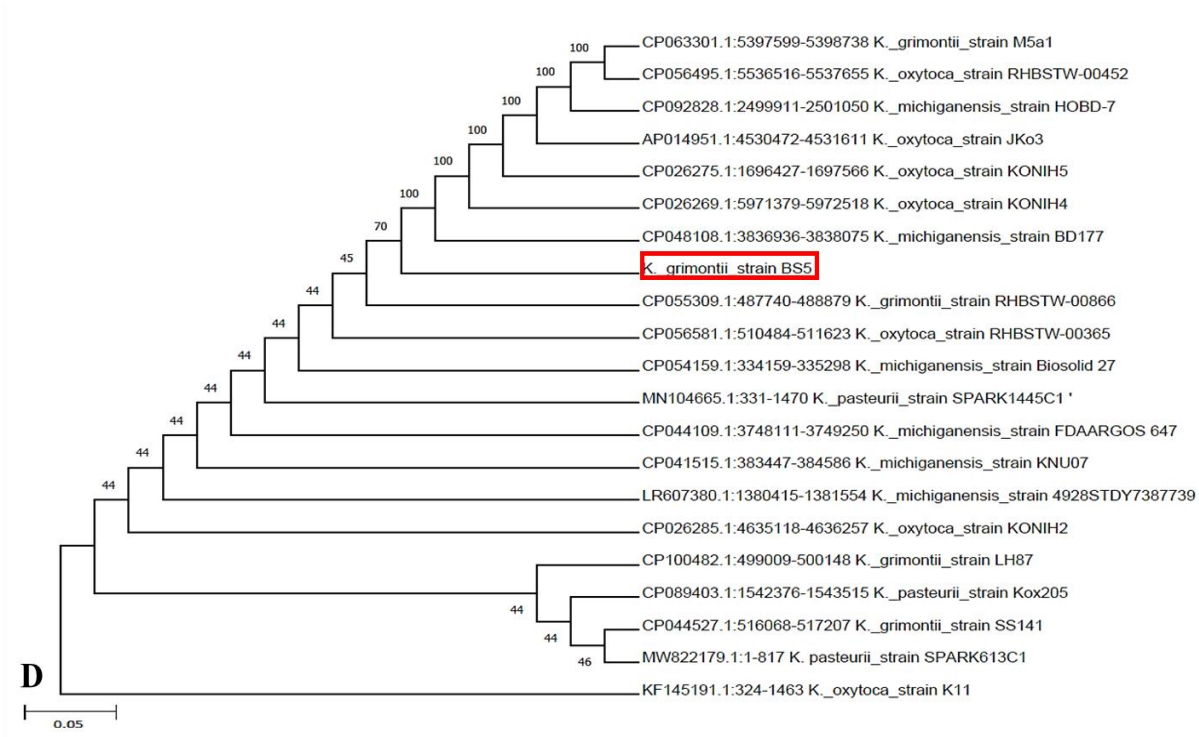

Table 10.1: Rootles neighbour joining tree that depicts phylogenetic relationships based on 16S rRNA nucleotide sequences within the species (a) *Aeromonas veronii*, (b) *Bacillus subtilis*, (c) *Comamonas testosteroni*, (d) *Klebsilla grimontii*. The trees were generated using Mega 11 package. The bootstrap values (numbers that estimates confidence levels expressed as percentages) were presented on the

branches and they were determined from 1000 replications and gene accession number and strain name are indicated on each isolate.

Appendix B: Analytical procedures

Appendix B1:\ COD analysis

- Switch on the Spectroquant® thermoreactor to the pre-set setting of 148 °C for two hours and let the thermoreactor heat to the desired temperature. (This will take approx. 10 min.)
- Place approximately 100ml distilled water into a 250ml beaker.
- When using COD solution, A and B for a range of 500 to 10000 mg/L.
- Pipette 2.2mL of COD solution A into a cell using P5000 pipette.
- Pipette 1.8mL COD solution B into the cells with COD solution A which was pipetted in using P5000.
- Using a new pipettetip, pipette 1ml of the sample into the cells sing P1000 pipette.
- Tightly attach the screw cap to the cells.
- Vigorously mix the cell with a shaker.
- Heat cells in the thermos reactor at 148 °C for 2 hours.
- Carefully remove the cells after 2 hours and place them in a test tube rack to cool. (Do not cool with cold water.)
- Wait 10 minutes, place them in the shaker again and leave in the test tube rack to cool at room temperature. (Cooling time is at least 30 minutes.)
- Place the cells in the Nova 60 for COD reading.
- When using the Nova 60, make sure that the indicator line on the cell lines up with the indicator line on the Nova 60. But when using COD solution for 500 to 10000 mg/L, put in the code 0.24. When using COD solution for 100 to 1500mg/L put in the code 0.23.
- When using COD solution, A and B for a range of 100 to 1500mg/L
- This procedure is exactly the same as for COD solution A and B for 500 to 10000 mg/L with the exception of:
- Add 0.30mL of COD solution A into the cell using P1000.
- Pipette 2.30mL COD solution B into the cell using P5000.
- Add 3mL of the sample into the cell that contains solution A and B using P5000 pipette.

Appendix B 2: Total suspended solids

Apparatus

- Glass microfibre filter discs, 5.5cm, without organic binder, Whatman type GF/F (0.7 Fm).

- Disposal aluminium dishes
- Tweezers
- Suction flask, 1000ml
- 47mm glass microanalysis filter holder (funnel, clamp and base).
- Drying oven for operation 103 to 105 °C.
- Muffle furnace for operation at 550± 50 °C.
- Desiccator.
- Analytical balance, capable of weighing 0.1mg, an RS232C interface and personal computer.
- Milli-Q® reagent grade water (ASTM Type-1 water), Millipore Corp., Bedford, MA.

Procedure for total suspended solids

- Insert the glass-fibre filter disc onto the base and a clamp funnel. While vacuum is applied, wash the filter disc with three successive 20mL volumes of Milli-Q® water. Remove all traces of water by applying the vacuum after the water has passed through. Remove the funnel from the base and place filter on the aluminium dish and ignite in the muffle furnace at 550± 50 °C for 30 min. Rewash the filter with an additional three successive 20mL volumes of Milli-Q® water, and dry it in an oven at 103 to 105 °C for 1 h. When dry, remove the dish from the oven, desiccate and weigh.
- Select the sample volume (200mL max) that will yield no more than 200mg of total suspended solids.
- Place the filter between the base and clamp, and add a small volume of Milli-Q® water so that the filter attaches to the base, and remove the water from the base.
- Shake the sample vigorously, then transfer the sample into the filter paper. Remove water by applying vacuum even after the water has passed through.
- Remove the filter from the base and dry for 1 hour at 103 to 105 °C. Cool in the desiccator and weigh.

Calculation for total suspended solids

TSS (mg/L) = (A-B) x 1000/C

Where A = Weight of filter and dish+ residue in mg.

B = Weight of filter and dish in mg.

C = Volume of sample filtered in mL.

APPENDIX C: Bradford's method

- 10 mg of crystal bovine serum albumin (BSA) was dissolved into 10 mM of 10 mL sodium phosphate. The standard curve was made from the stock.

- 50 µL of each of the standard samples containing a known concentration of BSA was added into the 96 wells microtiter plate (in duplicates).
- 150 µL of the Bradford reagent was added to each well that contained the standard sample and left to stand for 2 minutes.
- The absorbance of the standards was quantified using an Anthos Xenthal 1100 microtiter plate reader at an absorbance of 595 nm.
- A standard curve was constructed using the absorbance of the standard versus their concentration.
- A standard curve was then drawn for the diluted unknown protein concentration sample (1:10).
- The concentration was estimated using the regression line.

APPENDIX D: Biodefoamer activated sludge efficacy in the reduction of FOG, protein, TSS and COD.

Table 10.2: FOG concentration reduction in the aeration tank

Influent FOG concentration (mg/L)				FOG concentration tank (mg/L)			FOG reduction (%)		
Time (days)	Bio-AS	Syn-AS	CAS	Bio-AS	Syn-AS	CAS	Bio-AS	Syn-AS	CAS
0	53.3	29.6	53	550	500	530	53.3	29.6	53
1	75	58	69	250	280	270	75	58	69
2	85.3	74	66	114	114	140	85.3	74	66
3	84.2	73	66	113	144	128	84.2	73	66
4	82.3	74	72.3	85	100	76	82.3	74	72.3
5	85	66	74	58	72	74	85	66	74
6	87	60	73	46	62	94	87	60	73
7	91	58.2	70	28	86	102	91	58.2	70
8	91	56	70.4	22	140	52	91	56	70.4
9	91.1	50	70	30	128	57	91.1	50	70
10	94	50	62.5	28	402	300	94	50	62.5

Table 10.3: Protein reduction in the aeration tank

Influent Protein concentration (mg/L)				Protein concentration tank (mg/L)			Protein reduction (%)		
Time (days)	Bio-AS	Syn-AS	CAS	Bio-AS	Syn-AS	CAS	Bio-AS	Syn-AS	CAS
0	96	29.4	31	48	20	10	50.2	33.2	27
1	42.2	30	56.2	21	18	18	50.2	41.3	68
2	35.4	5.2	54.1	17.5	4.2	18	51	20.3	67.5
3	99.8	9	19.8	17	3.3	39.5	51.5	57.3	60.5
4	19	5	11.3	0.16	1.8	4.9	53	62.4	57
5	5.4	8	5	0.6	2.8	2.2	77	63	56
6	61.2	6	6.2	0.3	2	28	82	66	55

7	4	0.2	3.9	0.1	0.04	2	82.1	74	50
8	19.2	3.2	8	0.16	0.8	10	88.4	74.5	47
9	37	2	3	0.06	0.5	22	61	78	40
10	12	8	2	0.16	0.34	7.2	99	79	39

Table 10.4: TSS concentration reduction in the aeration tank

Influent TSS concentration (mg/L)				TSS concentration tank (mg/L)			TSS reduction (%)		
Time (days)	Bio-AS	Syn-AS	CAS	Bio-AS	Syn-AS	CAS	Bio-AS	Syn-AS	CAS
0	10000	9950	2000	1350	9950	2000	75.2	5.2	73
1	1900	1600	1800	1200	1600	1800	88	86	77
2	1050	1450	1700	1050	1450	1700	55.3	7	35
3	11000	10200	1100	1300	10200	1100	39	34	12
4	1000	990	1150	750	990	1150	51	1	12
5	1550	1150	1150	550	1150	1150	39	8	4.2
6	5550	5100	900	450	5100	900	43	6	74
7	1600	1550	690	100	1550	690	88	50	61
8	1300	1250	1000	110	1250	1000	87.1	22	60
9	1500	1300	800	200	1300	800	74.4	59	52
10	1600	1450	600	100	1450	600	86	50	50

Table 10.5: COD concentration reduction in the aerobic tank of a biodefomer supported AS

Influent COD concentration (mg/L)				COD concentration tank (mg/L)			COD reduction (%)		
Time (days)	Bio-AS	Syn-AS	CAS	Bio-AS	Syn-AS	CAS	Bio-AS	Syn-AS	CAS
0	10000	9950	2000	1985	4420	3960	56	47.1	32
1	1900	1600	1800	2210	3950	3535	38	61	2.75
2	1050	1450	1700	2565	3030	2030	37.3	63	13
3	11000	10200	1100	2434	3010	3650	44	37.2	2
4	1000	990	1150	2220	2840	3560	54	72	6.1
5	1550	1150	1150	1990	2835	4025	60	9.4	36.1
6	5550	5100	900	1765	2745	4955	61	9.2	50.5
7	1600	1550	690	1470	2580	4940	65	2	51
8	1300	1250	1000	1575	2320	5000	66	43	50.3
9	1500	1300	800	3020	2210	3160	65.2	41.1	8.6
10	1600	1450	600	1005	2200	4320	85.4	51	50.1

Table 10.6: FOG reduction in the secondary clarifier of a biodefoamer supported activated sludge

Influent FOG concentration (mg/L)				FOG concentration tank (mg/L)			FOG reduction (%)		
Time (days)	Bio-AS	Syn-AS	CAS	Bio-AS	Syn-AS	CAS	Bio-AS	Syn-AS	CAS
0	550	500	530	400	450	300	27.2	10	43.4
1	250	280	270	84	250	98	66.4	67	64

2	114	114	140	66	72	50	42	37	64.3
3	113	144	128	34	108	78	70	25	39.1
4	85	100	76	12	98	45	85	2	41
5	58	72	74	35	70	43	40	3	42
6	46	62	94	36	46	54	22	26	43
7	28	86	102	22	30	58	22.4	65	43.1
8	22	140	52	18	50	28	22.2	64.3	46.2
9	30	128	57	13	54	30	57	58	47.4
10	28	402	300	10	110	149	64.3	63.3	63

Table 10.7: Protein concentration reduction by the biodefoamer supported activated sludge secondary clarifier

Influent Protein concentration (mg/L)				Protein concentration tank (mg/L)			Protein reduction (%)		
Time (days)	Bio-AS	Syn-AS	CAS	Bio-AS	Syn-AS	CAS	Bio-AS	Syn-AS	CAS
0	48	20	10	13	7.7	10.2	3.2	61	65.2
1	21	18	18	0.5	7.2	12	94	40	62
2	17.5	4.2	18	0.3	2	12	94	59.4	33
3	17	3.3	39.5	0.04	2	13.2	98	77	48
4	0.16	1.8	4.9	0.04	1	0.34	99	64	89.3
5	0.6	2.8	2.2	0.04	1	0.81	93	92.2	80
6	0.3	2	28	0.1	2	10.3	93.4	50.2	77.2
7	0.1	0.04	2	0.2	0.04	1.2	27	59	40
8	0.16	0.8	10	0.04	0.6	3	74.1	60	73
9	0.06	0.5	22	0.05	0.1	9	20	64	12
10	0.16	0.34	7.2	0.01	2.1	1.4	71.4	3	57.5

Table 10.8: Reduction of TSS by a biodefoamer supported activated sludge secondary clarifier

Influent TSS concentration (mg/L)				TSS concentration tank (mg/L)			TSS reduction (%)		
Time (days)	Bio-AS	Syn-AS	CAS	Bio-AS	Syn-AS	CAS	Bio-AS	Syn-AS	CAS
0	5450	10500	7400	1350	9950	2000	75.2	5.2	73
1	9600	11500	7700	1200	1600	1800	88	86	77
2	2350	1550	2600	1050	1450	1700	55.3	7	35
3	2120	15400	1250	1300	10200	1100	39	34	12
4	1520	1000	1300	750	990	1150	51	1	12
5	900	1250	1200	550	1150	1150	39	8	4.2
6	900	5400	3420	450	5100	900	43	6	74
7	800	3100	1750	100	1550	690	88	50	61
8	850	1600	2500	110	1250	1000	87.1	22	60
9	780	3150	1650	200	1300	800	74.4	59	52
10	700	2900	1200	100	1450	600	86	50	50

Table 10.9: Efficiency of COD reduction by a biodefoamer supported activated sludge secondary clarifier

Influent COD concentration (mg/L)				COD concentration (mg/L)			COD reduction (%)		
Time (days)	Bio-AS	Syn-AS	CAS	Bio-AS	Syn-AS	CAS	Bio-AS	Syn-AS	CAS
0	4510	8355	5830	1985	4420	3960	56	47.1	32
1	3550	10 000	3635	2210	3950	3535	38	61	2.75
2	4095	8200	2325	2565	3030	2030	37.3	63	13
3	3760	4795	3725	2434	3010	3650	44	37.2	2
4	4200	10 000	3790	2220	2840	3560	54	72	6.1
5	4725	3130	6300	1990	2835	4025	60	9.4	36.1
6	9 500	3030	8 000	1765	2745	4955	61	9.2	50.5
7	4305	2630	2 467	1470	2580	4940	65	2	51
8	4520	4130	3070	1575	2320	5000	66	43	50.3
9	7950	3755	3460	3020	2210	3160	65.2	41.1	8.6
10	8890	4485	8650	1005	2200	4320	85.4	51	50.1